

NOTE TO USERS

This reproduction is the best copy available.

UMI

UNIVERSITY OF ALBERTA

Sedimentology and Stratigraphy of the Pedro Castle Formation

Southwest Grand Cayman, BWI

by

Astrid Elizabeth Arts



A thesis submitted to the Faculty of Graduate Studies and Research in partial fulfillment
of the requirements for the degree of **Master of Science**.

Department of Earth and Atmospheric Sciences

Edmonton, Alberta

Spring 2000



National Library
of Canada

Acquisitions and
Bibliographic Services

395 Wellington Street
Ottawa ON K1A 0N4
Canada

Bibliothèque nationale
du Canada

Acquisitions et
services bibliographiques

395, rue Wellington
Ottawa ON K1A 0N4
Canada

Your file *Voire référence*

Our file *Notre référence*

The author has granted a non-exclusive licence allowing the National Library of Canada to reproduce, loan, distribute or sell copies of this thesis in microform, paper or electronic formats.

The author retains ownership of the copyright in this thesis. Neither the thesis nor substantial extracts from it may be printed or otherwise reproduced without the author's permission.

L'auteur a accordé une licence non exclusive permettant à la Bibliothèque nationale du Canada de reproduire, prêter, distribuer ou vendre des copies de cette thèse sous la forme de microfiche/film, de reproduction sur papier ou sur format électronique.

L'auteur conserve la propriété du droit d'auteur qui protège cette thèse. Ni la thèse ni des extraits substantiels de celle-ci ne doivent être imprimés ou autrement reproduits sans son autorisation.

0-612-60089-0

Canada

ABSTRACT

The Pliocene Pedro Castle Formation on the southwest corner of Grand Cayman is composed of the 1) rhodolith *Amphistegina Trachyphyllia* facies, 2) *Amphistegina* rhodolith facies, 3) foram *Halimeda* rhodolith facies, 4) rhodolith, free living and branching coral *Amphistegina* facies, 5) *Stylophora Halimeda Amphistegina* facies, 6) *Halimeda Amphistegina* facies, and 7) rhodolith coralline red algae facies. The vertical succession of these facies are indicative of a transgressive succession. The development of this succession was influenced by antecedent topography, substrate type, water energy, and water depth. It appears that influences on sedimentation evolved as sea level gradually rose during the Pliocene. The timing of sedimentation for the Pedro Castle Formation is inconclusive due to the problematic correlation of this transgressive event to established sea level curves. A Pliocene Sea level of 30-35 m asl is similar to that seen in the Caribbean and globally.

*Do not go where the path may lead,
go instead where there is no path and leave a trail*

Author unknown

For my grade 4 teacher Mrs. Debra Fisher,
who had me make my first rock with white glue and pebbles from the playground,
I've never looked at rocks the same way again.

ACKNOWLEDGEMENTS

Hard to believe it's finally over; some days I felt this day would never come. I need to thank my supervisor Brian Jones for his unparalleled editing skills and lasting patience for this wayward student.

This thesis would not have been possible without the generosity of Helen Harquail, Otto Watler, Patrick Island Lagoon Estates and the Cayman Islands Water Authority who allowed us to drill on their land and acquire the cores used in this thesis. The drillers Ian Hunter, Kenton Phimester, Brent Wignall, Jen Vézina and Bill Kalbfleisch put in long hours in the hot sun to retrieve these cores and I thank them. Financial support of this research was provided by PanCanadian Petroleum, Husky Oil, and NSERC (grant A6090 to Brian Jones). The Cayman Islands Water Authority and Department of the Environment also provided logistical support during our stay on the island.

During my time at the U of A, there are so many individuals who helped me laugh and kept me sane. The Carbonate Group: Betsy Willson, Jason Montpetit, Dayve Hills, Jen Vézina and Paul Blanchon all made a huge difference in my life from teaching me the intricacies of the Mac to true warfare in the office. To Kim Jardine, thanks for making yours a second home and teaching me that everything looked different after a bottle of red wine. To Marianne MacKenzie, Betsy Willson, Julie Esdale, Leslie Driver, Devon Rowe and all the friends I made in grad school, you are what I will always remember. I want to thank the Ichnoboyz (you know who you are) for getting me in the bad books with my roommate, posting bond for me in Wyoming, occasionally letting me use your computer lab and most importantly providing a never ending supply of entertainment. To Shannon Nelson and Eric Hanson thanks for never making me feel bad for not being done and Crestar Energy for being so helpful and understanding. Isabel Hotchkiss and Judith Enarson helped me with every departmental issue I ever had and they saved me on more than one occasion. I am indebted to my family for their unending support and encouragement as well as a place to sleep every time I came back to Edmonton.

A special thanks to Jason Montpetit for his support, words of encouragement and friendship, remember the bunny plate is always there for you.

Gareth Jones, a man not of this world, your friendship and simple enjoyment of all things outdoors mean the world to me. Thanks for taking me to the edge and back.

One last special thanks to Bill Hannah for your friendship, encouragement, speedy typing skills, and patience as this thesis drew to a close. Thank you all so much.

TABLE OF CONTENTS

Chapter 1 Introduction	1
1.1 Introduction.....	1
1.2 History of Pedro Castle.....	1
1.3 Geographic and Geologic Framework.....	4
1.3.1 Location.....	4
1.3.2 Tectonic Setting.....	7
1.4 Stratigraphic Overview.....	9
1.5 Study Area.....	9
1.6 Objectives.....	13
1.7 Methods.....	13
1.7.1 Core Logging and Thin Section Petrography.....	13
Chapter 2 Stratigraphy	15
2.1 Stratigraphic Framework of the Cayman Islands.....	15
2.1.1 Brac Formation.....	17
2.1.2 Cayman Formation.....	17
2.1.3 Pedro Castle Formation.....	19
2.1.4 Ironshore Formation.....	19
2.2 Stratigraphy of the Study Area.....	20
2.3 Cayman Unconformity.....	26
2.4 Synopsis.....	27
Chapter 3 Sedimentology and Facies Architecture of the Pedro Castle Formation	31
3.1 Sedimentology.....	31
3.1.1 Definitions.....	31
3.1.2 Skeletal Allochems and Preservation.....	31
3.2 Facies of the Pedro Castle Formation.....	33

Rhodolith- <i>Amphistegina-Trachyphyllia</i> facies	35
<i>Amphistegina</i> -Rhodolith facies	35
Rhodolith-Free Living and Branching Coral- <i>Amphistegina</i> facies	38
Rhodolith-Coralline Red Algae facies	38
<i>Stylophora-Amphistegina-Halimeda</i> facies	41
Bivalve-Foram- <i>Halimeda</i> -Rhodolith facies	41
<i>Halimeda-Amphistegina</i> facies	41
3.3 Facies Architecture	45
3.3.1 Lower Valley Transect	45
3.3.2 Patrick Island Lagoon Transect	48
3.3.3 Western Transect	51
3.4 Synopsis	53
Chapter 4 Facies Interpretation	54
4.1 Introduction	54
4.2 Environmental Implications of Allochems	54
4.2.1 Foraminifera	54
<i>Amphistegina</i>	55
<i>Homotrema</i>	55
Globigerinids	55
4.2.2 Calcareous Algae	56
Green Algae (Codiaceae)	56
Red Algae (Corallinaceae)	56
4.2.3 Corals	57
<i>Stylophora</i>	57
<i>Trachyphyllia</i>	58
4.2.4 Bivalves and Gastropods	58
4.2.5 Echinoids	59
4.3 Facies Interpretation	59
4.3.1 Water Depth	59
4.3.2 Water Energy	60

4.3.3 <i>Water Circulation</i>	60
4.3.4 <i>Depositional Packages</i>	61
Depositional Package I	61
Depositional Package II	63
Depositional Package III	65
4.4 <i>Synopsis</i>	67
Chapter 5 Sea Levels	68
5.1 <i>Introduction</i>	68
5.2 <i>Sea Level History</i>	68
5.2.1 <i>Paleocene to Oligocene Sea Levels (65 – 25 Ma)</i>	70
5.2.2 <i>Miocene Sea Levels (25 – 5 Ma)</i>	71
5.2.3 <i>Pliocene Sea Levels (5 – 3.0 Ma)</i>	72
5.3 <i>Sea Level Interpretation</i>	74
5.4 <i>Synopsis</i>	77
Chapter 6 Conclusions	78
References	80
Appendix	88

LIST OF TABLES

Table		Page
Table 3.1	Facies in the dolostones of the Pedro Castle Formation.....	34
Table 3.2	Comparison of facies identified in the Pedro Castle Formation with those of Wignall 1995).....	47

LIST OF FIGURES

Figure	Page
Figure 1.1 Pedro (St. James) Castle before and after restoration.....	2
Figure 1.2 Grand Cayman's location in the Caribbean Sea.....	5
Figure 1.3 Study Area and surficial geology of Grand Cayman.....	6
Figure 1.4 Tectonic and bathymetric setting of the Cayman Islands in the central Caribbean area.....	8
Figure 1.5 Exposures of the Pedro Castle Formation along the southern coast of Grand Cayman.....	10
Figure 1.6 Karst on the Pedro Castle Formation at Great Pedro Point (Pedro Bluff).....	11
Figure 1.7 Man made exposures of the Pedro Castle (PCF) and Cayman (CF) formations at Pedro Castle Quarry.....	12
Figure 2.1 Table of Formations for the Cayman Islands.....	16
Figure 2.2 Location and geological map of the Cayman Islands.....	18
Figure 2.3 Location map showing localities discussed including the location of the Lower Valley, Newlands, Patrick Island Lagoon and Western Transects.....	21
Figure 2.4 Topography of Grand Cayman.....	22
Figure 2.5 Location Maps of Grand Cayman showing well and outcrop localities with elevations of Cayman Unconformity and thickness of the Pedro Castle Formation.....	23

Figure 2.6	Stratigraphic relationships of the Cayman, Pedro Castle and Ironshore Formations.....	24
Figure 2.7	Geometry of planed Pedro Castle and Cayman formations at Rogers Wreck Point.....	25
Figure 2.8	The Cayman Unconformity at Pedro Castle Quarry.....	28
Figure 2.9	Conceptual model showing the topography on the Cayman Unconformity.....	29
Figure 3.1	Exposure of the Pedro Castle Formation in Pedro Castle Quarry.....	32
Figure 3.2	Core photo of <i>Rhodolith-Amphistegina-Trachyphllia</i> facies.....	36
Figure 3.1	Core photo of <i>Amphistegina-Rhodolith</i> facies.....	37
Figure 3.1	Core photo of Rhodolith-Free Living and Branching Coral- <i>Amphistegina</i> facies.....	39
Figure 3.1	Core photo of Rhodolith-Coralline Red Algae facies.....	40
Figure 3.1	Core photo of <i>Stylophora-Amphistegina-Halimeda</i> facies.....	42
Figure 3.1	Core photo of Bivalve-Foram- <i>Halimeda-Rhodolith</i> facies.....	43
Figure 3.1	Core photo of <i>Halimeda-Amphistegina</i> facies.....	44
Figure 3.9	Location map showing positions of the Lower Valley, Patrick Island Lagoon and Western Transects.....	46
Figure 3.10	Facies distribution in the Pedro Castle Formation, Lower Valley Transect.....	49
Figure 3.11	Facies distribution in the Pedro Castle Formation, Patrick Island Lagoon Transect.....	50
Figure 3.12	Facies distribution in the Pedro Castle Formation, Western Transect.....	52
Figure 4.1	Depositional Sequence I.....	62

Figure 4.2	Depositional Sequence II.....	64
Figure 4.3	Depositional Sequence III.....	66
Figure 5.1	Third order sea level curves for the Tertiary.....	69
Figure 5.2	Third order sea level curves for the Pliocene.....	75

CHAPTER 1

INTRODUCTION

1.1 INTRODUCTION

This study of the Pliocene Pedro Castle Formation on the southwestern corner of Grand Cayman is part of continuing research in understanding the development and evolution of the Cayman Islands. The Pedro Castle Formation is rarely exposed in outcrop. A drilling program initiated in 1991 has recovered numerous subsurface examples of the Pedro Castle Formation. This subsurface information in conjunction with outcrop data has enabled a stratigraphic and sedimentologic analysis of the Pliocene on the southwestern part of Grand Cayman.

1.2 HISTORY OF PEDRO CASTLE

The Pedro Castle Formation, the focus of this thesis, derived its name from the proximal location of its type section to the historic Pedro Castle (Jones and Hunter 1989; Jones 1994). This castle has roots deeply seated in the history of the Cayman Islands. A narration of this history reveals a tumultuous past that provides a historical perspective to the name Pedro Castle.

Pedro Castle (Figure 1.1), built in 1780, is the oldest surviving building on the Cayman Islands. It is situated on the south coast of Grand Cayman, southeast of Savannah, on Pedro Bluff. The location of the castle adds to its mystery and allure. It is perched on a bluff fringed with rugged cliffs and the only seaward approach is from a small landing 2 km away. The upper story of the house commands a view of most of the island and the southern coast. For these reasons, the history of this building has been the subject of both stories and speculation for many generations. Its colourful yet curious history began with William Eden, the castle's owner. Eden, born in 1737, left Devizes, Wiltshire and came to Grand Cayman via Jamaica in 1765. This man is a mystery. His occupation



Figure 1.1. Pedro (St. James) Castle (A) Before restoration, February 1995. (B) After restoration, April 1997.

is unknown, his death is unexplained and his reason for building this great stone house on an isolated island is without answer. Eden's arrival on Grand Cayman came after his marriage, in Jamaica, to Dorothy Bodden, daughter of Governor Bodden. Dorothy died soon afterwards and Eden remarried Elizabeth Clark, sister of Robert Knowles Clark, in 1767. It was during his marriage to Elizabeth that Eden built the stone house he named St. James Castle. The castle was constructed by slaves using local materials and is modeled after English homes of that era. The castle itself is not what one would expect. It is not the grand structure commonly imagined when referring to a castle. But at its time of construction there were only 400 people on Grand Cayman and the typical house was simple, plaster walls and a thatch roof. By modern standards this building would not be worthy of the title but in comparison to the homes on the island in the late 1700's this building was truly a castle.

Through the years the castle has been a home, a meeting place, a gaol, a restaurant, and a bar. Today this building stands as a repository of much of the islands history. One of the most important events ever held in the castle was a public meeting on December 5th, 1831. At that meeting, it was decided to form the first elected parliament. For this reason the castle is often considered the birthplace of democracy in the Cayman Islands. Overall, the buildings scant history and strategic location have resulted in colourful stories linking it to the days of pirates and buried treasures. The most colourful of these stories belonged to a subsequent owner Thomas Hubbel in the 1950's. His stories of the castle included pirates, doubloons, cannons and antiquities from under the sea. To substantiate his claims he restored the structure, adding a crenellated tower and fabricated a new original owner, a Spaniard by the name of Pedro Gomez. He also carved a new date of construction, 1631, above one of the buildings arches. Historical fact refutes these claims but it is these stories, that have led to the development of local legends with tales of blood, doom and buried treasures in and around the great castle.

Pedro Castle survived two centuries of hurricanes, fires, robbery and neglect before the Cayman Government bought the historical building atop Pedro Bluff in 1992. The building has been restored to its original splendor (circa 1900) and has become the focus of a 7 acre heritage park. The Pedro St. James Castle, a name accrediting history and legend, contains information and history on the castle's colourful past. This restoration project was undertaken by the islands' tourism ministry and will commemorate this building as the birthplace of Democracy in the Caymans. Restoration commenced in May 1996 with the relaying of the cornerstone. Under this stone is a time capsule containing a \$1 Canadian coin, a May 1995 set of Cayman Islands stamps commemorating VE Day, a 1994 silver commemorative Cayman Islands Coin honouring the 200th anniversary of the wreck of the Ten Sails, and a microfiche copy of the May 11th, 1997 Caymanian Compass newspaper. To date, this is the most ambitious restoration project ever undertaken in the Cayman Islands. In the years to come, the Pedro St. James Castle will fittingly become a museum, housing all the historical and legendary truths of the Cayman Islands (Hirst 1910; Williams 1970; Shah 1996).

1.3 GEOGRAPHIC AND GEOLOGIC FRAMEWORK

1.3.1 Location

The Cayman Islands are situated between Jamaica and Cuba in the northwestern part of the Caribbean Sea (Figure 1.2). Grand Cayman (81°15'W, 19°20'N), the largest of the three islands (Figure 1.3), is approximately 480 km north-northwest of Jamaica and 240 km south of Cuba. The two smaller islands, Cayman Brac and Little Cayman, are located approximately 95 km north-northeast of Grand Cayman.

Grand Cayman is 30 - 35 km long (east to west) and 5 - 15 km wide (north to south) and encompasses an area of 197 km² (Spencer 1985). The island has a subdued topography, as most of it is less than 3 m above sea level.

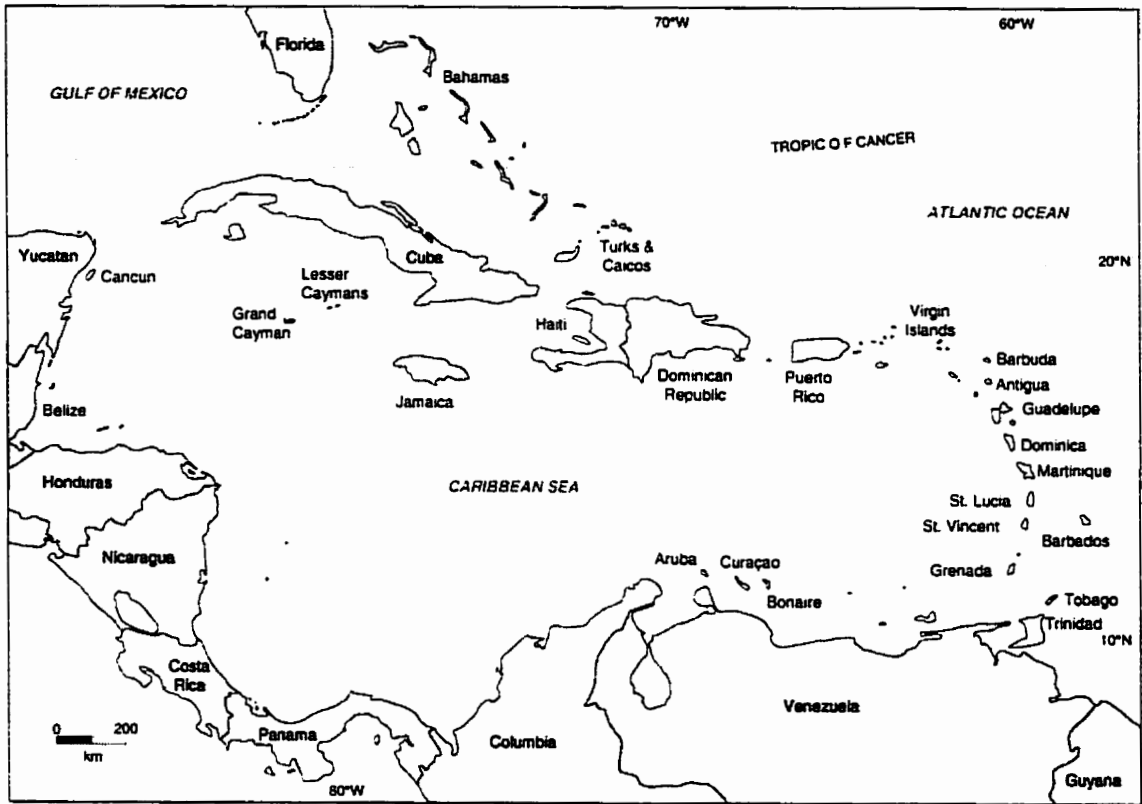


Figure 1.2. Grand Cayman's location in the Caribbean Sea (modified after Blanchon 1995).

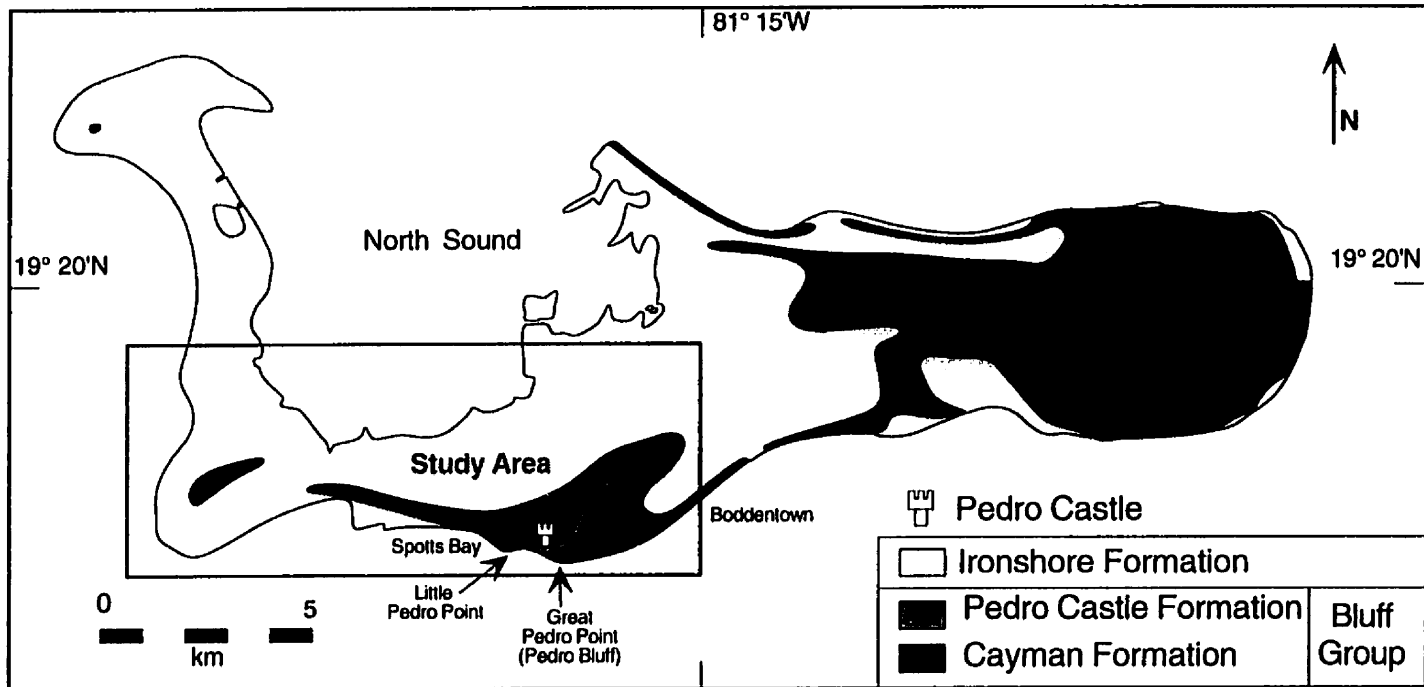


Figure 1.3. Study Area and surficial geology of Grand Cayman (modified after Jones *et al.* 1994b)

1.3.2 Tectonic Setting

The Cayman Islands are the only projecting peaks of the asymmetrical Cayman Ridge which extends from the Sierra Maestra of Cuba south to the Gulf of Honduras, where it disappears beneath sediment cover in the Yucatan Basin (Perfit and Heezen 1978). The north side of the Cayman Ridge, slopes gently into the Yucatan Abyssal Plain whereas the southern slope quickly drops more than 5000 m forming the northern margin of the Cayman Trench (Rosencrantz and Sclater 1986).

The Cayman Trench is 100 - 150 km wide, 1200 km long and reaches depths in excess of 6000 m (Perfit and Heezen 1978). This trench marks the present day location of the strike slip boundary between the northern Caribbean Plate and the North American Plate. The Oriente Transform Fault defines this boundary along the northern and eastern edge, whereas the Swan Island Transform Fault delineates the southern and western edge. Movement of the North American Plate is sinistral relative to the Caribbean Plate. These faults are separated by the Mid-Cayman Rise; a north south spreading center located southwest of Grand Cayman (Figure 1.4). Since the opening of the Mid-Cayman Rise, 30-40 Ma ago, the Cayman Trench has been displaced 190 km relative to the North American Plate (Leroy *et al.* 1996).

The Cayman Ridge was predominantly a shallow carbonate bank until it began to subside during the Miocene (Perfit and Heezen 1978; Hallam 1984). Each of the Cayman Islands are situated on independent fault blocks that are elevated above the general level of the Cayman Ridge. Perfit and Heezen (1978) have estimated the rates of subsidence for this ridge at 6 cm/Ka along the northern Caribbean margin. Localized uplift during the late middle Miocene elevated the Cayman Islands, Swan Islands, Jamaica, and most of southern Cuba above sea level, whereas the surrounding areas continued to fault and subside.

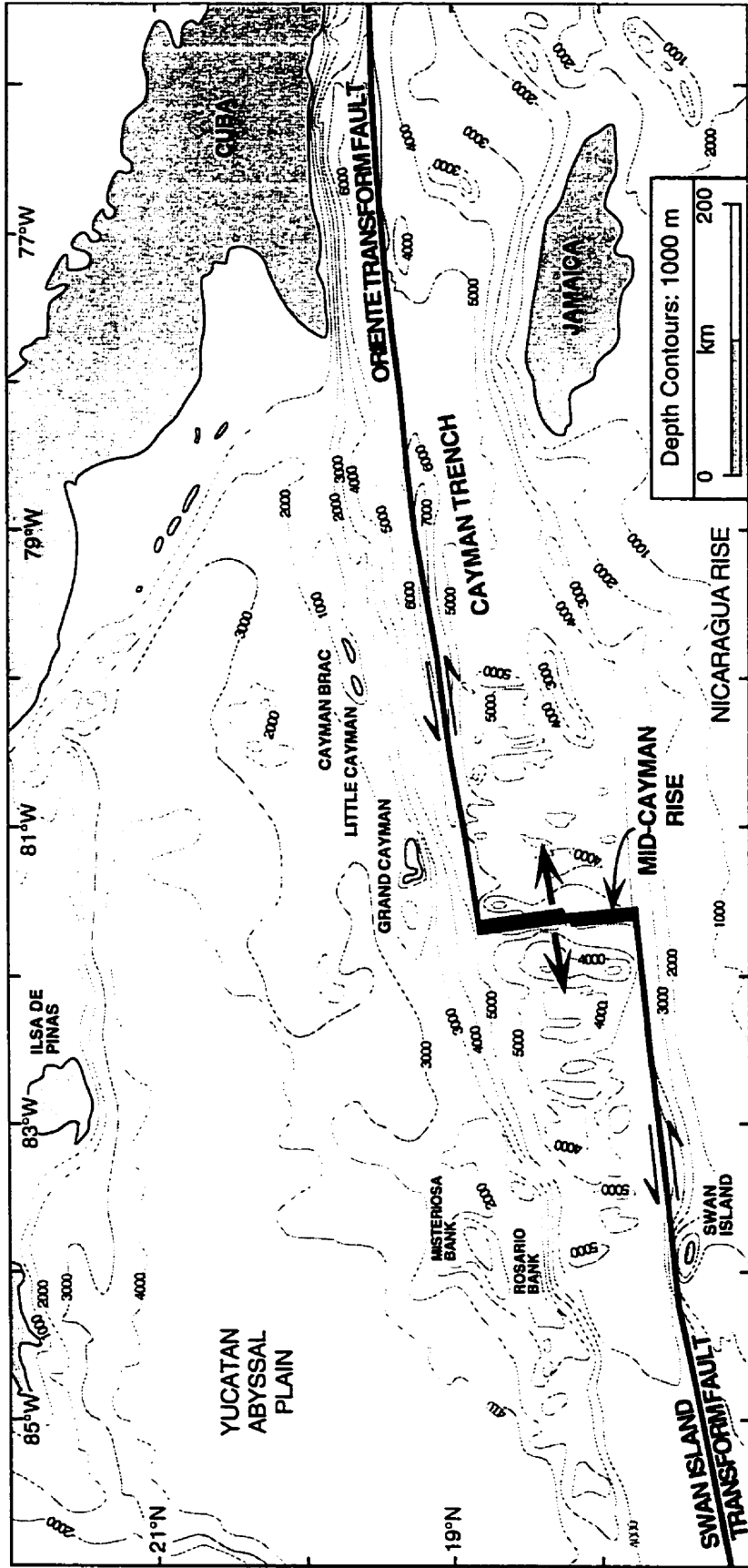


Figure 1.4. Tectonic and bathymetric setting of the Cayman Islands in the central Caribbean area (modified after Pleydell *et al.* 1990).

1.4 STRATIGRAPHIC OVERVIEW

On the Cayman Islands strata at the surface and in the shallow subsurface belong to the Brac, Cayman, Pedro Castle, and Ironshore formations. The Cayman Unconformity delineates the contact between the Cayman and Pedro Castle formations (Jones and Hunter 1994). The Pedro Castle Unconformity defines the boundary between the Pedro Castle and Ironshore formations. The Brac, Cayman, and Pedro Castle formations, which constitute the Bluff Group, are Tertiary in age (Jones *et al.* 1994a) whereas, the Ironshore Formation is Pleistocene in age (Woodroffe *et al.* 1983; Vézina 1997). On Grand Cayman the Cayman, Pedro Castle, and Ironshore formations are found in subsurface and surface exposures. Each formation has variable lateral and vertical distribution (Figure 1.3). The Pedro Castle Formation is the focus of this study.

1.5 STUDY AREA

The study area is located in the southwest corner of Grand Cayman (Figure 1.3). It extends east to west, from Bodden Town to the sunny beaches of the western coastline. It is bounded to the north by the south shore of North Sound and to the south by the coastline.

This area is unique in that it contains the only natural exposures of the Pedro Castle Formation on Grand Cayman. Although most of the area is covered in vegetation, the Pedro Castle Formation outcrops along the coast (Figure 1.5) as rugged cliffs attaining heights of 12' - 21.5' (3.7 m - 6.6 m). Along the coast, the Cayman Unconformity is visible (Jones and Hunter 1994) and accentuated by a change in the morphology of the karsted surface (Figure 1.6). Man made exposures of the Pedro Castle Formation are found at Pedro Castle Quarry (Figure 1.7).

Of the 8 m exposed in Pedro Castle Quarry, the upper 2.5 m is composed of the Pedro Castle Formation. This locality is the type section for the Cayman and Pedro Castle



Figure 1.5. Exposures of the Pedro Castle Formation along the southern coast of Grand Cayman. Photo taken from Spotts Bay.

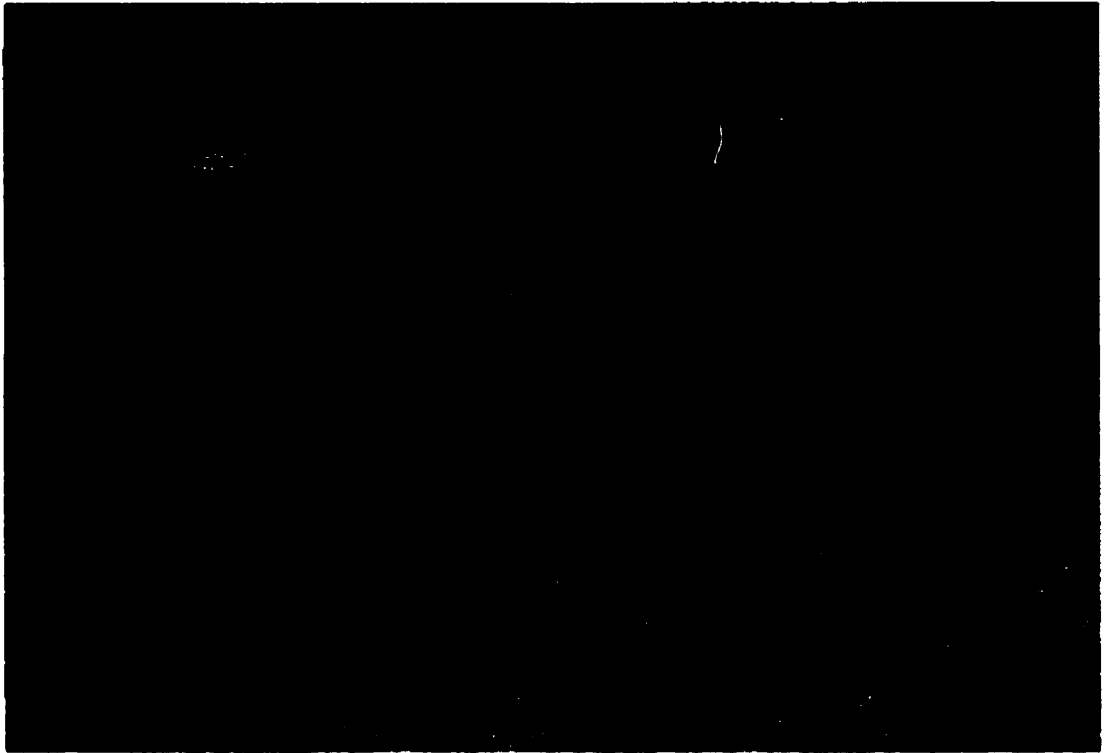


Figure 1.6. Karst on the Pedro Castle Formation at Great Pedro Point (Pedro Bluff).

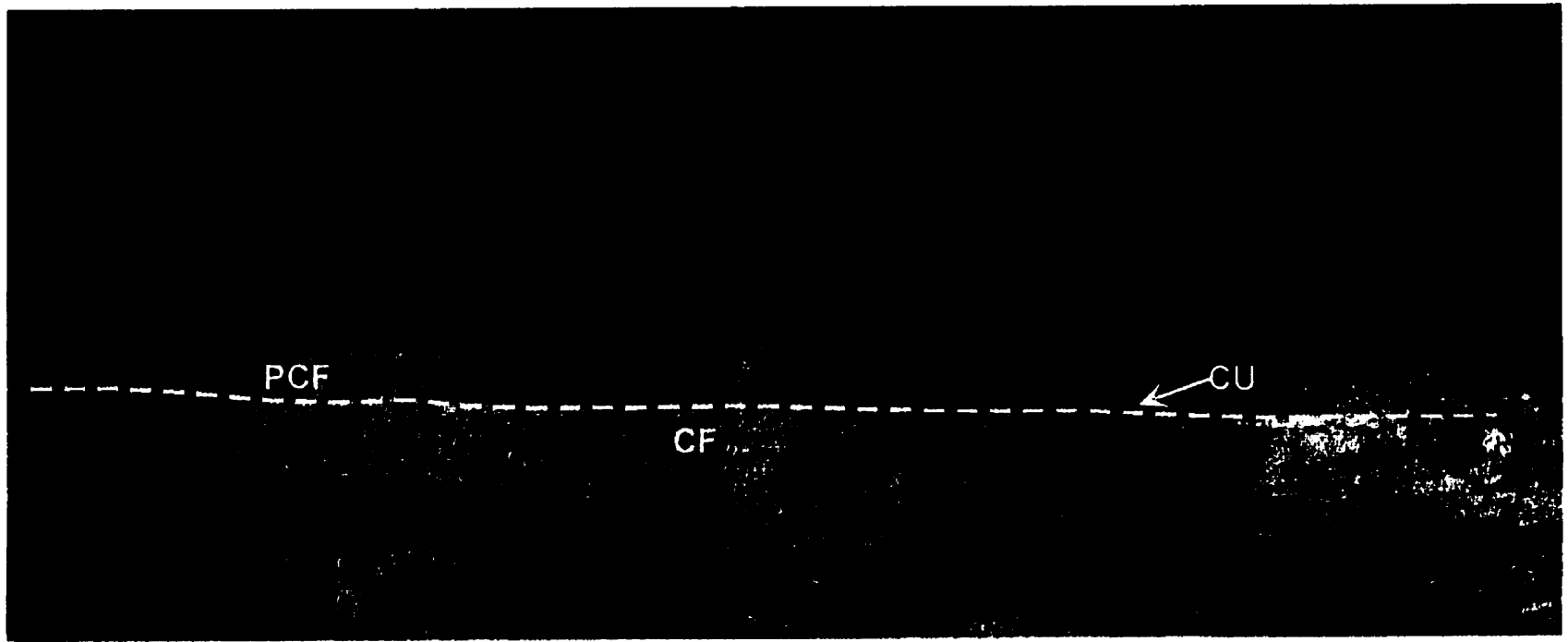


Figure 1.7. Man made exposures of the Pedro Castle (PCF) and Cayman (CF) formations at Pedro Castle Quarry. The Cayman Unconformity (CU) is the contact between these units. Quarry wall is approximately 8.5 m high.

formations. The contact between these formations is clearly exposed (Jones and Hunter 1989).

1.6 OBJECTIVES

The objectives of this study are as follows:

1. to describe the sedimentological characteristics and facies architecture of the Pedro Castle Formation in the study area,
2. to describe the physical characteristics of the Cayman Unconformity and to characterize the effects that the topography of that surface had on the depositional regime of the Pedro Castle Formation, and
3. to establish a Pliocene sea level that resulted in the deposition of the Pedro Castle Formation

1.7 METHODS

A drilling program initiated in 1991 has to date drilled 57 wells on Grand Cayman, 15 within the study area. Of these 15 wells, 10 contain the Pedro Castle Formation (Appendix A). Core recovery was facilitated by the use of a continuous coring Winke Exploration Diamond Drill, manufactured by JKS BOYLES. Under ideal conditions this drilling system is capable of penetrating depths up to 120 m. The recovered core is approximately 3.5 cm in diameter and has been split for logging. Unfavorable subsurface conditions in the study area prevented coring past depths of 35 m.

1.7.1 Core Logging and Thin Section Petrography

Slabbed core and accessible outcrops were logged by identifying the biota present and the textural relationships found in the rock. The textures are described using Dunham's (1962) Classification scheme as modified by Embry and Klovan (1971). A more detailed study of the core was made possible using thin section microscopy. The 50

x 75 mm thin sections were ground to approximately 30 μm and stained for calcite, using Alizarin Red S. The staining procedures followed those of Dickson (1965). The thin sections were examined using transmitted light.

CHAPTER 2

STRATIGRAPHY

2.1 STRATIGRAPHIC FRAMEWORK OF THE CAYMAN ISLANDS

The geology of the Cayman Islands has undergone considerable revision since its original description by Matley in 1924. Matley's work was based on information gathered on an eleven day reconnaissance survey, five of which were spent on Grand Cayman. He assigned exposed strata to the Bluff Limestone and the Ironshore Formation. The Bluff Limestone forms the core of each island and received its name from its resistant nature, as it characteristically crops out as bluffs or cliffs. The Ironshore Formation forms a low coastal terrace on the periphery of each island. The name Ironshore was derived from a local term used for the low rocky type of shore that these rocks produced. The Bluff Limestone described as a white, massive, and commonly semi-crystalline limestone with poorly preserved fossils, was assigned a Tertiary age on the basis of its coral and foraminifera fauna. The Ironshore Formation was defined as a white and cream colored consolidated coral sand and marl, containing abundant well preserved coral heads which were used to date this formation to the Pleistocene epoch (Matley 1924a; 1924b; 1925; 1926).

Unfortunately, inherent lithologic inferences associated with the term Bluff Limestone caused considerable confusion regarding the composition of this unit. Later work by Jones *et al.* (1984), Pleydell (1987), and Pleydell and Jones (1988), showed that this unit was composed predominantly of dolostone, not limestone as originally proposed by Matley (1924a; 1924b; 1925; 1926). Consequently, Jones and Hunter (1989) advocated changing the term Bluff Limestone to Bluff Formation, so that all lithologic connotations would be removed from the name. The Bluff Formation was subsequently elevated to group status (Jones *et al.* 1994b) and divided into the disconformity bounded Brac, Cayman, and Pedro Castle formations (Figure 2.1).

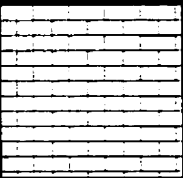
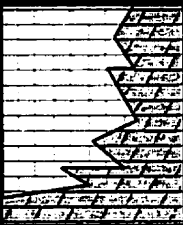


AGE	LITHOTYPE	UNIT	LITHOLOGY	BIOTA	
PLEIST.		IRONSHORE FORMATION <i>unconformity</i>	<i>Limestone</i>	<i>Corals (VC)</i> <i>Bivalves (VC)</i> <i>Gastropods (C)</i>	
PLIOCENE		PEDRO CASTLE FORMATION <i>unconformity</i>	<i>Dolostone (fabric retentive), dolomitic limestone and limestone</i>	<i>Foraminifera (VC)</i> <i>Corals (C)</i> <i>Bivalves (LC)</i> <i>Gastropods (C)</i> <i>Red Algae (C)</i> <i>Halimeda (R)</i>	
M. MIOCENE		BLUFF GROUP	CAYMAN FORMATION <i>unconformity</i>	<i>Dolostone (fabric retentive and destructive)</i>	<i>Corals (VC)</i> <i>Bivalves (LC)</i> <i>Rhodoliths (LC)</i> <i>Red algae (LC)</i> <i>Foraminifera (LC)</i> <i>Halimeda (R)</i> <i>Gastropods (R)</i>
L. OLIGOCENE			BRAC FORMATION	<i>Limestone and sucrosic dolostone (fabric-destructive) with pods of limestone</i>	<i>Bivalves (VC)</i> <i>Gastropods (C)</i> <i>Foraminifera (VC)</i> <i>Red algae (R)</i>

Figure 2.1. Table of Formations for the Caymans Islands. VC = very common; C = common; LC = locally common; R = rare (modified after Jones *et al.* 1994a).

The outcrop distribution of the Tertiary and Pleistocene strata on the Cayman Islands is variable (Figure 2.2). The Ironshore and Cayman formations crop out on all three islands, whereas exposures of the Pedro Castle Formation are limited to Grand Cayman and Cayman Brac. The Brac Formation, at the base of the Bluff Group, is limited to vertical exposures on Cayman Brac.

2.1.1 Brac Formation

The Brac Formation, named after its type locality on the northeast end of Cayman Brac, is at least 33 meters thick. This late Lower Oligocene formation (Jones *et al.* 1994a) is predominately formed of limestones (wackestones to grainstones). On the south coast of Cayman Brac, the formation is composed of sucrosic dolostone that contains isolated pods of limestone. Biotas characteristically found in the Brac Formation include numerous *Lepidocyclina*, with lesser numbers of red algae, echinoid plates, and other foraminifera. Corals are absent apart from rare *Porites* fragments in the 2 meters below the Brac-Cayman unconformity. Bivalves and gastropods are also found in the Brac Formation but are restricted to one bed near the upper boundary. This formation has yet to be found on Grand Cayman or Little Cayman (Jones 1994).

2.1.2 Cayman Formation

The Cayman Formation disconformably overlies the Brac Formation. It is questionably lower - middle Miocene in age (Jones *et al.* 1994a). This unit, which is at least 170 meters thick, is composed of fabric-retentive microcrystalline dolostones. The biota of the Cayman Formation is more diverse than that in the Brac Formation. *Lepidocyclina* is not found above the Brac - Cayman unconformity. Instead, *Amphistegina* is the dominant foraminifera in the Cayman Formation. Other biota found in this formation include corals (massive domal, branching, free living), bivalves,

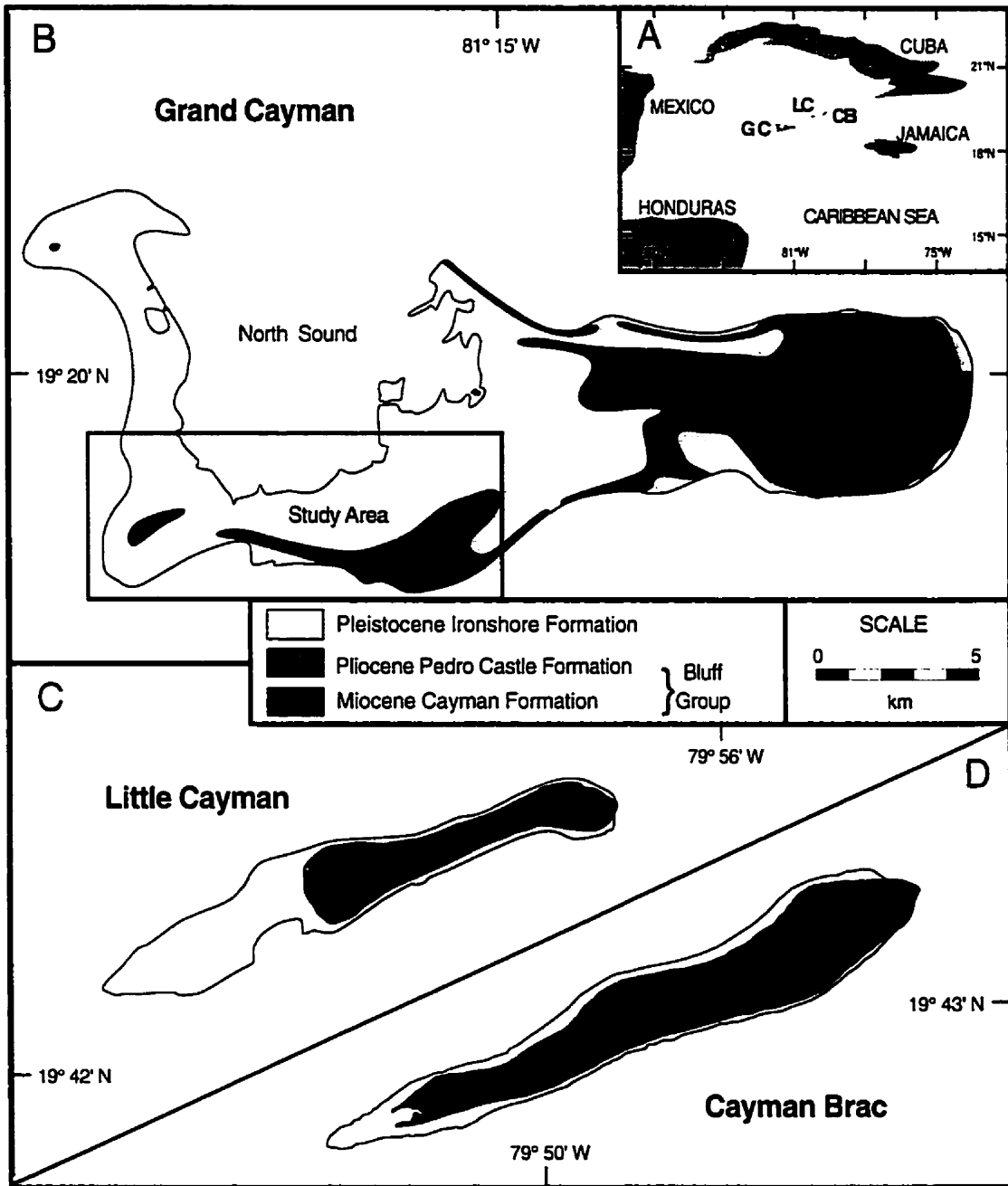


Figure 2.2. A) Location map showing the Cayman Islands, Grand Cayman (GC), Little Cayman (LC), and Cayman Brac (CB). B) Geological map of Grand Cayman showing study area. C) Geological Map of Little Cayman. D) Geological map of Cayman Brac (modified after Hunter and Jones 1989).

gastropods, foraminifera, *Halimeda*, red algae (free living and rhodoliths), and echinoids (Jones 1994).

2.1.3 Pedro Castle Formation

The uppermost stratigraphic unit in the Bluff Group is the Pedro Castle Formation. This unit, which disconformably overlies the Cayman Formation, is up to 28 m thick in wells SH#3 (Jones *et al.* 1994b) and OWP#2. The Pedro Castle Formation, which is Pliocene in age (Jones *et al.* 1994a), is composed of an off - white to cream colored, rubbly weathering dolostone, limestone, or dolomitic limestone. This unit, which is relatively soft compared to the dolostones of the underlying Cayman Formation, contains free - living and branching corals, foraminifera (dominantly *Amphistegina*), bivalves, gastropods, red algae (free living and rhodoliths), and echinoids (Jones 1994).

2.1.4 Ironshore Formation

The Ironshore Formation rests unconformably on the Tertiary Bluff Group. This unit is generally less than 9 m thick (Jones 1994) and commonly forms a thin veneer over the Bluff Group. This Pleistocene unit (Woodroffe *et al.* 1983; Vézina 1997; Vézina *et al.* 1999) is typically formed of friable, poorly consolidated reefal limestones, calcarenites, and oolitic limestones that are cemented by calcite (Jones 1994). This formation is divided into four unconformity bound units that represent highstands from the last four interglacial periods (Vézina 1997; Vézina *et al.* 1999). The depositional architecture of the Ironshore Formation on Grand Cayman was described by Shourie (1993). To date, dolomite has not been found in this unit. The Ironshore Formation is characterized by a well preserved diverse fauna of corals (Hunter and Jones 1988; Jones and Hunter 1990), bivalves, gastropods (Cerridwen 1989; Cerridwen and Jones 1991), and tunicate spicules (Jones 1990).

2.2 STRATIGRAPHY OF THE STUDY AREA

The Cayman, Pedro Castle, and Ironshore formations are found in natural exposures and core recovered from the study area (Figure 2.3).

The Cayman Formation underlies the entire study area and is known to be at least 170 m thick from well LV#3 recently drilled at the Lower Valley Reservoir site. This unit is also found in outcrop as a ridge that parallels the southern coastline.

The ridge, developed on the Cayman Formation, is a prominent discontinuous peripheral feature on Grand Cayman (Figure 2.4). It parallels the north, south and east coasts and attains heights > 6 m. This ridge is a subtle but important topographic feature on the otherwise low-lying island. The formation of this peripheral ridge has been attributed to erosional processes during the terminal Miocene (Jones and Hunter 1994).

Messinian (terminal Miocene) erosion resulted in the uneven removal of the upper portion of the Cayman Formation, creating the Cayman Unconformity. The topography on this Unconformity is of variable relief (Figure 2.5A). It generally rises inland from the coast and then drops to depths of up to 25 m bsl in the study area.

The Pedro Castle Formation was found in 10 of the 15 wells drilled in the study area (Figure 2.3). This unit generally fills topographic lows on the top of the Cayman Formation (Figure 2.6, 2.7) and assuming deposition was uniform across the island, the original thickness may have been greater than 44 m. This thickness estimate is based on the base of the formation at 28 m bsl in OWP#2 to exposures that are 16 m asl near Pedro Castle (Figure 2.5A, B). Today, the variable thickness of the formation (Figure 2.5B) reflects late Pliocene - early Pleistocene erosion that removed most of this formation from much of the island.

The Pedro Castle Unconformity delineates the boundary between the Pedro Castle and Ironshore formations. This unconformity represents an erosive event that took place in post-Pliocene times. This drop in sea level initiated the partial to complete removal of the

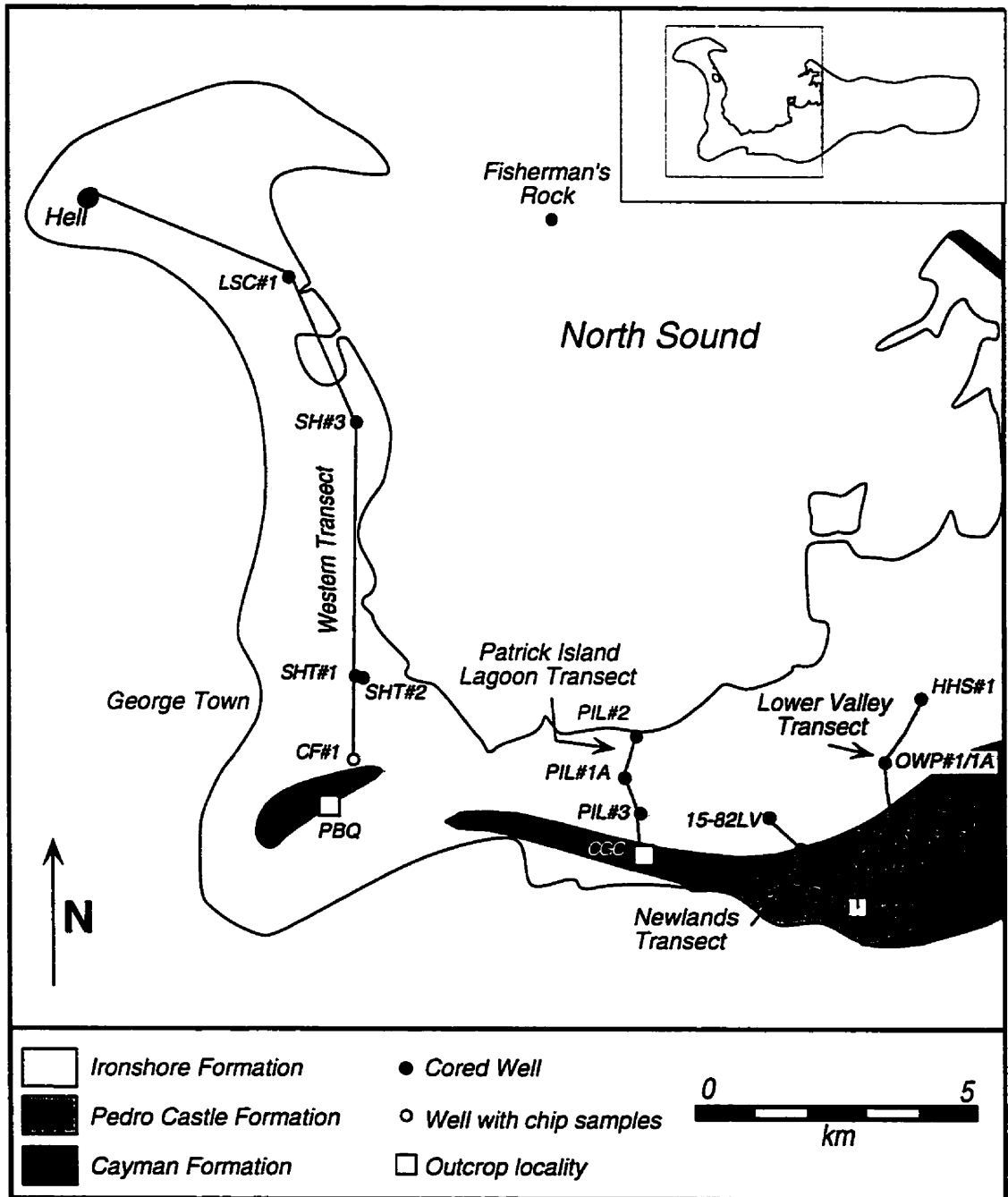


Figure 2.3. Location map showing localities discussed including the location of the Lower Valley Transect, Newlands Transect, Patrick Island Lagoon Transect, and Western Transect (modified after Jones and Hunter 1994).

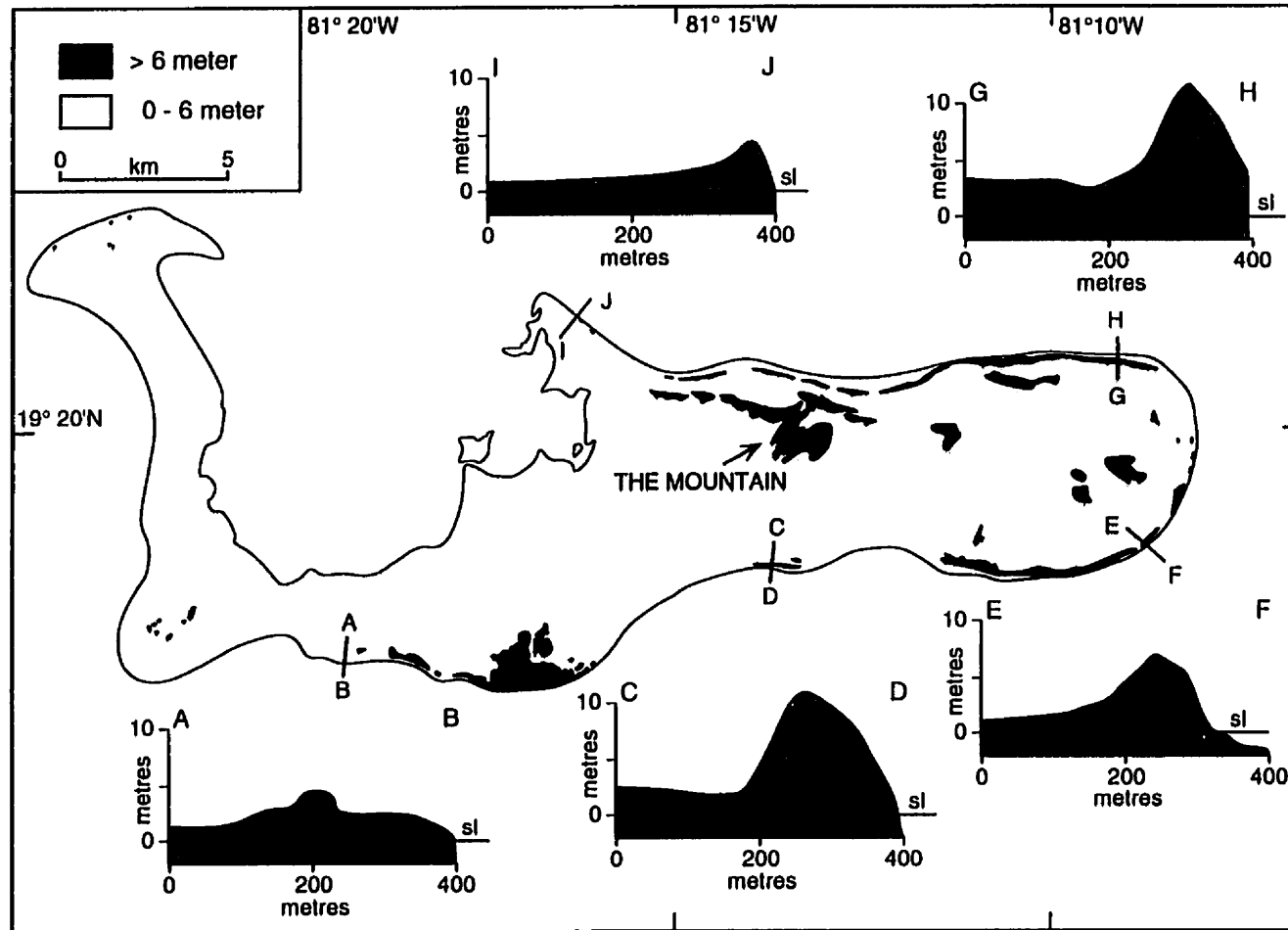


Figure 2.4. Topography of Grand Cayman. The areas with elevations of greater than 12 m are so small that they have been omitted from this map for the sake of simplicity. This map is based on the 1988 topographic maps published by the Cayman Islands Government. The topographic transects showing the peripheral rim were constructed using spot heights obtained from the 1:2500 scale topographic maps that give spot heights as determined by photogrammetry (modified after Jones and Hunter 1994).

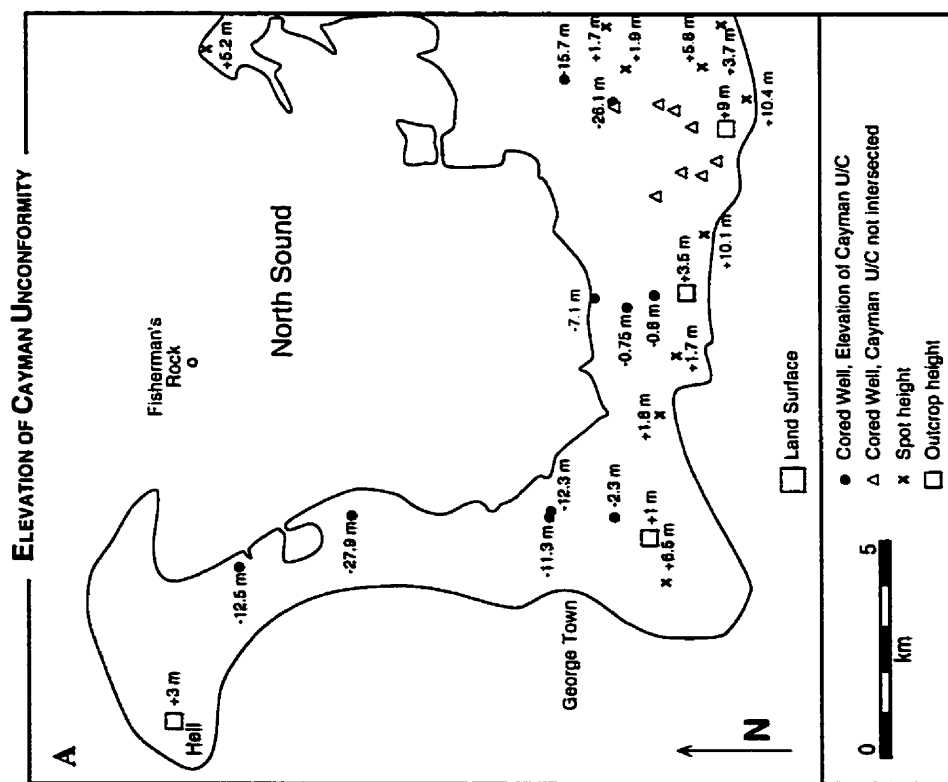
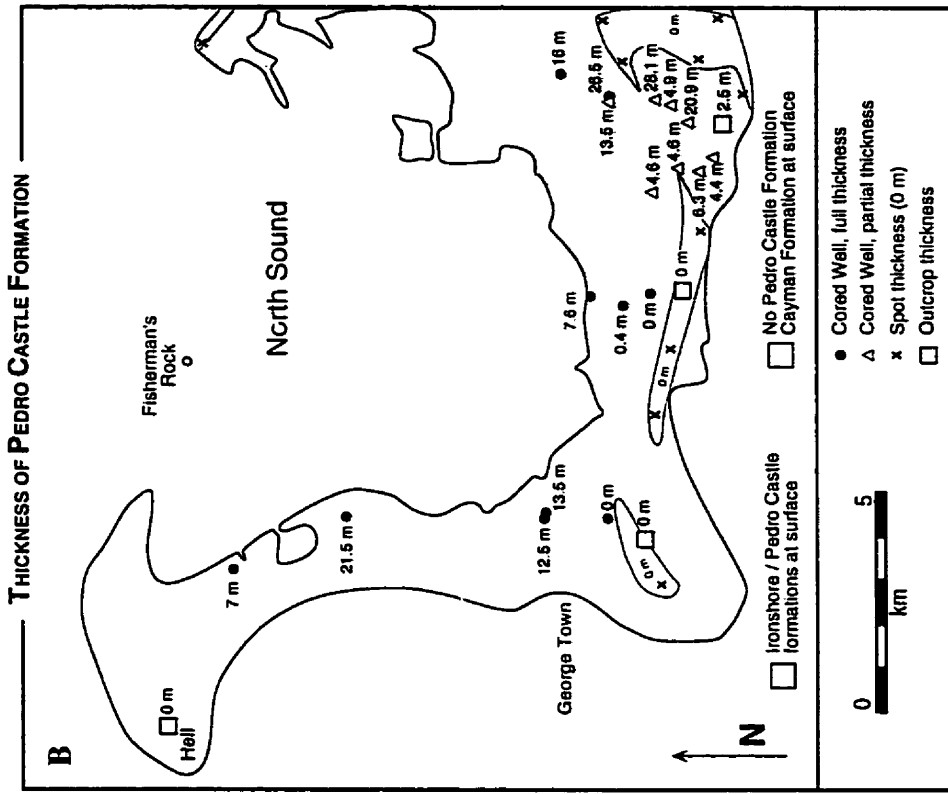


Figure 2.5. Location Maps of Grand Cayman showing well and outcrop localities. A) Elevations of Cayman Unconformity, heights are relative to present day sea level. B) Thickness of the Pedro Castle Formation at various localities.

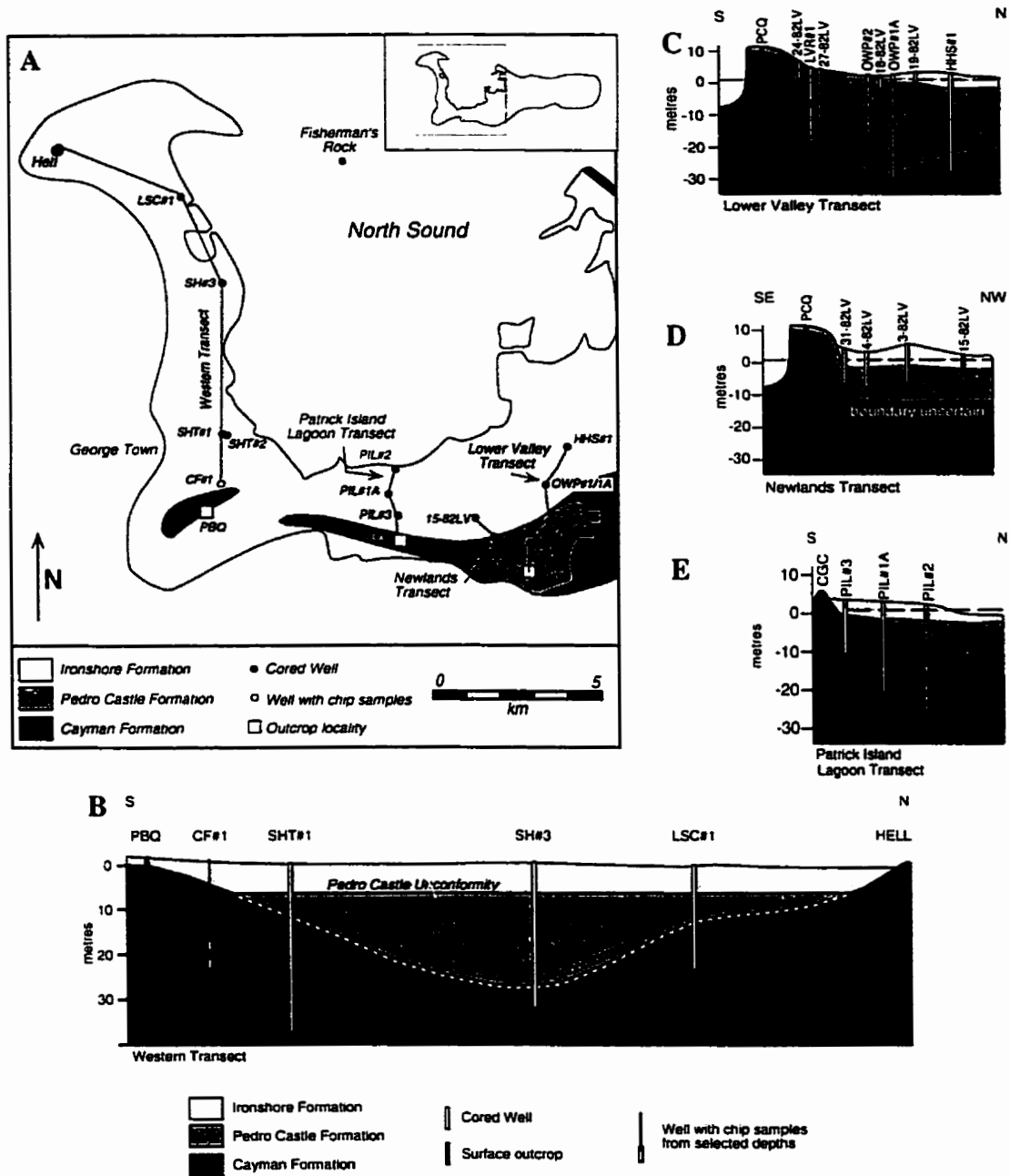


Figure 2.6. Stratigraphic relationships of the Cayman, Pedro Castle and Ironshore formations. (A) Map of the western part of Grand Cayman showing the location of the Western, Patrick Island Lagoon, Newlands and Lower Valley transects. (B) Western Transect (C) Lower Valley Transect (D) Newlands Transect (E) Patrick Island Lagoon Transect. Note in each transect the irregular topography of the Cayman Unconformity and the nearly horizontal nature of the Pedro Castle Unconformity (modified from Jones and Hunter 1994).

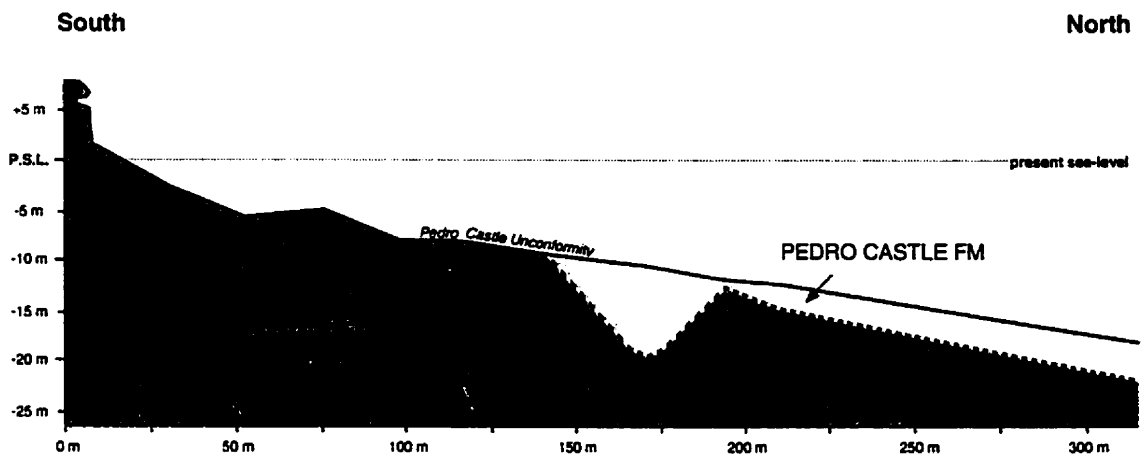
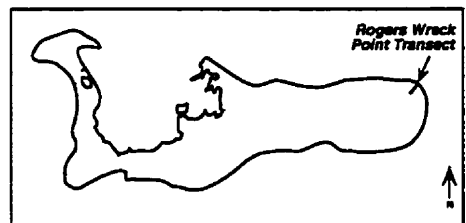


Figure 2.7. Geometry of planed Pedro Castle and Cayman Formations at Rogers Wreck Point. Cayman Unconformity (dashed line) shows a karst related topography and has been truncated by the overlying Pedro Castle Unconformity (solid line) (modified after Vézina 1997).



Pedro Castle Formation from most of Grand Cayman. This erosive event planed the top of the Pedro Castle Formation (Figure 2.6, 2.7) and in some localities (most of the eastern end of the island) removed it entirely. In areas where the Pedro Castle Formation is absent, the Pedro Castle Unconformity truncates or merges with the Cayman Unconformity. This situation is found at many localities on Grand Cayman (Figures 2.6, 2.7). At Paul Bodden's Quarry (PBQ), on the west end of the island, the Pedro Castle Unconformity merges with the Cayman Unconformity (Jones and Hunter 1994). There, the Ironshore Formation directly overlies the Cayman Formation. Nevertheless, dolostones of the Pedro Castle Formation fill worm and sponge borings developed on the top of the Cayman Formation. The presence of the Pedro Castle Formation at PBQ (at 0.5-1 m asl) suggests that the formation was removed by erosional processes before deposition of the limestones that now form the Ironshore Formation.

In the study area, the Ironshore Formation generally forms a thin veneer, ~1 m thick over most of the Tertiary strata. The formation increases in thickness towards the western arm of the island where it attains thicknesses up to 17 m (Shourie 1993). Recovery of this formation in wells is generally poor. Outcrop distribution is also minimal due to the low relief of the land in the area.

2.3 CAYMAN UNCONFORMITY

The Cayman Unconformity, between the Cayman and Pedro Castle formations, developed during the Messinian (terminal Miocene), 5 - 6.7 Ma ago (Jones and Hunter 1994). Sea Level during this time reached a temporary lowstand that caused the 'Messinian Salinity Crisis' (MSC) leading to the deposition of thick evaporite successions in the Mediterranean (Hsü *et al.* 1977). As a result of this eustatic drop in sea level many isolated oceanic islands, such as Grand Cayman, became subaerially exposed and subsequently karsted. Aharon *et al.* (1993) stated that the drop in sea level was sudden and the resulting

lowstand lasted for a period of 1.5 million years. The Cayman Unconformity therefore must have developed during this time (Jones and Hunter 1994).

The position of the Cayman Unconformity has been difficult to delineate because it is not exposed in most areas of Grand Cayman. This subtle feature (Figure 2.8A,B) is only identified in 4 outcrops on the island and is conspicuously absent from massive exposures on the east end. The absence of the unconformity in outcrops can be attributed to removal by later erosion or burial beneath the Pedro Castle and Ironshore Formations. The implementation of the drilling and coring program in 1991, provided new information regarding the position of this unconformity. Consequently, Jones and Hunter (1994) constructed a conceptual model showing the topography that developed on the Cayman Unconformity by the end of the Miocene (Figure 2.9). The topography on the unconformity is the result of progressive bedrock dissolution by meteoric and groundwater activity during the Messinian. Preferential dissolution of the carbonates on the interior of the island resulted in the formation of a prominent peripheral rim that surrounded a deep depression. This rim contained many breaches, the most significant being Pedro Gap on the south coast (Figure 2.9). This gap, located between Spotts and Pedro Castle, is approximately 1 km wide and 50 m deep. The resultant topography from the dissolution process resembled an atoll-like structure with two distinct geographical areas, the western and eastern zones. The western zone is a bowl-shaped depression that has its base at least 50m below the top of the southern peripheral rim. The more subdued eastern zone was not subject to the same degree of dissolution and lies 20-30 m above the base of this western depression (Jones *et al.* 1994b). A comparison of the model and location map shows that North Sound is located over a remnant of the depression designated as the western zone.

2.4 SYNOPSIS

The current stratigraphic framework of Grand Cayman consists of three unconformity bounded units, the Cayman, Pedro Castle, and Ironshore formations. In the

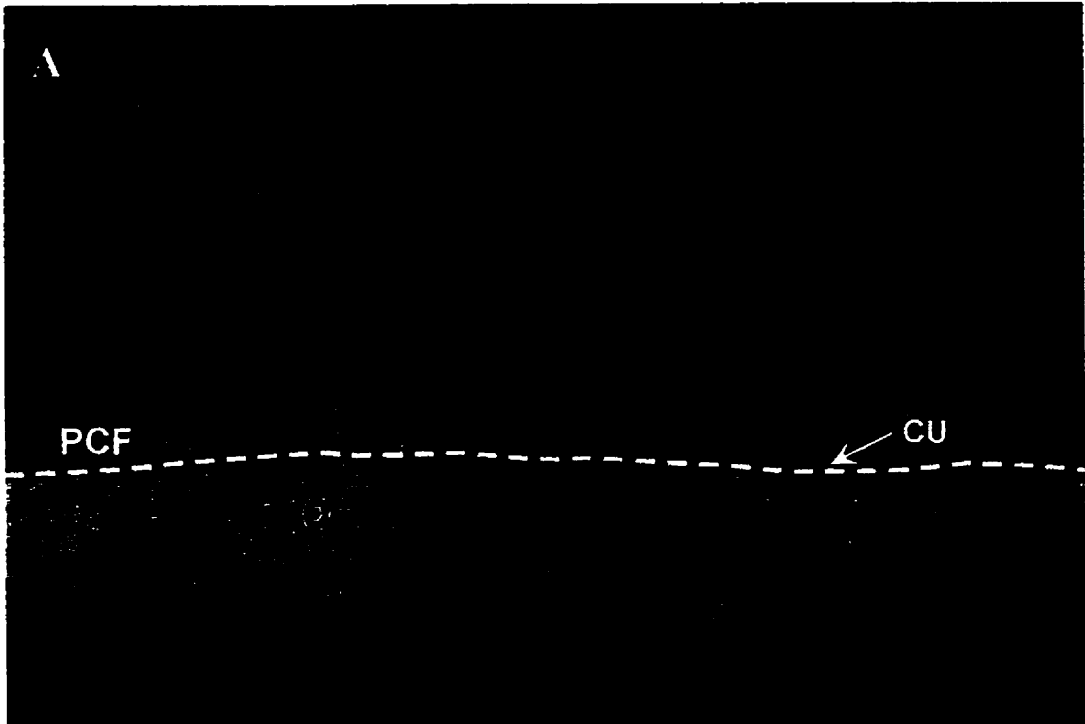


Figure 2.8. The Cayman Unconformity (A) Pedro Castle Quarry: Exposure of the Cayman Unconformity (CU) between the Cayman Formation (CF) and the Pedro Castle Formation (PCF). Quarry wall is approximately 8.5 m high. (B) Close up of the Cayman Unconformity (CU). *Cliona* (sponge) borings (Cb) are commonly found extending below the contact of the Cayman Formation (CF) and the Pedro Castle Formation (PCF). Pen is 14 cm long.

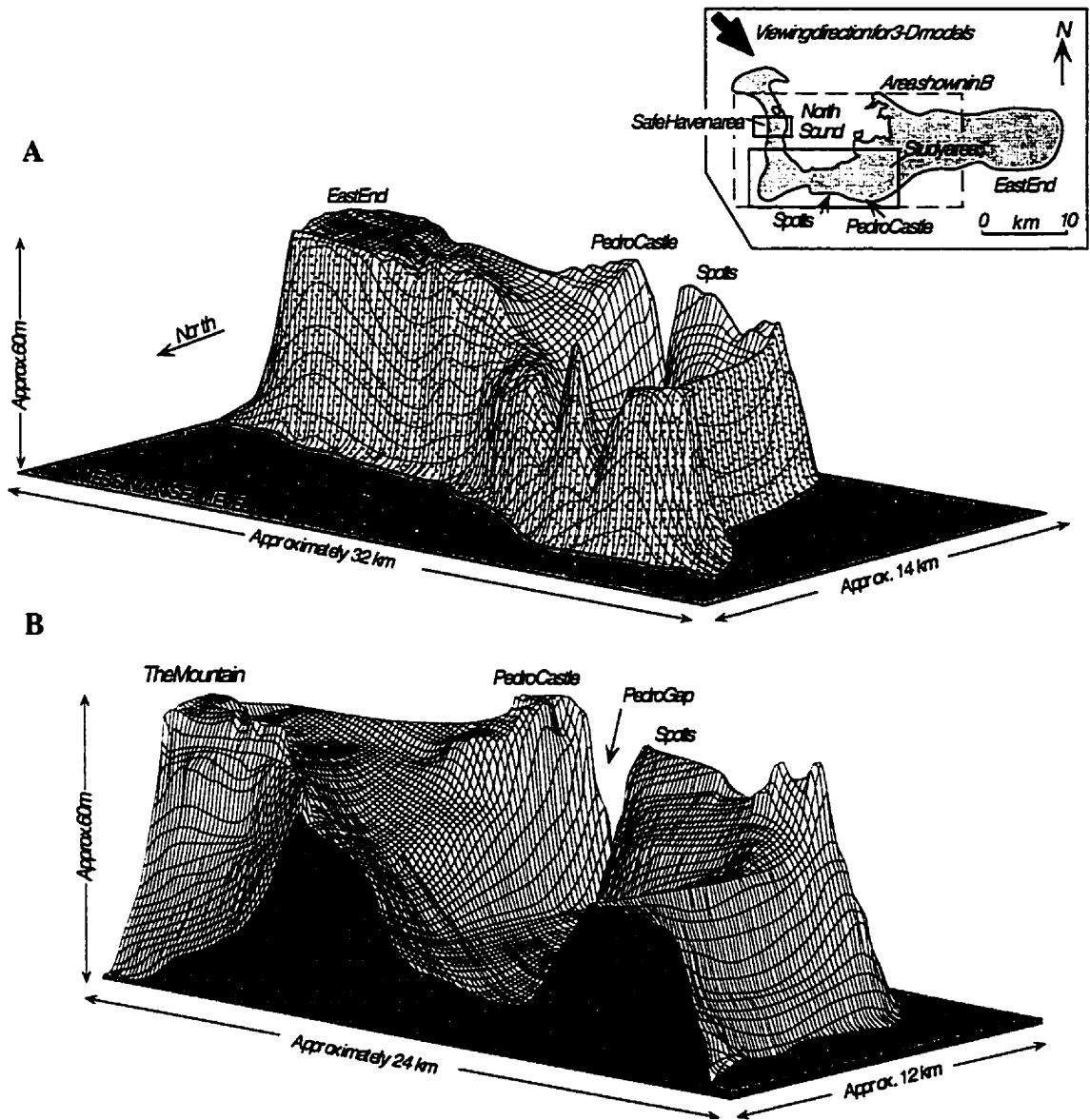


Figure 2.9. A) Conceptual model showing the topography on the Cayman unconformity. B) More detailed version of (A) showing the topography on the Cayman unconformity (modified after Jones and Hunter 1994).

study area, all three units are found in surface and subsurface exposures. During the terminal Miocene, the top of the Cayman Formation underwent extensive karsting that led to the development of the Cayman Unconformity. The resultant topography resembled an atoll-like structure with a peripheral rim enclosing a low-lying interior. The Pedro Castle Formation filled in the erosional lows that had developed on the top of the Cayman Formation. The original thickness of the Pedro Castle Formation is unknown, because later erosion planed off the top of this unit and removed much of this original thickness. The Ironshore Formation caps these units as a thin veneer over much of the area.

CHAPTER 3

SEDIMENTOLOGY AND FACIES ARCHITECTURE OF THE PEDRO CASTLE FORMATION

3.1 SEDIMENTOLOGY

3.1.1 *Definitions*

Facies in the Pedro Castle Formation have been described using a two-fold method. Megafossils (> 2 cm) and the surrounding matrix (including fossils < 2 cm) are described separately. Both are classified by Embry and Klovan's (1971) modifications to Dunham's (1962) classification scheme. This method is used because the study incorporates large exposures (meters – 10 meters) and drill core (3.5 cm diameter). When combining and interpreting data of different scales there are many inherent problems. First, facies classification will vary depending upon the scale of observation. Outcrops permit meter scale observations whereas drill core restricts observations to the 3.5 cm core diameter. As a result, what may be considered a mudstone in core may be classified as a floatstone in outcrop. This is mainly because megafossils are under-represented in core (Figure 3.1). In Pedro Castle Quarry, there are many large (>10 cm) well preserved free-living corals. In core recovered from the study area, these large corals are generally absent. This is a function of the distribution of the corals and the fact that the core will commonly not intersect them. Consequently, the interpretation of core data alone can produce a skewed view of the environment. The two fold method of classification is utilized to overcome the problems associated with incorporating outcrop and core data. Similar procedures were used by Jones and Hunter (1994b), Wignall (1995), and Montpetit (1998).

3.1.2 *Skeletal Allochems and Preservation*

The Pedro Castle Formation is composed of a variety of skeletal allochems. Free-living corals (e.g. *Trachyphyllia*) and branching corals (e.g. *Stylophora*, *Porites*) are

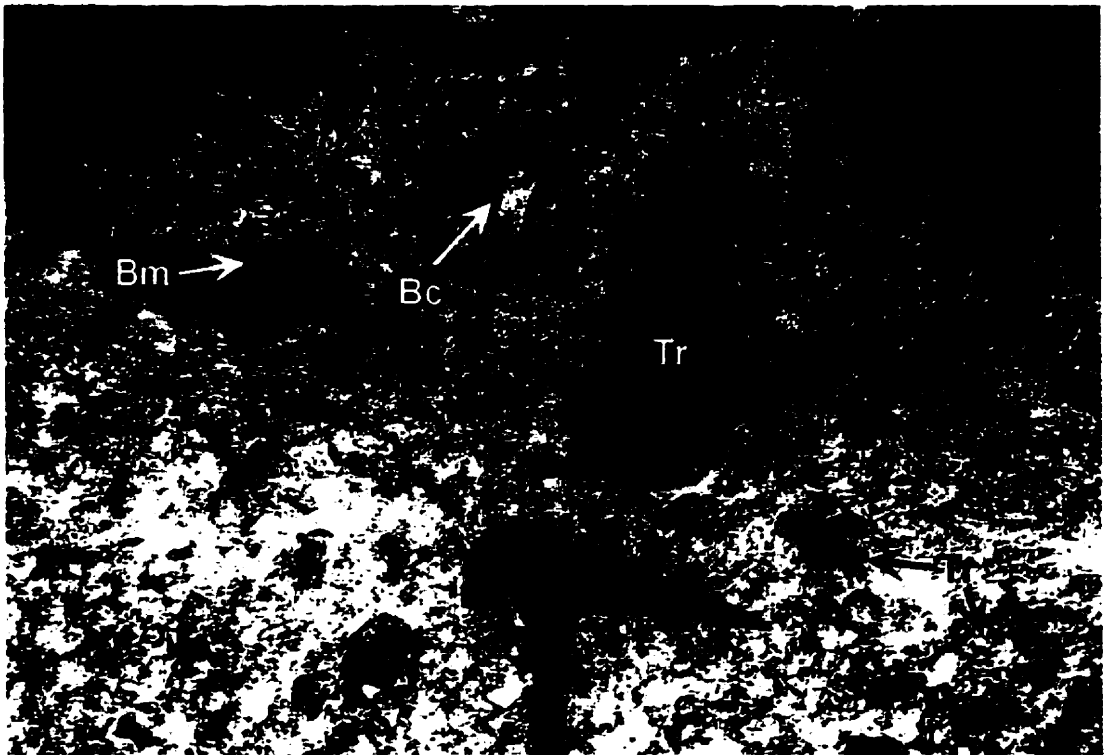


Figure 3.1. Exposure of the Pedro Castle Formation in Pedro Castle Quarry (PCQ). Note abundance of large fossils: *Trachyphyllia* molds (TR), bivalve shell mold (Bm) and bivalve shell cast (Bc). Head of Hammer is 17 cm long.

common whereas colonial corals (e.g. *Montastrea*, *Leptoseris*) are rare. Other large allochems (>2cm) include rhodoliths. The matrix includes numerous benthic forams (*Amphistegina*, *Sphaerogypsina*, miliolinids, fusilinids). *Amphistegina* is the dominant benthic species throughout the formation. *Halimeda*, bivalves, gastropods, encrusting and branching Homotrematidae, echinoderms, rhodoliths (< 2 cm), encrusting and coralline red algae, and planktonic forams (globorotalids) are found in varying numbers in the matrix.

The preservation of these allochems is variable. *Stylophora*, *Trachyphyllia*, and *Montastrea* are invariably leached and are identified by morphology and corallite molds. This leaching commonly reveals mud filled sponge borings in the coral (*Entobia* - cf. Pleydell, 1987). *Porites* are preserved as recognizable fragments, either as hollow or external mud molds. Foraminifera tests (*Amphistegina*, *Sphaerogypsina*, miliolids, fusilinids, *Homotrema*, *Sporadotrema*, globorotalids) are replaced by fabric retentive dolomite or are leached (to varying degrees) and are therefore evident only as molds. Coralline red algae are most commonly preserved by fabric retentive dolomites. Echinoderms are replaced by dolomite and are evident in thin section as uniaxial crystals that are commonly surrounded by syntaxial overgrowths. Bivalves and gastropods are commonly leached and preserved as molds that are filled with calcite cement. *Halimeda* are preserved as mud casts or hollow molds.

3.2 FACIES OF THE PEDRO CASTLE FORMATION

The Pedro Castle Formation in the study area can be divided into seven facies, all composed of dolostone (Table 3.1). Facies delineation is on the basis of biota content and texture.

FACIES	SKELETAL ALLOCHEMS	COATED GRAINS	DOMINANT ALLOCHEMS	RARE ALLOCHEMS	TEXTURE
Rhodolith Amphistegina Trachyphyllia	Trachyphyllia Stylophora Montastrea Amphistegina Halimeda Sphaerogypsina Molluscs Homotrema Sporadotrema Echinoderms	Rhodoliths large - abundant	MEGAFOSSILS Rhodoliths Trachyphyllia MATRIX Amphistegina	MEGAFOSSILS Stylophora Montastrea MATRIX Sphaerogypsina Homotrema Sporadotrema	Floatstone in a wacke- packstone matrix
Amphistegina Rhodolith	Amphistegina Halimeda Sphaerogypsina Molluscs Homotrema Sporadotrema Echinoderms	Rhodoliths small - common	MATRIX Amphistegina Rhodoliths	MATRIX Homotrema Sporadotrema	Packstones with local grainstones
Rhodolith Free Living & Branching Coral Amphistegina	Trachyphyllia Stylophora Porites Amphistegina Halimeda Sphaerogypsina Molluscs Homotrema Sporadotrema Coralline Red Algae	Rhodoliths large - abundant small - rare	MEGAFOSSILS Rhodoliths Trachyphyllia Stylophora MATRIX Amphistegina	MEGAFOSSILS Porites MATRIX Coralline Red Algae Sphaerogypsina Halimeda	Floatstone in a wackestone matrix
Rhodolith Coralline Red Algae	Porites Amphistegina Sphaerogypsina Molluscs Homotrema Coralline Red Algae	Rhodoliths small - common	MATRIX Rhodoliths Coralline Red Algae	MEGAFOSSILS Porites MATRIX Amphistegina Sphaerogypsina Molluscs Homotrema	Mudstone
Stylophora Halimeda Amphistegina	Trachyphyllia Stylophora Porites Amphistegina Halimeda Sphaerogypsina Molluscs Homotrema Sporadotrema Coralline Red Algae	Rhodoliths small - moderate	MEGAFOSSILS Stylophora MATRIX Amphistegina Halimeda	MEGAFOSSILS Porites Trachyphyllia MATRIX Molluscs Coralline Red Algae	Floatstone in a wacke- packstone matrix
Bivalve Foram Halimeda Rhodolith	Stylophora Trachyphyllia Porites Amphistegina Halimeda Sphaerogypsina Molluscs Homotrema Sporadotrema Coralline Red Algae	Rhodoliths small - abundant	MATRIX Amphistegina Sphaerogypsina Halimeda Rhodoliths	MEGAFOSSILS Stylophora Trachyphyllia Porites MATRIX Molluscs Sporadotrema	Pack- wackestones with local grainstones
Halimeda Amphistegina	Amphistegina Halimeda Molluscs	Rhodoliths small - rare	MATRIX Amphistegina Halimeda Rhodoliths	MATRIX Molluscs	Wacke- mudstone

Table 3.1. Facies in the dolostones of the Pedro Castle Formation

Rhodolith-*Amphistegina*-*Trachyphyllia* facies

This facies is best described as a *Trachyphyllia*, rhodolith floatstone with an *Amphistegina* wackestone matrix (Figure 3.2). Rhodoliths greater than 2 cm in diameter dominate this facies. The shape of these rhodoliths is dependent upon the composition of the nuclei, which varies locally and includes *Halimeda*, shell fragments, lithoclasts, and/or coral fragments. Smaller rhodoliths (1-2 cm) tend to be spherical to prolate whereas larger rhodoliths (> 2 cm) are discoidal to bladed. The white red algal layers of the rhodoliths contrast sharply with the light to medium brown mud matrix. These algal layers commonly alternate with layers of an encrusting homotremidae. There is a notable vertical decrease in the size of the rhodoliths in this facies. The coral biota is dominated by the free-living coral *Trachyphyllia*, with *Montastrea* and *Stylophora* being scattered throughout. These corals are leached and preserved as external molds. The matrix locally varies from a wackestone to a packstone. Amongst the randomly oriented smaller allochems, *Amphistegina* dominates with *Halimeda* being locally common.

***Amphistegina*-Rhodolith facies**

Numerous *Amphistegina* and spherical rhodoliths, less than 1 cm in diameter, are the most abundant allochems in this facies (Figure 3.3). *Amphistegina*, the dominant allochem, has variable preservation (intact, partial - completely leached). Allochems are randomly distributed in the packstones of this facies. Grainstones are found locally. Biota found in smaller concentrations include external molds of *Halimeda*, partially leached - replaced *Sphaerogypsina*, and leached mollusc fragments. Encrusting and branching (*Sporadotrema*) varieties of Homotrematidae are present in even lesser numbers. This facies can be distinguished from other rhodolith-bearing facies by the notable absence of larger (>2 cm in diameter) rhodoliths and coral megafossils in conjunction with an overall low abundance and diversity of biota.



Figure 3.2. Core photo of the Rhodolith *Amphistegina Trachyphyllia* Facies from OWP#1A. Rhodoliths (Rh) and *Trachyphyllia* mold (Tr) have been highlighted. Note rhodolith with colonial coral nucleus (Rcc) at top of core. Core is 3.5 cm in diameter.



Figure 3.3. Core photo of the *Amphistegina* Rhodolith Facies from OWP#2. *Amphistegina* (A) and rhodoliths (Rh) have been highlighted. Core is 3.5 cm in diameter.

Rhodolith-Free Living and Branching Coral-*Amphistegina* facies

The floatstones of this facies are characterized by a diverse faunal assemblage that includes high concentrations of corals and rhodoliths (Figure 3.4). This unit contains the free-living coral *Trachyphyllia* along with numerous branching corals (including *Stylophora* and *Porites*). Rhodoliths, greater than 2 cm in diameter, are the dominant larger allochem (> 2 cm) whereas small rhodoliths, 1-2 cm in diameter, are found in lesser numbers. All rhodoliths are spherical to prolate in shape. Their shape is a function of the nucleus morphology, which is commonly composed of coral fragments or branches. All corals in this facies are leached and preserved as external molds. The wackestone matrix contains numerous *Amphistegina*, lesser numbers of molluscs, *Homotrema*, *Sporadotrema*, *Sphaerogypsina*, and coralline red algae. Although *Halimeda* is generally rare, it is locally abundant. The bimodal size distribution of rhodoliths and the presence of branching corals distinguish this facies from the Rhodolith - *Amphistegina* - *Trachyphyllia* Facies.

Rhodolith-Coralline Red Algae facies

The mudstones of this facies contain minor concentrations of coralline red algae and scattered spherical rhodoliths that are less than 1 cm in diameter (Figure 3.5). Other allochems, including *Porites*, *Sphaerogypsina*, molluscs and encrusting *Homotrema*, are generally rare and small (less than 5 mm long). The bioclasts commonly have a thin, circumgranular algal coating. The coralline red algae generally has a crudely planar orientation. This facies is easily identified by its predominance of coralline red algae and general lack of other biota.

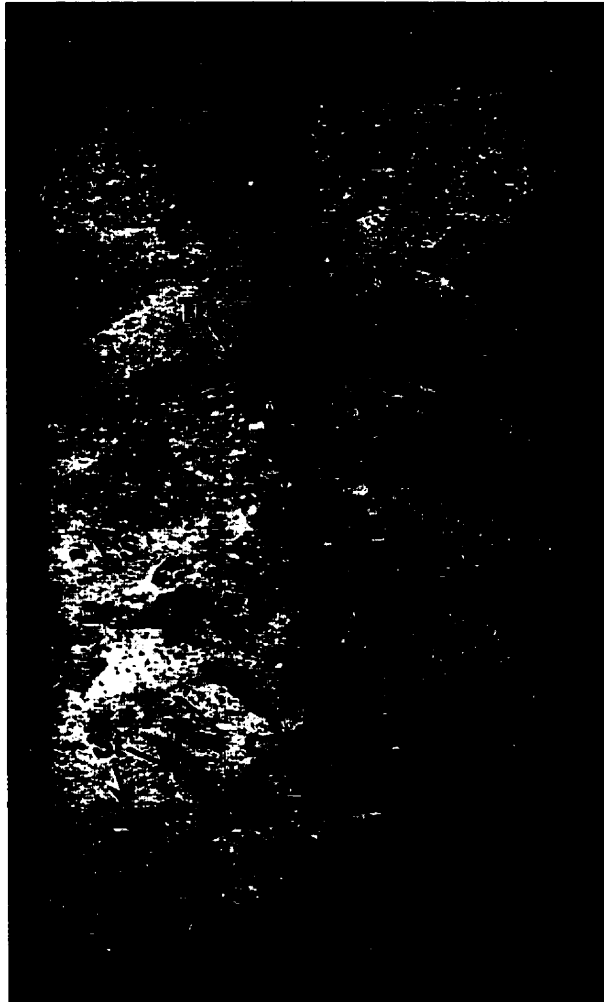


Figure 3.4. Core photo of the Rhodolith Free Living and Branching Coral *Amphistegina* Facies from OWP#1A. *Trachyphyllia* (Tr), *Stylophora* molds (St) and *Sphaerogypsina* (S) have been highlighted. Core is 3.5 cm in diameter.



Figure 3.5. Core photo of the Rhodolith Coralline Red Algae Facies from OWP#1. Rhodoliths (Rh) and Coralline Red Algae (CA) have been highlighted. Core is 3.5 cm in diameter.

***Stylophora-Amphistegina-Halimeda* facies**

Numerous *Stylophora* dominates this facies (Figure 3.6). This branching coral has a diameter of 5-10 mm and is commonly fragmented. It is invariably leached and the molds are commonly partially filled with calcite cement. Other corals found in this facies include *Porites* fragments and scattered *Trachyphyllia*. These corals have a random orientation. The matrix of this floatstone facies is a wackestone to packstone but does include local patches of grainstone. The matrix is dominated by amphistegid forams and *Halimeda* fragments. Other skeletal allochems include *Sphaerogypsina*, coralline red algae, mollusc fragments, rhodoliths (< 2 cm in diameter), encrusting and branching Homotrematidae, all in lesser numbers. Allochems in the matrix are randomly orientated.

Bivalve-Foram-Halimeda-Rhodolith facies

This facies is distinct because it contains large disarticulated bivalve shells and a diverse biota (Figure 3.7). *Amphistegina* and *Sphaerogypsina*, which are the dominant forams, are found with *Halimeda* plates and rhodoliths. The matrix varies from a wackestones to packstones, and locally grainstones. Molluscs, encrusting and branching varieties of Homotrematidae, free-living (*Trachyphyllia*) and branching corals (*Porites*, *Stylophora*) are scattered throughout the facies. Rhodoliths, less than 1 cm in diameter, are most commonly prolate in shape. This shape can be attributed to *Halimeda* being the most common nuclei. Skeletal material in the matrix is commonly leached and the matrix is light beige in color.

***Halimeda-Amphistegina* Facies**

The wackestones to mudstones of this facies contain a sparse biota (Figure 3.8). *Amphistegina*, *Halimeda*, and rhodoliths are the only identifiable allochems. Rhodoliths with unidentifiable nuclei are less than 1 cm diameter. *Amphistegina* are partially to



Figure 3.6. Core photo of the *Stylophora Halimeda Amphistegina* Facies from OWP#1. *Stylophora* molds (St), *Halimeda* molds (H) and *Amphistegina* (A) are highlighted. Core is 3.5 cm in diameter.



Figure 3.7. Core photo of the Bivalve Foram *Halimeda* Rhodolith Facies from LVR#1. Bivalve mold (Bm), *Halimeda* (H) and rhodoliths (Rh) are highlighted. Core is 3.5 cm in diameter.



Figure 3.8. Core photo of the *Halimeda Amphistegina* Facies from OWP#1A. *Halimeda* (H) and *Amphistegina* (A) have been highlighted. Core is 3.5 cm in diameter.

completely leached and *Halimeda* are invariably dissolved. Most bioclasts in this facies are less than 5 mm long. These mudstones and wackestones tend to interfinger vertically and laterally with each other.

3.3 FACIES ARCHITECTURE

Three stratigraphic cross sections, the Lower Valley, Patrick Island Lagoon, and Western transects show the variable vertical and lateral facies distribution in the Pedro Castle Formation on the western half of Grand Cayman (Figure 3.9). The Lower Valley and Patrick Island Lagoon transects embody the facies distribution in wells and outcrops examined during this study. The Western Transect integrates one core examined in this study (SHT#1) with previous work by Wignall (1995). Many of the facies defined during this study can be correlated with those defined by Wignall (1995) (Table 3.2).

The Lower Valley Transect provides the most extensive view of the vertical and lateral facies variation in the Pedro Castle Formation. This transect was examined in the most detail and therefore serves as the key in understanding the facies in this formation

3.3.1 Lower Valley Transect

The Lower Valley Transect reveals distinct north-south facies variations (Figure 3.10). The basal Rhodolith *Amphistegina Trachyphyllia* facies, which is 4.5-6 m thick, directly overlies the Cayman Unconformity (Figure 3.10). Although this unit occupies a consistent stratigraphic position above the Cayman Unconformity, it lies at varying elevations relative to sea level. This indicates that this facies is related, in some manner, to the Cayman Unconformity.

In wells LVR#1 and OWP#2, the basal Rhodolith *Amphistegina Trachyphyllia* facies is overlain by the *Amphistegina* Rhodolith facies (Figure 3.10). To the north in well OWP#1A, this facies (< 1.5 m thick) is located 3 m above the upper contact of the

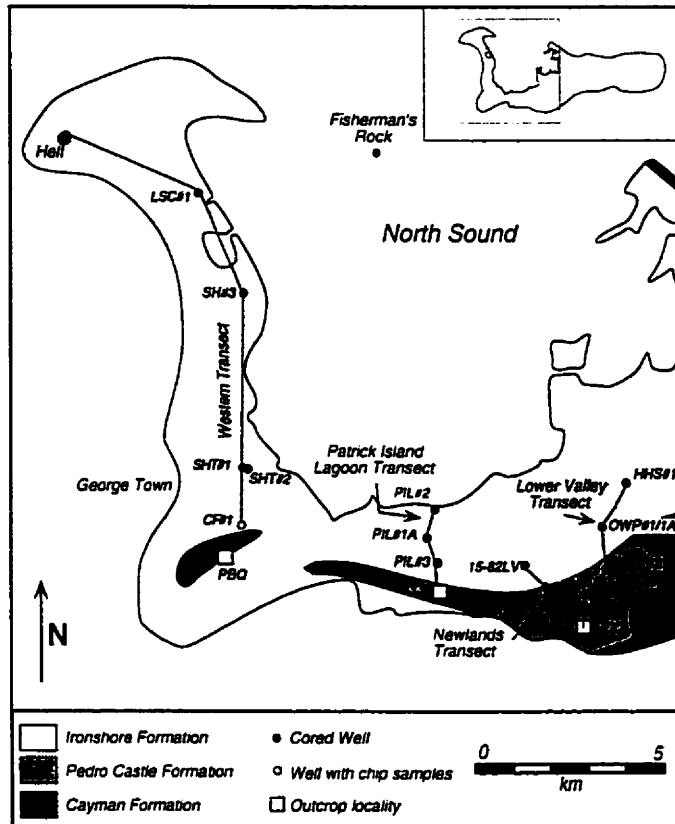


Figure 3.9. Location map showing positions of the Lower Valley, Patrick Island Lagoon and Western Transects.

FACIES	WIGNALL 1995
<i>Rhodolith-Amphistegina-Trachyphyllia</i>	Rhodolith-Foraminifera- <i>Halimeda</i>
<i>Amphistegina</i> -Rhodolith	_____
Rhodolith-Free Living & Branching Coral- <i>Amphistegina</i>	_____
Rhodolith-Coralline Red Algae	_____
<i>Stylophora-Halimeda-Amphistegina</i>	<i>Stylophora</i> -Mollusc-Foraminifera
<i>Stylophora-Halimeda-Amphistegina</i>	Mollusc- <i>Halimeda</i> -Foraminifera
Bivalve-Foram- <i>Halimeda</i> -Rhodolith	Foraminifera-Mollusc
<i>Halimeda-Amphistegina</i>	_____
_____	Solitary Coral-Foraminifera- <i>Halimeda</i>
_____	<i>Halimeda</i> -Mollusc

Table 3.2. Comparison of facies identified in this study of the Pedro Castle Formation with those delineated by Wignall (1995) in the Safe Haven area.

Rhodolith *Amphistegina Trachyphyllia* facies (Figure 3.10). This facies has not been found in the northern wells (Figure 3.9).

In LVR#1, the Bivalve Foram *Halimeda* Rhodolith facies directly overlies the *Amphistegina* Rhodolith facies (Figure 3.10). In the OWP#1A well, the Bivalve Foram *Halimeda* Rhodolith facies, which is over 7.6 m thick, contains a 0.6 m thick interval of the *Amphistegina* Rhodolith facies 3 m above the top of the Rhodolith *Amphistegina Trachyphyllia* facies. The Bivalve Foram *Halimeda* Rhodolith facies is, however, absent from well OWP#2 (Figure 3.10). This facies has not been found north of well OWP#1A.

The Rhodolith Free Living and Branching Coral *Amphistegina* facies directly overlies the Bivalve Foram *Halimeda* Rhodolith facies in well LVR#1 where it is ~ 4.5 m thick (Figure 3.10). This facies is also found locally in wells OWP#1A and OWP#1 (Figure 3.10).

Most of the upper part of the Pedro Castle Formation in the Lower Valley Transect is formed of the *Stylophora Halimeda Amphistegina* facies (Figure 3.10). This facies, however, overlies different units in each well (Figure 3.10). Locally, thin layers of the Rhodolith Free Living and Branching Coral *Amphistegina* facies, the *Halimeda Amphistegina* facies, and the Rhodolith Coralline Red Algae facies are intercalated with the *Stylophora Halimeda Amphistegina* facies. The *Halimeda Amphistegina* facies is 0.6-0.9 m thick and restricted to wells OWP#1 and OWP#1A. The Rhodolith Coralline Red Algae facies is near horizontal and restricted to wells north of OWP#2. It is less than 1.5 m thick and is found at two stratigraphic levels 1.2 m apart in well OWP#1.

3.3.2 Patrick Island Lagoon Transect

In the Patrick Island Lagoon Transect, which is 5 km west of the Lower Valley Transect, the Pedro Castle Formation is formed entirely of the Rhodolith *Amphistegina Trachyphyllia* facies (Figure 3.11). As in the Lower Valley Transect, this facies directly

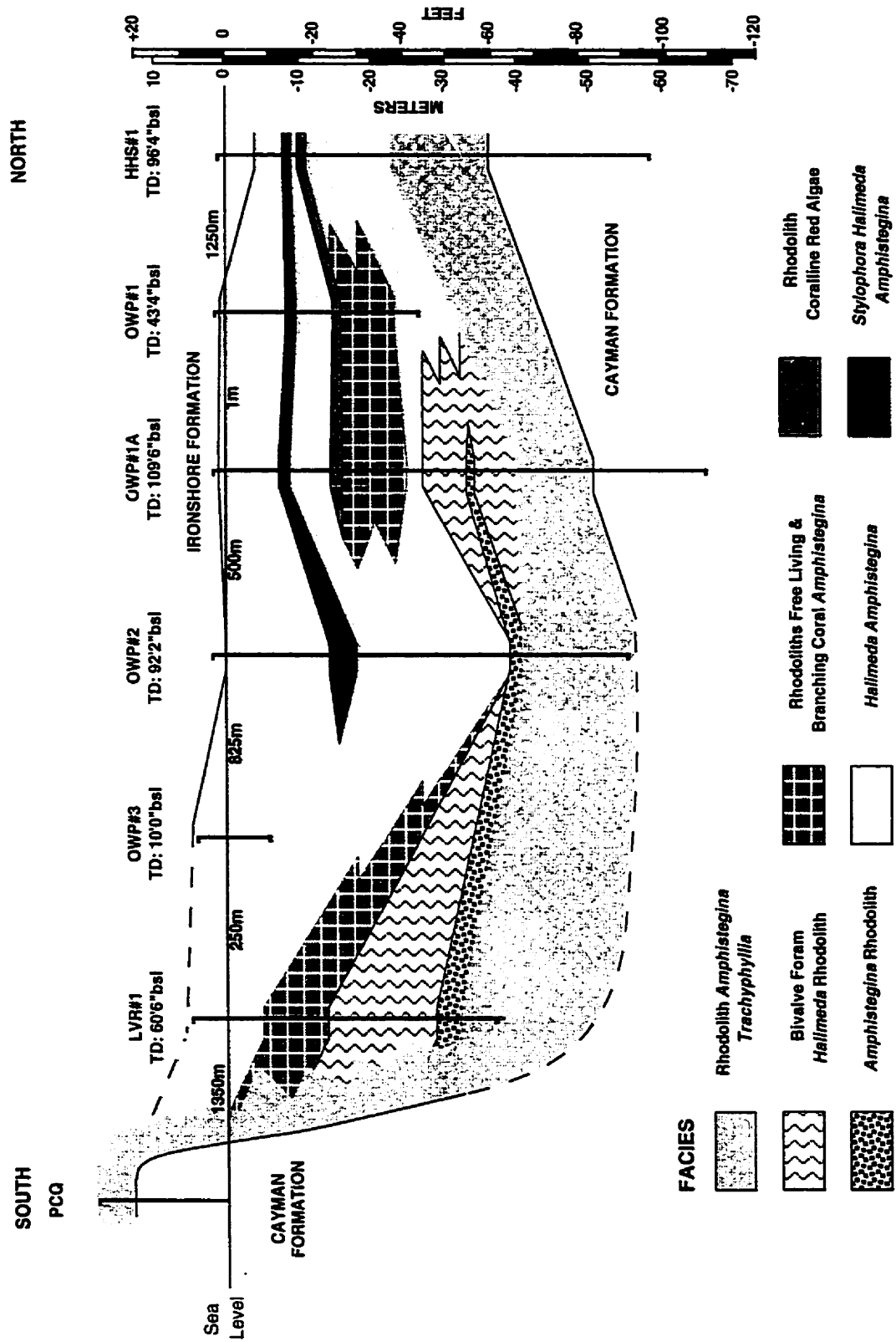


Figure 3.10. Facies distribution in the Pedro Castle Formation, Lower Valley Transect.

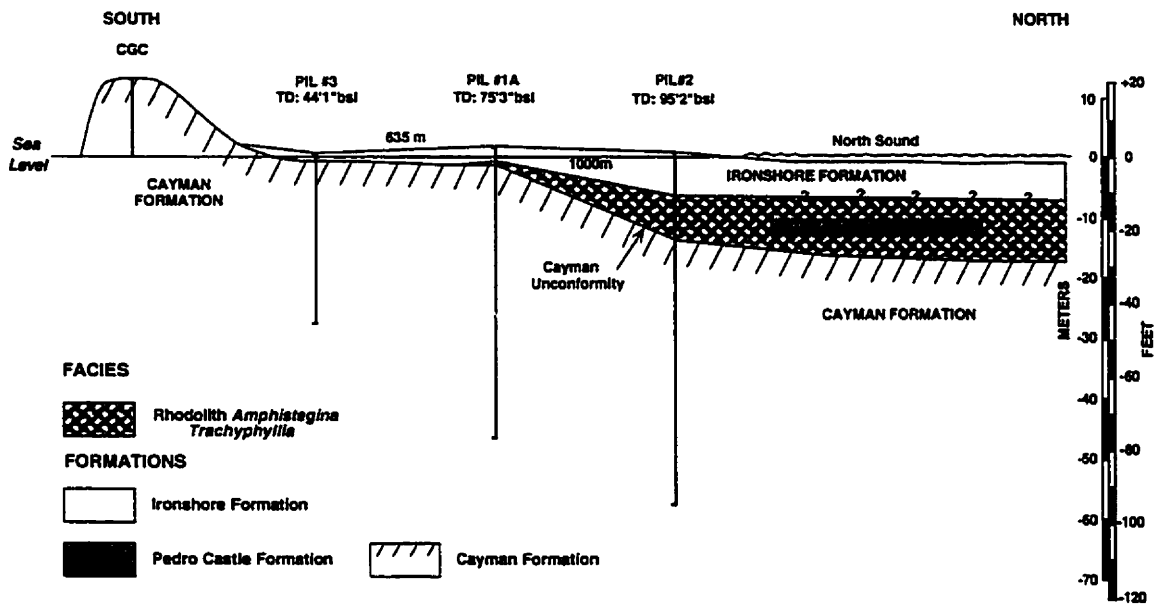


Figure 3.11. Facies distribution in the Pedro Castle Formation, Patrick Island Lagoon Transect.

overlies the Cayman Unconformity. In this transect the formation increases to ~ 3 m thick at its northern end (PIL#2).

3.3.3 Western Transect

The Western Transect, which lies ~ 5 km to the west of the Patrick Island Lagoon transect, shows distinct north south facies variations (Figure 3.12). Along this transect, the Pedro Castle Formation encompasses five facies (Figure 3.12). Three of these facies were also found in the Lower Valley.

As in other transects the Rhodolith *Amphistegina Trachyphyllia* facies forms the basal facies in this transect (Figure 3.12). It is 4.6-6.1 m thick and directly overlies the Cayman Unconformity.

In well SH#3, the Bivalve Foram *Halimeda* Rhodolith facies directly overlies the Rhodolith *Amphistegina Trachyphyllia* facies in well SH#3 (Figure 3.12). The Bivalve Foram *Halimeda* Rhodolith facies is 6.1-7.6 m thick and approximately 3 m above the base of this facies is a 0.3-0.6 m interval of the Solitary Coral Foram *Halimeda* facies.

The Bivalve Foram *Halimeda* Rhodolith facies is overlain, in well SH#3, by the *Halimeda* Mollusc and Coral Foraminifera *Halimeda* facies. These intervals do not have equivalents in the Lower Valley and appear to be restricted to the Safe Haven area. Further information regarding their distribution can be found in Wignall (1995).

The uppermost facies in well SH#3 is the *Stylophora Halimeda Amphistegina* facies which directly overlies the *Halimeda* Mollusc facies (Wignall 1995). This facies is also found at two other depths in the well with a total thickness < 3 m. It is found ~ 3 m below the top of the formation and is vertically bound on either side by the *Halimeda* Mollusc facies. It is also found as an approximately 0.6 m lens at the base of the formation, where it is bound on the upper and lower contacts by the Rhodolith *Amphistegina Trachyphyllia* facies.

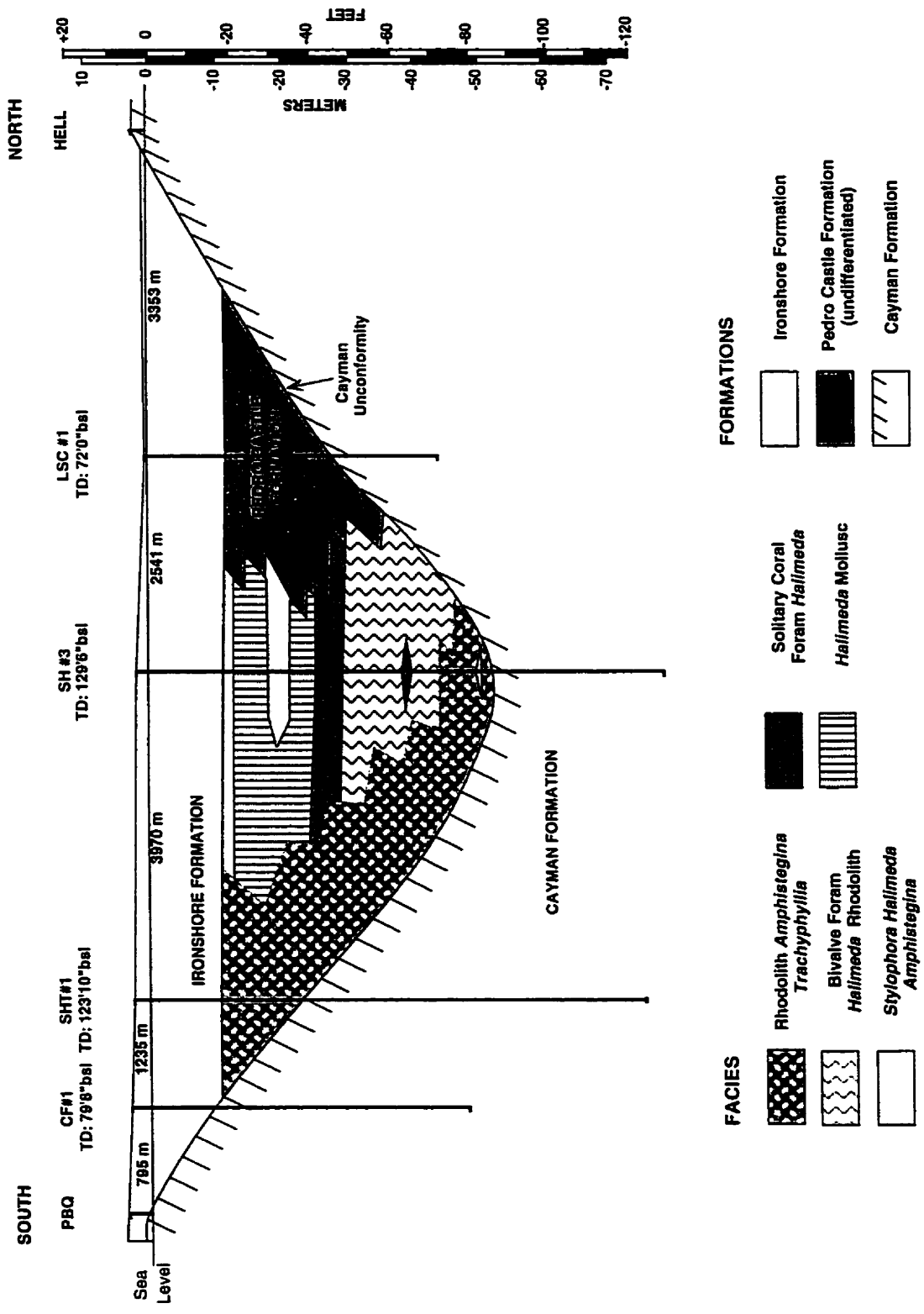


Figure 3.12. Facies distribution in the Pedro Castle Formation, Western Transect. Facies in SH#3 from Wignall (1995).

Comparison of the Lower Valley (Figure 3.10), Patrick Island Lagoon (Figure 3.11) and Western (Figure 3.12) transects show east-west variations in facies. West of the Lower Valley Transect, the Pedro Castle Formation thins and is composed strictly of the Rhodolith *Amphistegina Trachyphyllia* facies. In the Western Transect (Figure 3.12), north of well SHT#1, the formation thickens and facies diversity increases (Wignall 1995).

Generally, facies within the Pedro Castle Formation in the Lower Valley Transect, Patrick Island Lagoon Transect and Western transect are easily recognizable, uniform in thickness, laterally restricted and vertically confined.

3.4 SYNOPSIS

The dolostones of the Pedro Castle Formation are divided into seven facies. These facies are delineated on the basis of biota and texture. These units are laterally restricted, vertically confined and of uniform thickness and each contain characteristics that make them distinct and easily recognizable.

CHAPTER 4

FACIES INTERPRETATION

4.1 INTRODUCTION

Facies analysis provides insight to the paleoenvironment of a given horizon and can be a useful way of comparing local sea level history to established eustatic sea level curves. There are inherent problems when utilizing plants and animals such as rhodoliths, trachyphyllid and stylophorid corals, foraminifera, red and green algae, echinoids, gastropods and bivalves to determine paleoenvironments and paleo-sea levels. Identifying biota indicative of any one environment is difficult due to the adaptive nature of these marine plants and animals. Thus, when examining outcrop or core, the fossil assemblage and abundance, rather than presence of a particular organism are the more important indicators of paleoenvironment.

4.2 ENVIRONMENTAL IMPLICATIONS OF ALLOCHEMS

The ecology of dominant flora and fauna in a sequence can provide significant insight into the paleoenvironment of deposition. Once an understanding of the diverse habitats these organisms thrive in is achieved, an interpretation on the environment of deposition can be made.

4.2.1 *Foraminifera*

Foraminifera are unicellular or acellular organisms, 1-10 mm in size, that may secrete a mineralized chambered test. Water depth and temperature dictate the distribution of foraminifera. Water depth governs the amount of light that reaches the symbiotic algae known to be associated with many foraminiferal species as well as regulating the hydrostatic pressure on the animal. Benthonic forams live on the sea floor and are abundant constituents of lagoonal, back reef and shallow neritic settings.

Encrusting forams commonly coat sea grasses in the back reef/lagoonal setting and are characterized by a flat ventral side. Planktonic forams typically live in surface waters down to 1000m and upon death rain down to the sea floor. The tests of planktonic forams are extremely delicate and cannot withstand significant abrasion (Scoffin 1987).

Amphistegina

Amphistegina, a common Caribbean reefal taxon, is the most abundant foram found in the Pedro Castle Formation. This benthonic genus principally inhabits reef, near reef and carbonate bank environments in water depths not much greater than 100 m (Cushman 1954; Crouch and Poag 1979). *Amphistegina* has a widespread distribution and cannot be characterized as diagnostic of any one environment (Cushman 1954). These forams live primarily as epibionts on sea grasses and hard substrates, but may also live in or on soft sediments (Crouch and Poag 1979; Hottinger 1975). The presence of thinner walled tests and a generally flatter, more lenticular test shape has been attributed to lower light levels and quieter waters (Hallock 1981; Hallock *et al.* 1986).

Homotrema

Homotrema is a cranberry-red to pink sessile foraminifera that commonly encrusts the lower surfaces of shells, corals, and shoal or reef detritus (MacKenzie *et al.* 1965). This sciaphilic foram is found most abundantly in lagoons and is rarely found in deeper waters (Cushman 1954). The presence of encrusting forams, such as *Homotrema*, implies the presence of a stabilized substrate (Gill and Hubbard 1986).

Globigerinids

Globigerinids are planktonic forams that are commonly incorporated into outer shelf and slope sediments. These delicate forams are most abundant in deep-water oozes

(Cushman 1954). The presence of globigerinids in lagoonal deposits argues for a bank margin open to the sea with no reef restriction (Gill and Hubbard 1986)

4.2.2 *Calcareous Algae*

Algae are aquatic plants that manufacture their own food using photosynthetic energy and lack the vascular tissue of the higher plants (Scoffin 1987).

Green Algae (Codiaceae)

Codiaceae algae are abundant constituents of lagoonal/back reef environments. Green algae, utilizing a hardy rootsystem, colonize reefs, flat bottom plains of sand, rubble and hard substrates.

Halimeda, a common form of green algae, is a major contributor to carbonate sediments. These plants are common throughout the carbonate factory and may live down to depths of 70 m but are most productive in depths < 15 m (Hine *et al.* 1988, Liddell *et al.* 1988). Most species of *Halimeda* prefer hard substrates but may live in sandy environments (Goreau 1963).

Red Algae (Corallinaceae)

Articulate corallines (Corallinoideae) and crustose corallines (*Melobesioideae*) are common constituents in the sediments of the Pliocene on Grand Cayman. Articulated coralline red algae are randomly branched plants that typically grow in small tangled clumps. These free living algae are more delicate than the crustose varieties and generally live in shaded sheltered settings (Humann 1993). These plants prefer stabilized substrates and disintegrate into sand shaped sedimentary particles upon death (Gill and Hubbard 1986).

Crustose varieties of Corallinaceae algae are commonly preserved in rhodoliths. Factors which limit rhodolith distribution include light, salinity, turbidity, hydraulic

energy and nuclei supply. Hydraulic energy and nuclei supply are the two most important variables dictating rhodolith development in tropical lagoons (Hills 1998). To develop rhodoliths, the level of hydraulic energy must be within a specific 'window'. Too much energy cause the brittle algal thallus to be abraded and destroyed whereas, too little energy may suffocate the alga in fine sediment (Hills 1998). Rhodoliths will typically develop in areas that are protected from open water. Coralline algal growth form has been used as an indicator of environment. A laminar growth form implies the nodules were overturned frequently by waves or currents whereas, a columnar or branched form implies nodules were immobile in quiet water (Bosellini and Ginsberg 1971). The true value of growth form as indicators of environment has come under some scrutiny (Reid and McIntyre 1988). Algal nodules have been found actively growing in a variety of non muddy environments to depths of up to 90 m (Adey *et al.* 1982; Bosence 1983; Reid and McIntyre 1988; Minnery 1990; Littler *et al.* 1991).

4.2.3 Corals

Hermatypic scleratinian corals flourish in the photic zone at depths less than 100m (Wells 1967). These corals are limited by the requirements of their symbiotic zooxanthellae to warm, normally marine waters of the tropics. The clearer the water the greater the depth of vigorous coral development. The principle limiting factor being the amount of light. These corals grow most successfully and most abundantly within the zone of wave action at depths < 20 m. These filter feeding corals generally prefer a firm non muddy substrate

Stylophora

Stylophora is a zooxanthellate coral that became extinct in the Caribbean at the end of the Pliocene (Wineberg 1994). At that time, approximately 80% of coral species living in the Caribbean became extinct and more than 60% of the species now living in

the Caribbean originated (Budd *et al.* 1998). *Stylophora* is similar in appearance and habitat to *Acropora cervicornis* (Gill and Hubbard 1985). Like *Acropora cervicornis*, *Stylophora* preferred deeper, clear, calm waters out of the range of surf action and has a similar bathymetric range of 0-50 m (Hunter 1994). This highly photophilic genus was most successful in competing for light by out growing competitors.

Trachyphyllia

Trachyphyllia, is a solitary coral that became extinct in the Caribbean at the end of the Tertiary. Recent varieties of this genus flourish today in the Indo-Pacific. This genus prefers silty to sandy substrates and has a bathymetric range of 5-40 m. Its cup shape implies it grew upward in rapid response to sedimentation (Hunter 1994).

4.2.4 Bivalves and Gastropods

Bivalves, epifaunal and infaunal varieties, are found in abundance at all latitudes. The shells of these creatures are relatively resistant to fragmentation due to their dense structure. Generally, thicker shelled varieties live in areas of higher water turbulence. The disarticulated, fragmented and encrusted nature of the shells implies that the animals were epifaunal or semi -infaunal

Gastropods have a widespread distribution in fresh and salt waters of all latitudes. Marine gastropods tend to be smaller in size than their fresh water counterparts and thinner shelled varieties more common in colder deeper waters. The dense skeletal structure of gastropods generally inhibits fragmentation, though excessive wear may leave only the thicker centre of the spiral (columella).

4.2.5 *Echinoids*

Echinoids are exclusively marine and a common element of the benthic fauna in tropical and temperate seas. Upon death the organic material of the echinoderm decays and individual plates, ossicles and spines disarticulate. During burial, calcite cement precipitates as syntaxial rims in optical continuity with the single calcite crystals of the echinoid plate.

4.3 FACIES INTERPRETATION

Seven facies have been identified in the Lower Valley, Patrick Island Lagoon and Western transects. These facies can be divided into depositional packages I, II and III. Depositional package I contains the Rhodolith *Amphistegina Trachyphyllia*, Bivalve Foram *Halimeda* Rhodolith, and *Amphistegina* Rhodolith facies. Depositional package II is composed of the Rhodolith Free Living and Branching Coral *Amphistegina* facies. The *Halimeda Amphistegina*, Rhodolith Coralline Red Algae and *Stylophora Halimeda Amphistegina* facies comprise depositional package III. Each of these packages contain facies that have similar environments of deposition.

Some generalizations can be made regarding water depth, energy and circulation before a full discussion on the interpretation of the paleoenvironment is presented.

4.3.1 *Water Depth*

The presence of *Halimeda* and photophyllic corals (*Stylophora*, *Trachyphyllia*, *Porites*) throughout the Pedro Castle Formation support that deposition occurred in the photic zone. The photic zone may reach depths down to 100 m in clear waters (Tucker and Wright 1990). The carbonate factory is most prolific at depths less than 20 m and framework corals are most prolific in depths less than 15 m (Tucker and Wright 1990).

The absence of framework corals and general scarcity of biota (sequence is predominantly wackestone and floatstone) indicates that sedimentation of the Pedro Castle Formation took place in depths greater than 15 m. The dominance of muddier matrices (general lack of grainstones and rudstones) may further support deeper water conditions.

4.3.2 *Water Energy*

The sediments of the Pedro Castle Formation indicate that water energy conditions varied throughout deposition. Higher energy conditions are suggested by the presence of large rhodoliths and fragmented branching and free living corals. The associated high energy matrices are dominated by packstones, with local grainstones. Wackestone matrices associated with baffling corals may also indicate higher energy. Quieter energy conditions are associated with a low diversity and abundance of biota. Matrices attributed to lower energy conditions are composed of wackestones and mudstones. Generally, the three packages in the study area exhibit higher energy conditions at the base of the Pedro Castle Formation followed by sequentially quieter conditions towards the top.

4.3.3 *Water Circulation*

Water circulation in a lagoon is typically restricted due to the presence of a barrier, commonly a reef. The ridge present on the erosional Cayman Unconformity would have provided a substantial barrier during the early phases of deposition of the Pedro Castle Formation. The ridge would have restricted water circulation over much of the island and created a quiet interior atoll-like lagoon. As deposition continued and water depths increased the effect of the ridge would have been lessened as later deposition was controlled by water depth. The presence of breaches in the ridge, such as

the Pedro Gap in the study area, would have increased circulation and allowed for the development of a more open marine biotic assemblage.

4.3.4 Depositional Packages

Depositional Package I

Depositional Package I (Figure 4.1) is composed of the basal Rhodolith *Amphistegina Trachyphyllia* facies which is found throughout the study area. Also included in this package are the Bivalve Foram *Halimeda* Rhodolith, and *Amphistegina* Rhodolith facies.

Each of the facies in this initial sequence imply higher energy conditions than seen elsewhere in the formation. The matrices found in the three facies of this sequence are wackestones to packstones with local grainstones. The wackestones are still higher energy deposits as they are associated with baffling corals. These grain supported matrices suggest a turbid, higher energy environment that did not permit fines to settle out. The biotas present in the 3 facies further support a higher energy depositional regime. The dominance of rhodoliths throughout this initial sequence places deposition within the range of waves and currents. Wave and current action would have frequently overturned the rhodoliths, giving the algae the laminar growth form that evenly coated the nodules. The basal Rhodolith *Amphistegina Trachyphyllia* facies is representative of the initial transgression. The ubiquitous nature of this facies can be attributed to the initial colonization of the Cayman Unconformity as Pliocene waters flooded the area. Rhodoliths, *Amphistegina* and *Trachyphyllia* prefer non muddy environments and the solidified Cayman Unconformity would have provided an ideal substrate for their development. Water depth increased throughout deposition of this sequence. This is evidenced by the absence of the coral *Trachyphyllia* in the upper 2 facies of this sequence. Sea level was rising too rapidly to maintain continued growth of this coral.

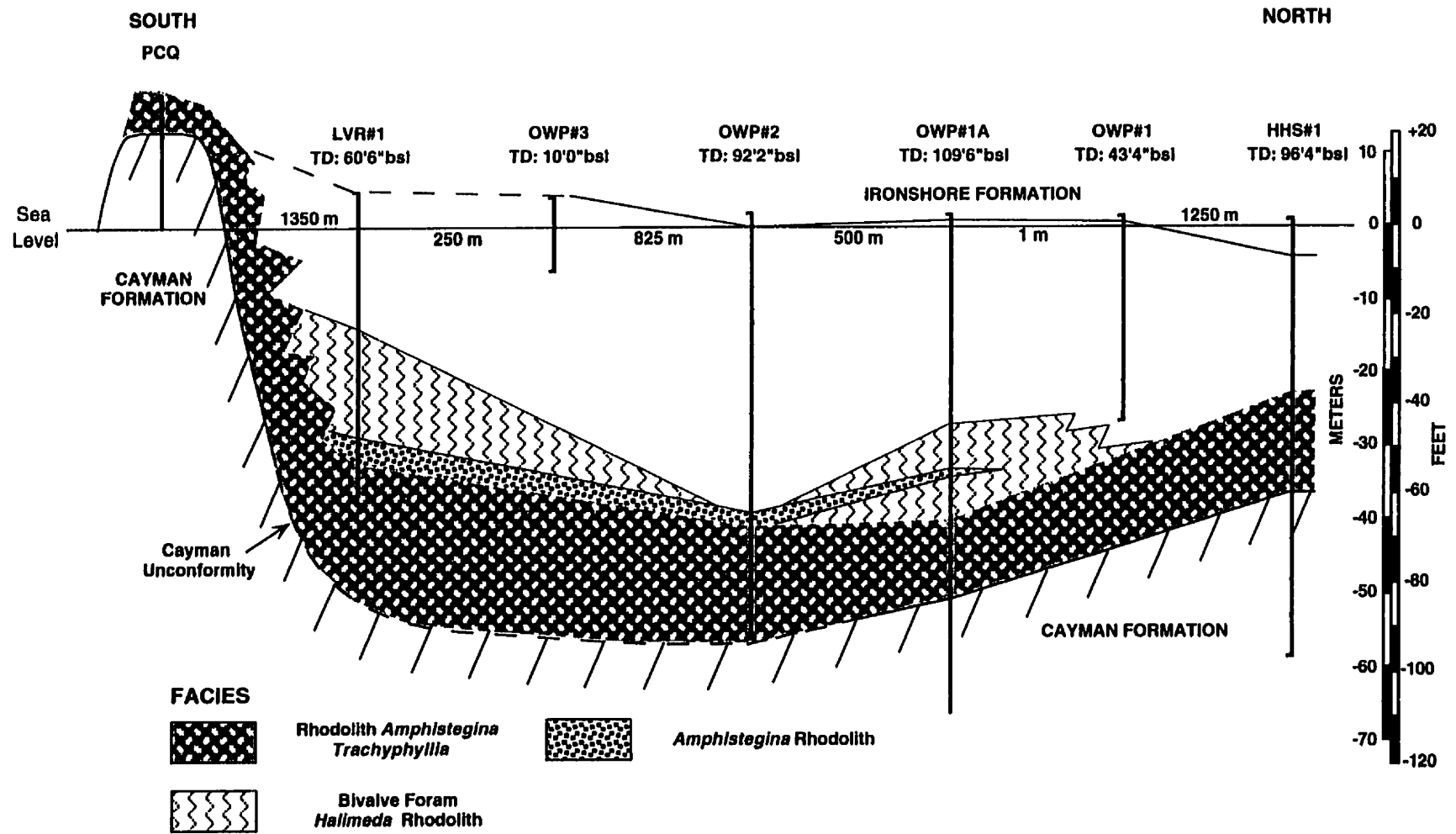


Figure 4.1. Depositional Package I

The following *Amphistegina* Rhodolith and Bivalve Foram *Halimeda* Rhodolith facies represent the initial stages of the quiescent Pliocene lagoon. Forams and *Halimeda* become the dominant organisms and by the end of this package *Halimeda* thickets dominated the floor of the lagoon with benthic forams and bivalves being other dominant fauna.

The lack of major reef development, the changes in biotic assemblages throughout deposition and the dominance of packstone to grainstone matrices suggests these rocks were deposited in a rapidly deepening lagoon. The peripheral ridge would have been an active barrier during deposition of this initial sequence. This barrier created an interior lagoon that achieved a maximum water depth of 15-20 m.

Depositional Package II

Depositional Packages II and III were deposited penecontemporaneously. The relationship between these two packages is best described after the environmental interpretation is presented.

Depositional Package II (Figure 4.2) is composed of the Rhodolith Free Living and Branching Coral *Amphistegina* facies. The transition from Depositional Package I to II is marked by the stabilization of sea level. Free living (*Trachyphyllia*) and branching corals (*Stylophora*) flourished in high numbers indicating sea level was no longer rising at a fast pace. Rhodoliths were still dominant and are of similar morphology to those present in Depositional Package I. The overall high diversity and abundance of biota in this sequence indicate the Pliocene lagoon had unrestricted circulation. The matrix in this sequence is a wackestone. The association of this matrix with baffling corals implies it is a relatively higher energy deposit. In general the Pedro Castle lagoon had a firm non-

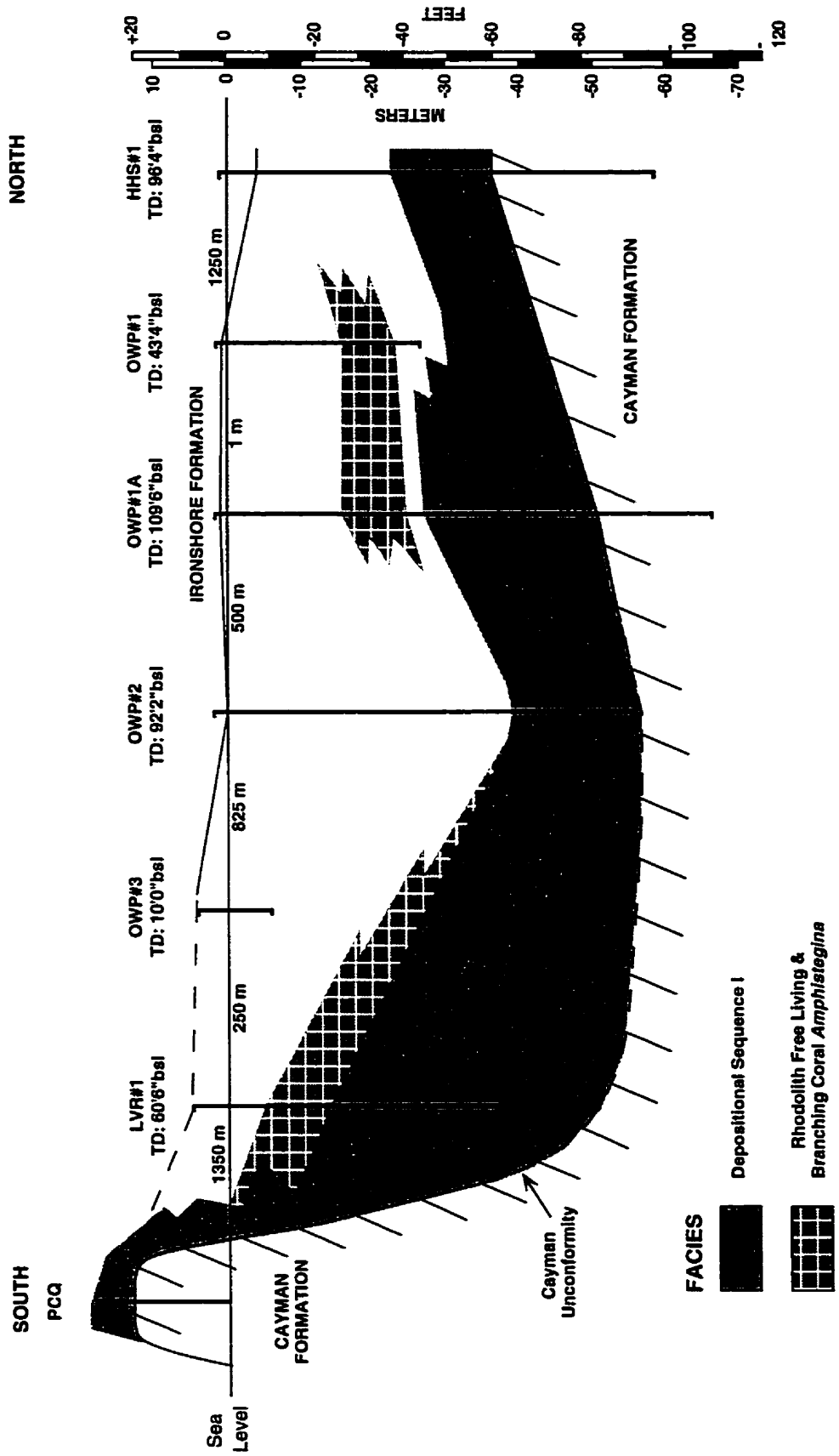


Figure 4.2. Depositional Package II

muddy sea floor, was turbulent, rich with nutrients and stable enough to support the active development of corals.

This sequence is a collection of healthy, diverse patch reefs growing behind the barrier ridge. The presence of the Pedro gap may have kept conditions open km's behind the ridge as sea level slowly rose.

Depositional Package III

Depositional Package III (Figure 4.3) is composed of the *Stylophora Halimeda Amphistegina*, *Halimeda Amphistegina* and Rhodolith Coralline Red Algae facies. This sequence is characterized by an increase in water depth with localized restriction as sea level rose.

The *Stylophora Halimeda Amphistegina* facies was deposited throughout the duration of Depositional Sequence III and is coeval with the other two facies. The transition from Depositional Sequences I and II is marked by the disappearance of rhodoliths and *Trachyphyllia*. *Stylophora*, a branching coral most prolific in deeper waters, becomes the dominant animal in the study area. The abundance of this coral indicates the Pedro Castle lagoon was deep, calm and out of the range of surf action. At the end of Depositional Sequence III this facies was deposited over most of the study area.

The *Halimeda Amphistegina* and Rhodolith Coralline Red Algae facies develop in the central parts of the lagoon as water levels continue to rise. As circulation restriction develops, there is a decrease in the diversity, abundance and size of allochems. The matrix reflects these deepening conditions as it is composed of wackestones to mudstones. Megafossils are conspicuously absent as these two facies are completely composed of matrix allochems. These two facies represent localized restriction in water circulation in an ever deepening lagoon.

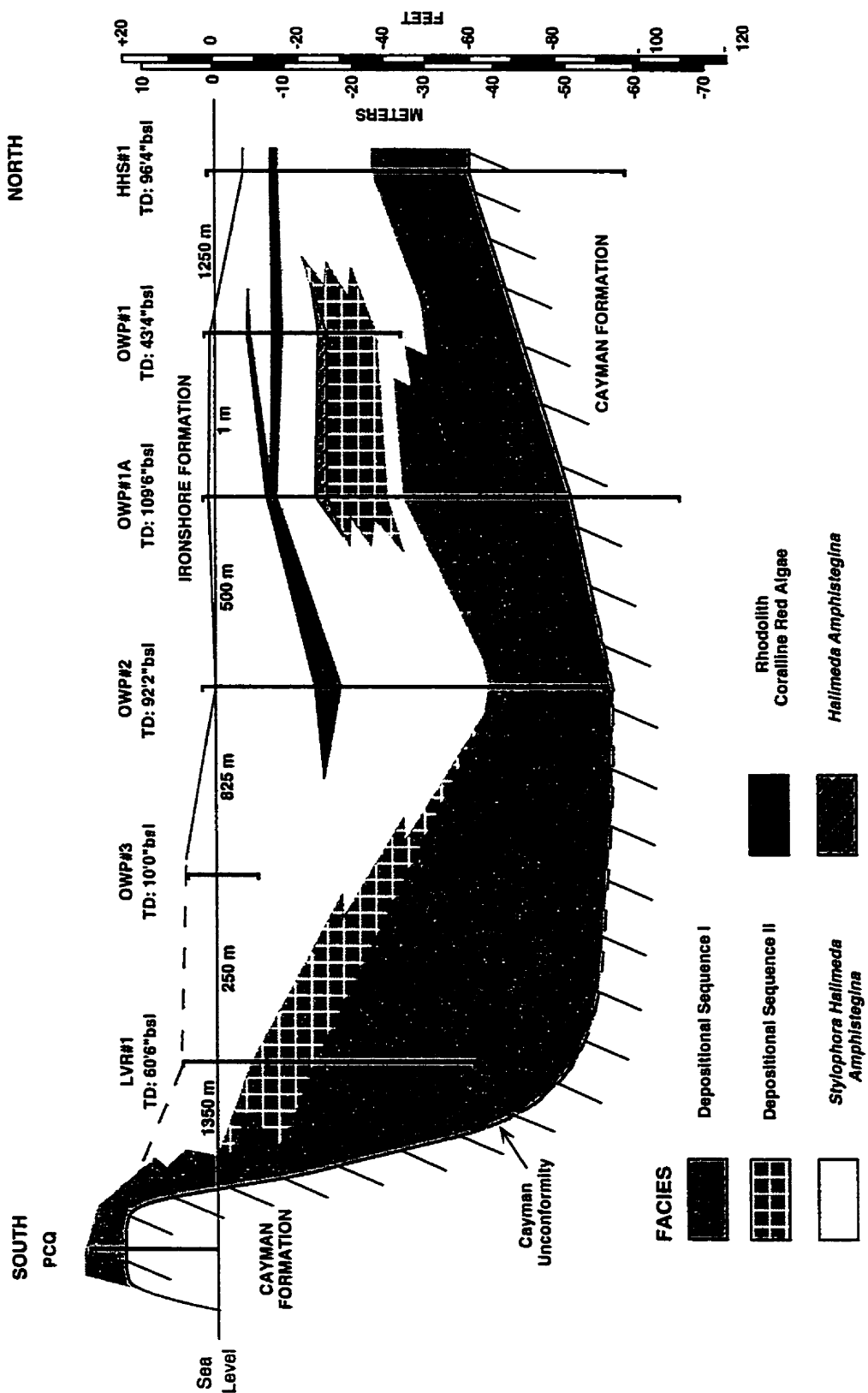


Figure 4.3. Depositional Package III

By the end of the Pliocene the Pedro Castle lagoon had a healthy diverse deeper water assemblage of corals, forams and green algae. Bathymetry was the most important factor controlling faunal distribution as the Cayman Ridge was submerged and no longer acting as an energy baffle. This sequence represents the deepest waters seen in the study area. Water depth for this final sequence was on the order of 25-35m but possibly deeper.

Depositional Sequences II and III represent changing conditions within the Pedro Castle lagoon. The patch reefs of Depositional Sequence II thrive when lagoonal conditions are at a moderate depth and unrestricted. Once sea level started to rise a deeper water assemblage became dominant. During the deposition of the final sequence parts of the lagoon became restricted and a more stressed assemblage is present.

4.4 SYNOPSIS

The 7 facies identified in the Pedro Castle Formation can be divided into 3 depositional packages. These packages were deposited in waters deeper than 15 m in an atoll-like lagoon. The assemblages present record a transgressive event during the Pliocene. During early deposition the peripheral ridge was an important energy baffle whereas in later deposition bathymetry was the most important control.

CHAPTER 5

SEA LEVELS

5.1 INTRODUCTION

The depositional and diagenetic history of Grand Cayman has been dictated by global changes in sea level. Understanding the cause of changes in eustatic sea level is critical to understanding the geologic history of Grand Cayman.

5.2 SEA LEVEL HISTORY

Changes in eustatic sea level are well documented for the Phanerozoic (Vail *et al.* 1977; Hallam 1984; Haq *et al.* 1987). 'Vail Curves' show global changes of sea level on different orders of cyclicity. First order cycles are global changes that occur on a 200-400 Ma timescale whereas; second order cycles occur every 10-100 Ma. Third order cycles occur every 1-10 Ma and have the best resolution for eustatic sea level changes during the Tertiary (Figure 5.1)

Due to variation in the dating of events, the Tertiary timescale of Hayes and Frakes (1973) is utilized here. It should be noted that variation in dating by different authors is a controversy over time scale definitions rather than the exact timing of events.

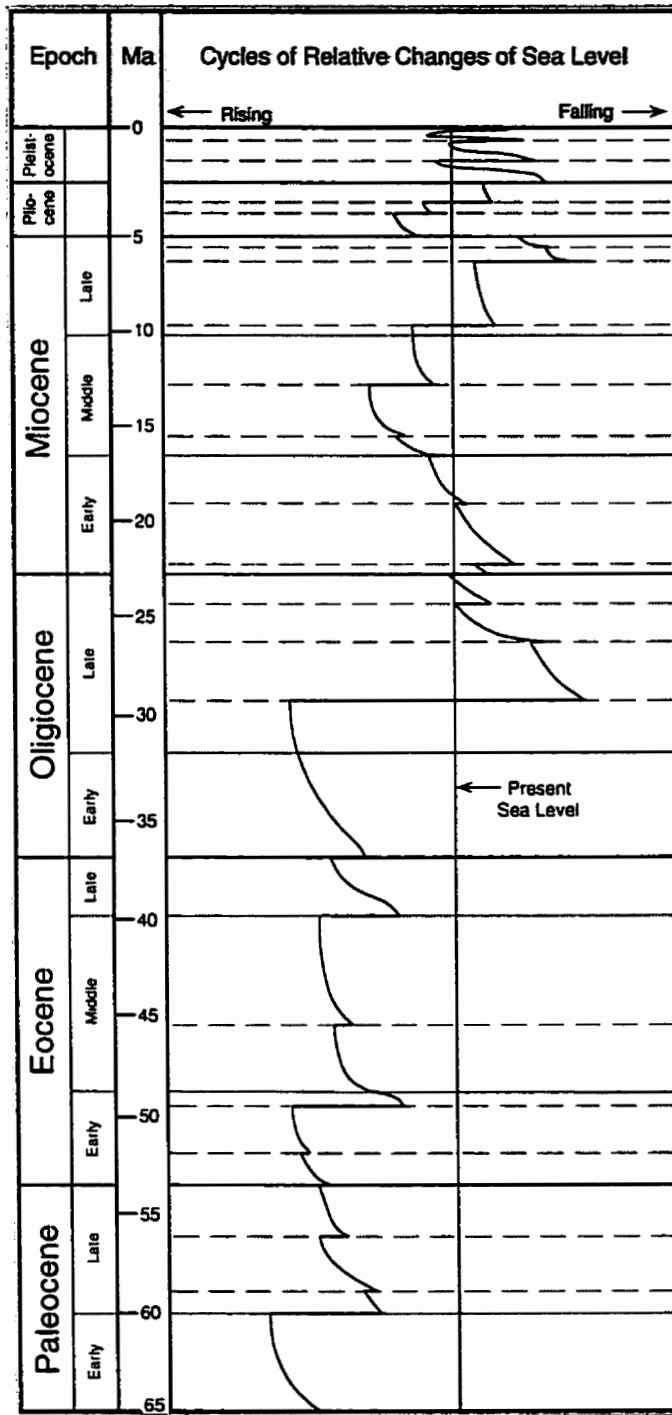


Figure 5.1. Third order sea level curves for the Tertiary (Vail *et al.* 1977)

5.2.1 Paleocene to Oligocene Sea Levels (65 - 25 Ma)

Plate tectonic activity in the Paleocene changed ocean circulation patterns permitting antarctic glaciation in the Late Oligocene. The initial rifting of the Australian-Antarctic continent in the Paleocene sent Australia drifting northward at approximately 5 cm/yr. (Kennett *et al.* 1975). This continental divergence was the first step in developing circumpolar circulation around Antarctica. Once established it would change the climate to one that would be conducive to continent wide glaciation.

By the Eocene, glaciation had commenced on Antarctica (Margolis and Kennett 1971; Geitzenauer *et al.* 1968) but was limited by the temperate climate that still persisted on the continent (Hayes and Frakes 1973). Australia was imposing a shallow water barrier to circumpolar circulation preventing the full development of a cool Antarctic climate. Australia's continual northward drift finally resulted in the configuration of circumpolar circulation and the initiation of major Antarctic glaciation in the Early Oligocene (Kennett *et al.* 1972; Hayes and Frakes 1973). As ice built up on Antarctica, a gradual drop in sea level was felt globally. The magnitude of this Middle Oligocene drop in sea level has been estimated at up to 100 m (Hayes and Frakes 1973). As sea level continued to drop, many isolated oceanic islands, including Grand Cayman, became subaerially exposed. The unconformity on the top of the Brac Formation would have developed at this time.

5.2.2 Miocene Sea Levels (25 - 5 Ma)

Slowly advancing Antarctic ice continued to lower sea level during the Early and Middle Miocene (Kemp and Hayes 1975). The culmination of this cooling episode in the Late Miocene resulted in the abrupt, dramatic expansion of continental ice on Antarctica (Hodell and Kennett 1986). Mercer and Sutter (1982) stated that Antarctic glaciation alone was insufficient to appreciably lower sea level. They proposed that Northern Hemisphere glaciation, chiefly in North America away from the Atlantic coast, played an instrumental role in the eustatic lowering of sea level during the terminal Miocene (Messinian). The uplift of the Himalayan-Tibetan Plateau may have been the driving force behind this dramatic increase in glaciation (Fort 1996; Filippelli 1997). The uplift of the Himalayan Range and adjacent Tibetan Plateau (~7 Ma) would have changed atmospheric circulation and increased the drawdown of atmospheric CO₂ resulting in global cooling and increased continental ice buildup.

The magnitude of the Messinian eustatic drop in sea level has been the subject of much debate with estimates ranging from 30 m (Aharon *et al.* 1993), 40 m (Berggren and Haq 1976; McKenzie *et al.* 1984), 40-60 m (Hodell and Kennett 1986), 40-70 m (Kennett 1967), 50-70 m (Adams *et al.* 1977), 80 m (Cita and Ryan 1979), 70-100 m (Loutit and Keigwin 1982), 75-125 m (Lincoln and Schlanger 1987) to 180 m (Pigram *et al.* 1992) below present sea level. These lowstand positions were derived from areas outside of the Caribbean. Jones and Hunter (1994) estimated that the Messinian drop in sea level to be

at least 41 m below present sea level, based on evidence from Grand Cayman. This Messinian lowstand was a contributing factor in the well documented desiccation of the Mediterranean, which resulted in the deposition of a thick evaporite succession (Hsü *et al.* 1973; Adams *et al.* 1977; Hsü *et al.* 1977). This lowstand is recorded on the eustatic sea level curve (Figure 4.1) of Vail *et al.* (1977) and is thought to have lasted for approximately 1 Ma (Hayes and Frakes 1973; Berggren and Haq 1976; McKenzie *et al.* 1984; Aharon *et al.* 1993). The Cayman Unconformity developed during this time (Jones and Hunter 1994).

5.2.3 Pliocene Sea Levels (5 – 3.0 Ma)

The Miocene-Pliocene boundary, approximately 5.0 Ma, marked the end of glacial advancement in the Antarctic and the commencement of an interglacial period. Melting of the Antarctic ice sheet and the associated rise in sea level flooded the Mediterranean basin and ended the Messinian Salinity Crisis (Hsü *et al.* 1973). The onset of these events marked the beginning of a period of global warming.

Pliocene warming is characterized by increased ocean temperatures, in higher latitudes, by 3-5°C above present conditions (Hecht 1990; Dowsett *et al.* 1992; Cronin and Dowsett 1993). The cause of the warmer climates and the extent of Antarctic ice retreat in the Early Pliocene (5.0-3.5 Ma) has been the subject of much debate (Pickard *et al.* 1988; Dowsett *et al.* 1992; Harwood and Webb 1998; Stroeve *et al.* 1998). Many

mechanisms have been discussed as possible causes of Pliocene warming. Hecht (1990) proposed that 'Greenhouse' gases (e.g. CO₂) were at high levels in the atmosphere and were the culprit of the elevated global temperatures. The causes of those elevated CO₂ levels, however, is still in question. McKenzie *et al.* (1984) suggested that the cessation of the salinity crisis in the Mediterranean may also have triggered climatic changes but the reason behind that is also in question. Cronin and Dowsett (1993) suggested that changes in oceanic circulation patterns associated with the emergence of the Isthmus of Panama was the cause of ice retreat in Antarctica. The emergence of this land barrier would have first restricted deep circulation during the latest Miocene earliest Pliocene and its final emergence ~3 Ma would have created the final barrier to surface circulation (Dowsett *et al.* 1992). This land barrier would have blocked the free flow of water between the equatorial Pacific and Atlantic oceans, thus intensifying the gulf stream and diverting warm waters into higher northern latitudes (Hecht 1990; Coates 1992; Dowsett *et al.* 1992; Cronin and Dowsett 1993). Similarly, warm water could also be transmitted to high southern latitudes where they would upwell around Antarctica (Broecker and Denton 1989). Warmer temperatures at higher latitudes would have altered climatic conditions and initiated the retreat of ice in the Antarctic (McKenzie *et al.* 1984) and Northern Hemisphere (Mercer and Sutter 1982). This glacial retreat elevated sea level to three maximum highstands in the Pliocene at approximately 4.6, 4.0 and 3.5 Ma.

Pliocene sea level fluctuations (Figure 5.2) were documented by Haq *et al.* (1987). The Pliocene commenced with an initial highstand (H1), followed by a small drop in sea level at approximately 4.2 Ma (H2). This first highstand (H1), peaking at 4.6 Ma, has estimated magnitudes of 29-36 m (Wardlaw and Quinn 1991), 50 m (Hayes and Frakes 1973), 70 m (McKenzie *et al.* 1984), to 75 m (Pickard *et al.* 1988) above present sea level. Following this highstand (H1), sea level quickly rebounded reaching a second maximum at approximately 4.0 Ma (H2) and then dramatically fell approximately 3.8 Ma. Whether or not H1 and H2 are separate highstands or one single event is open to conjecture. The scale of observation will dictate if one or two highstands would be identifiable. Continued glacial retreat in the Antarctic elevated sea level to a third Pliocene highstand (H3) at approximately 3.5 Ma. This rise in sea level has varying estimates regarding its magnitude ranging from 25-35 m (Cronin and Dowse 1993), 30-35 m (Hecht 1990), 20-25 m (Wardlaw and Quinn 1991), to 40 m (Shackleton and Opdyke 1977) above present sea level. This third highstand (H3) is of shorter duration and lower magnitude than the first highstand (H1).

5.3. SEA LEVEL INTERPRETATION

The geological record on Grand Cayman is inconclusive with respect to which Pliocene highstand was responsible for deposition of sediments that now form the Pedro Castle Formation. Strontium dates for the limestones of the Pedro Castle Formation give

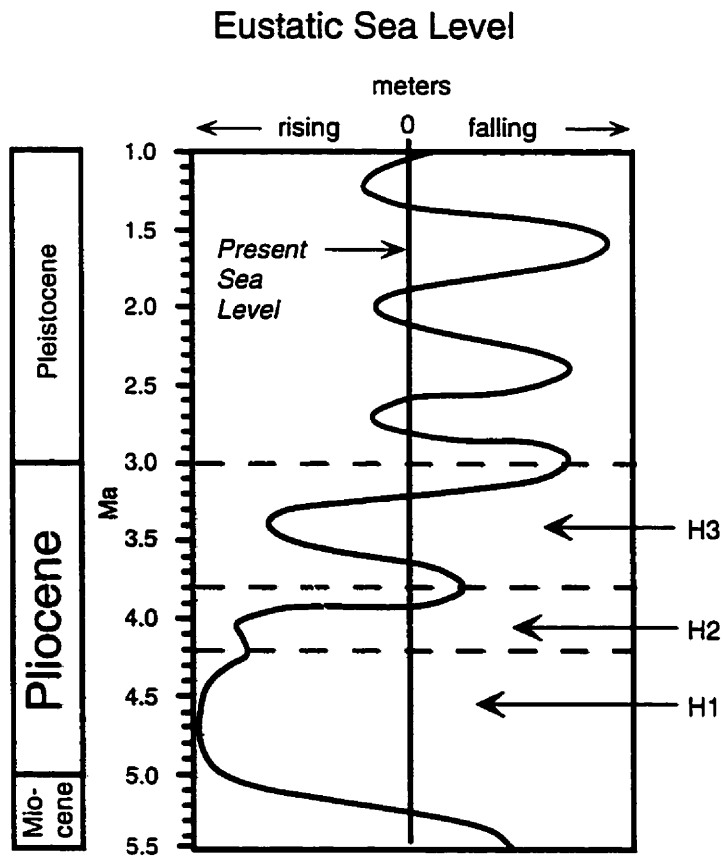


Figure 5.2. Third order sea level curves for the Pliocene (modified from Haq *et al.* 1987; Krantz 1991).

ages of 3-5 Ma (Jones *et al.*, 1994b). Over these 2 Ma only one transgressive cycle is recognized in the Pedro Castle Formation by this study and that of Wignall (1995). It is difficult to determine which Pliocene transgressive event the Pedro Castle Formation represents (Figure 5.2). In attempts to further delineate the timing of deposition, sedimentation rates of 0.1 - 0.5 cm/ka for back lagoon settings are used (Tucker and Wright 1990). For the 44 metres of Pedro Castle Formation found in the Lower Valley, lengths for deposition vary from 88,000 – 440,000 years. The first, second and third highstands developed over 900,000, 200,000 and 400,000 years respectively. The calculated time frames for sedimentation all fall within the margins of each transgressive event. Since the Pedro Castle Formation is unconformity bounded and part of the formation may be missing, it is difficult to resolve which highstand this sequence is related to. This sequence is, however, most likely a result of the first highstand in the Pliocene. It is more likely to remove sediment from the top of a sequence rather than the base. It is safe to say that sedimentation of the Pedro Castle Formation was terminated by a drop in sealevel associated with the onset of Pleistocene glaciation in the Northern Hemisphere (Shackleton and Cita 1976). The Pedro Castle Unconformity represents this drop in sea level. Unfortunately, until another transgressive cycle is found in the Pedro Castle Formation in the Caymans, the exact timing of the transgressive cycle seen by Wignall (1995) and this study will remain inconclusive.

Estimates for the magnitude of Pliocene sea level of the Pedro Castle Formation in the Lower Valley is 30-35 m above present day sea level. This is based on a minimum sea level of 16 m above present, as the Pedro Castle Formation outcrops at this height at Pedro (Great) Bluff near Pedro Castle. The facies at that locality is unknown due to karsting on the formation. In close proximity to that locality, at Pedro Castle Quarry, the Rhodolith *Amphistegina Trachyphyllia* facies of the Pedro Castle Formation is exposed at 11.5 m asl. This facies is presumably present at Pedro Bluff as it ubiquitously overlies the Cayman Unconformity. This facies represents a water depth of 15-20 m based on the faunal assemblage and similarities to modern settings.

5.4. SYNOPSIS

Pliocene sea level variations are due to a complex series of tectonic events that have their origins in the Paleocene. The Pedro Castle Formation is estimated to have been deposited in a maximum water depth of 30-40 m based on the current position and depositional water depth of the uppermost facies. Since only one cycle of sea level change is seen to date in the Pedro Castle Formation the exact timing of the related highstand may be at 4.6, 4.0 or 3.5 Ma.

CHAPTER 6

CONCLUSIONS

The examination of accessible outcrop and 10 cores from the Pliocene Pedro Castle Formation on the southwest corner of Grand Cayman has led to the following conclusions:

- 1) The Pliocene highstand during the deposition of the Pedro Castle Formation was probably 30 – 35 m above present day sea level.
- 2) The Pedro Castle Formation is composed of 7 facies that can be separated into depositional packages I, II and III. Each of these packages contain facies that have accumulated in similar depositional environments.
- 3) Sediments of the Pedro Castle Formation were deposited in waters deeper than 15m in an atoll-like lagoon. The facies succession in the Pedro Castle Formation records a transgressive event.
- 4) Earliest deposition of the Pedro Castle Formation (Depositional Package I) was deposited in a rapidly deepening lagoon. The lagoon was surrounded by the peripheral ridge, which influenced sedimentation. The maximum water depth during that period was 15-20 m.
- 5) Later deposition of the Pedro Castle Formation (Depositional Package II, III) was primarily controlled by bathymetry because the peripheral ridge was no longer an

active barrier. The facies in these packages indicate that sea level was rising slowly until water depths of 25-35m were present.

- 6) One transgressive cycle is recognized in the Pedro Castle Formation on Grand Cayman. The exact timing of this transgressive cycle is unknown because of the problems associated with the correlation of it to any one of the three transgressive events currently recognized in eustatic sea level curves for the Pliocene.

REFERENCES

- Adams, C.G., Benson, R.H., Kidd R.B., Ryan, W.B.F., and Wright, R.C., 1977, The Messinian salinity crisis and evidence of Late Miocene eustatic changes in the world ocean: *Nature*, v. 269, p. 383-386.
- Adey, W.H., Townsend, R.A., and Boykins, W.T., 1982, The crustose coralline algae (Rhodophyta: *Corallinaceae*) of the Hawaiian Islands: *Smithsonian Contributions to Marine Sciences*, v. 15, p.1-74.
- Aharon, P., Goldstein, L.S., Wheeler, C.W., and Jacobson, G., 1993, Sea-level events in the South Pacific linked with Messinian salinity crisis: *Geology*, v. 21, p. 771-775.
- Berggren, W.A., and Haq, B.U., 1976, The Andalusian stage (Late Miocene): biostratigraphy, biochronology and paleoecology: *Palaeogeography, Palaeoclimatology, Palaeoecology*, v. 20, p. 67-129.
- Bosellini, A., and Ginsburg, R.N., 1971, Form and internal structure of Recent algal nodules (rhodolites) from Bermuda: *Journal of Geology*, v. 79, p. 669-682.
- Bosence, D.W.J., 1983, The occurrence and ecology of Recent rhodoliths – a review, *in* Peryt, T.M., ed., *Coated Grains*: New York, Springer-Verlag, p.225-242.
- Blanchon, P.A., 1995, Controls on Modern Reef Development around Grand Cayman [unpublished Ph.D. thesis]: University of Alberta.
- Broecker, W.S., and Denton, G.H., 1989, The role of ocean-atmosphere reorganizations in glacial cycles: *Geochimica et Cosmochimica Acta*, v. 53, p. 2465-2501.
- Budd, A.F., Petersen, R.A., and McNeill, D.F., 1998, Stepwise faunal change during evolutionary turnover: A case study from the Neogene of Curacao, Netherlands Antilles: *Palaios*, v. 13, p. 170-188.
- Cerridwen, S.A., 1989, Paleoecology of Pleistocene mollusca from the Ironshore Formation, Grand Cayman, B. W. I. [unpublished M.Sc. thesis]: University of Alberta.
- Cerridwen, S.A., and Jones, B., 1991, Distribution of bivalves and gastropods in the Pleistocene Ironshore Formation, Grand Cayman, British West Indies: *Caribbean Journal of Science*, v. 27, p. 97-116.
- Cita, M.B., and Ryan, W.B.F., 1979, The Bou Regreg section of the Atlantic coast of Morocco. Evidence, timing and significance of a Late Miocene regressive phase: *Rivista Italiana di Paleontologia e Stratigraphia*, v. 84, p. 1051-1082.

- Cronin, T.M., and Dowsett, H.J., 1993, PRISM: Warm Climates of the Pliocene, *Geotimes*: no.11, p. 17-19.
- Crouch, R.W., and Poag, C.W., 1979, *Amphistegina Gibbosa* D'orbigny from the California borderlands: The Caribbean connection: *Journal of Foraminiferal Research*, v. 9, no. 2, p. 85-105.
- Cushman, J.A., Todd, R., and Post, R.J., 1954, Recent foraminifera of the Marshall Islands Bikini and nearby atolls: U.S. Geological Survey Professional Paper, v. 260-H, p. 319-377.
- Dickson, J.A.D., 1965, A modified staining technique for carbonates in thin section: *Nature*, v. 205, p. 587.
- Dowsett, H.J., and Cronin, T.M., 1990, High Eustatic sea level during the middle Pliocene: evidence from the southeastern U.S. Atlantic Coastal Plain: *Geology*, v. 18, p. 435-438.
- Dowsett, H.J., Cronin, T.M., Poore, R.Z., Thompson, R.S., Whatley, R.C., and Wood, A.M., 1992, Micropaleontological Evidence for increased Meridional Heat Transport in the North Atlantic Ocean during the Pliocene: *Science*, v. 258, p. 1133-1135.
- Dunham, R.J., 1962, Classification of carbonate rocks according to their depositional texture, *in* Hamm, W.E., ed., *Classification of carbonate rocks*: American Association of Petroleum Geologists, p. 108-121.
- Embry, A.F., and Klovan, J.E., 1971, A Late Devonian reef tract on northeastern Banks Island, NWT: *Bulletin of Canadian Petroleum Geology*, v. 19, p. 730-781.
- Filippelli, G.M., 1997, Intensification of the Asian monsoon and a chemical weathering event in the late Miocene-early Pliocene: Implications for late Neogene climate change: *Geology*, v. 25, no. 1, p. 27-30.
- Fort, M., 1996, Late Cenozoic environmental changes and uplift on the northern side of the central Himalaya: a reappraisal from field data: *Palaeogeography, Palaeoclimatology, Palaeoecology*, v. 120, p. 123-145.
- Gill, I.P., and Hubbard, D.P., 1985, Subsurface sedimentology of the Miocene-Pliocene Kingshill Limestone, St. Croix, U.S.V.I., *in* Crevello, P.D., and Harris, P.M., eds., *Deep-water carbonates: buildups, turbidites, debris flows and chalks; a core workshop*: SEPM Core Workshop, v.6, p.431-460.
- Geitzenauer, K.R., Margolis, S.V., and Edwards, D., 1968, Evidence consistent with Eocene glaciation in a South Pacific deep sea sedimentary core: *Earth Planetary Science Letters*, v.4, p.173-177.

- Goreau, T.F., 1963, Calcium carbonate deposition by coralline algae and corals in relation to their roles as reef-builders: *Annals of the New York Academy of Sciences*, v.109, p. 127-167.
- Hallam, A., 1984, Pre-Quaternary sea level changes: *Annual Review of Earth and Planetary Sciences*, v. 12, p. 205-243.
- Hallock, P., 1981, Light dependence in *Amphistegina*: *Journal of Foraminiferal Research*, v. 11, no. 1, p. 40-46.
- Hallock, P., Forward, L.B., and Hansen, H.J., 1986, Influence of environment on the test shape of *Amphistegina*, *Journal of Foraminiferal Research*, v. 16, no. 3, p. 224-231.
- Harwood, D.M., and Webb, P.N., 1998, Glacial Transport of Diatoms in the Antarctic Sirius Group: Pliocene Refrigerator, *GSA Today*: v. 8, no. 4, p. 1-8.
- Hayes, D.E., and Frakes, L.A., 1973, General Synthesis, Deep Sea Drilling Project Leg 28, in Hayes, D.E., Frakes, L.A., *et al.*, eds., *Initial Reports of the Deep Sea Drilling Project: Washington (U.S. Government Printing Office)*, v. 28, p. 919-942.
- Haq, B.V., Hardenbol, J., and Vail, P.R., 1987, Chronology of fluctuating sea levels since the Triassic, *Science*, v.235, p. 1156-1167.
- Hecht, J., 1990, Global warming: back to the future, *New Scientist*: no. 12, p. 38-41.
- Hills, D, 1998, Rhodolite Development in the Modern and Pleistocene of Grand Cayman [unpublished M.Sc. Thesis]: University of Alberta.
- Hine, A.C., Harris, M.W., Locker, S.D., Hallock, P., Peebles, M., Tedesco, L., Mullins, H.T., Snyder, S.W., Belknap, D.F., Gonzales, J.L., Neumann, A.C., and Martinez, J., 1994, Sedimentary infilling of an open seaway: Bawihka Channel, Nicaraguan Rise: *Journal of Sedimentary Research*, v. B64, no. 1, p. 2-25.
- Hine, A.C., Hallock, P., Harris, M.W., Mullins, H.T., Belknap, D.F., and Jaap, W.C., 1988, *Halimeda* bioherms along an open seaway: Miskito Channel, Nicaraguan Rise, SW Caribbean Sea: *Coral Reefs*, v.6, p. 173-178.
- Hirst, G.S.S., 1910, *Notes on the History of the Cayman Islands: Kingston, Jamaica*, Printed 1967 by P.A. Benjamin Manf. Co., 412 p.
- Hodell, D.A., and Kennett, J.P., 1986, Late Miocene - Early Pliocene Stratigraphy and Paleoceanography of the South Atlantic and Southwest Pacific Oceans: A Synthesis: *Paleoceanography*, v. 1, no. 3, p. 285-311.

- Hottinger, L., 1975, Late Oligocene Larger Foraminifera from Koko Guyot, Site 309, *in* Gardner, J.V., ed., Initial Reports of the Deep Sea Drilling Project: Washington (U.S. Government Printing Office), v. 32, p. 825-826.
- Hsü, K.J., Ryan, W.B.F., and Cita, M.B., 1973, Late Miocene Desiccation of the Mediterranean: *Nature*, v. 242, p. 240-244.
- Hsü, K.J., Montadert, L., Bernoulli, D., Cita, M.B., Ericson, A., Garrison, R.E., Kidd, R.B., and others, 1977, History of the Mediterranean salinity crisis: *Nature*, v. 267, p. 399-403.
- Humann, P., 1993, Reef Coral Identification: New World Publications, 252 p.
- Hunter, I.G., and Jones, B., 1988, Corals and paleogeography of the Pleistocene Ironshore Formation on Grand Cayman, B. W. I.: Proceedings of the Sixth International Coral Reef Symposium, p. 431-435.
- Jones, B., 1990, Tunicate spicules and their syntaxial overgrowths: examples from the Pleistocene Ironshore Formation, Grand Cayman, British West Indies: *Canadian Journal of Earth Sciences*, v. 27, p. 525-532.
- Jones, B., 1994, Geology of the Cayman Islands, *in* Brunt, M.A., and Davies, J.E., eds., *The Cayman Islands: Natural History and Biogeography*: Netherlands, Kluwer Academic Publishers, p. 13-49.
- Jones, B., and Hunter, I.G., 1989, The Oligocene-Miocene Bluff Formation on Grand Cayman: *Caribbean Journal of Science*, v. 25, p. 71-85.
- Jones, B.J., and Hunter, I.G., 1990, Pleistocene paleogeography and sea level on the Cayman Islands, British West Indies: *Coral Reefs*, v. 9, p. 81-91.
- Jones, B., and Hunter, I.G., 1994, Messinian (Late Miocene) karst on Grand Cayman, British West Indies: An example of an erosional sequence boundary: *Journal of Sedimentary Research*, v. B64, p. 531-541.
- Jones, B., Hunter, I.G., and Kyser, K., 1994a, Revised stratigraphic nomenclature for Tertiary strata of the Cayman Islands, British West Indies: *Caribbean Journal of Science*, v. 30, p. 53-68.
- Jones, B., Hunter, I.G., and Kyser, T.K., 1994b, Stratigraphy of the Bluff Formation (Miocene-Pliocene) and the newly defined Brac Formation (Oligocene), Cayman Brac, British West Indies: *Caribbean Journal of Science*, v. 30, p. 30-51.
- Jones, B., Lockhart, E.B., and Squair, C., 1984, Phreatic and vadose cements in the Tertiary Bluff Formation of Grand Cayman Island, British West Indies: *Bulletin of Canadian Petroleum Geology*, v. 32, p. 382-397.

- Kemp, E.M., and Hayes, D.E., 1975, Paleoclimate Significance of Diachronous Biogenic Facies, Leg 28, Deep Sea Drilling Project, *in* Hayes, D.E., Frakes, L.A., *et al.*, eds., Initial Reports of the Deep Sea Drilling Project: Washington (U.S. Government Printing Office), v 28, p. 909-917.
- Kennett, J.P., 1967, Recognition and correlation of the Kapitean Stage (Upper Miocene, New Zealand): *New Zealand Journal of Geology and Geophysics*, v. 10, p. 1051-1063.
- Kennett, J.P., Burns, R.E., Andrews, J.E., Churkin jr., M., Davies, T.A., Dumitrica, P., Edwards, A.R., Galehouse, J.S., Packham, G.H., and van der Lingen, G.J., 1972, Australian-Antarctic Continental Drift, Palaeocirculation Changes and Oligocene Deep-Sea Erosion: *Nature Physical Science*, v. 239, p. 51-55.
- Kennett, J.P., Houtz, R.E., Andrews, P.B., Edwards, A.R., Gostin, V.A., Hajos, M., Hampton, M.A., Jenkins, D.G., Margolis, S.V., Ovenshine, A.T., and Perch-Nielsen, K., 1975, Cenozoic paleoceanography in the Southwest Pacific Ocean, Antarctic glaciation and development of the Circum-Antarctic current, *in* Kennett, J.P., Houtz, R.E., *et al.*, ed., Initial Drilling Reports of the Deep Sea Drilling Project: Washington (U.S. Government Printing Office), p. 1155-1170.
- Krantz, D.E., 1991, A Chronology of Pliocene Sea level Fluctuations: The US Middle Atlantic Coastal Plain Record: *Quaternary Science Reviews*, v. 10, p. 163-174.
- Leroy, S., Mercier de Lépinay, B., Mauffret, A., and Pubellier, M., 1996, Structural and Tectonic Evolution of the Eastern Cayman Trough (Caribbean Sea) from Seismic Reflection Data: *AAPG Bulletin*, v. 80, p. 222-247.
- Liddell, W.D., Ohlhorst, S.L., and Boss, S.K., 1988, The significance of Halimeda as a space occupier and sediment producer, 1-750m north Jamaica, *in* 6th International Coral Reef Symposium, Proceedings, Townsville, Australia, 1988, v. 3, p. 127-138.
- Lincoln, J.M., and Schlanger, S.O., 1987, Miocene sea level falls related to the geologic history of Midway Atoll: *Geology*, v. 15, p. 454-457.
- Littler, M.M., Littler, D.S., and Hanisak, M.D., 1991, Deep water rhodolith distribution, productivity, and growth history at sites of formation and subsequent degradation: *J. Exp. Mar. Biol. Ecol.*, v. 150, p. 163-182.
- Loutit, T.S., and Keigwin, L.D., Jr., 1982, Stable isotopic evidence for latest Miocene sea level fall in the Mediterranean region: *Nature*, v. 300, p. 163-166.
- MacKenzie, F.T., Kulm, L.D., Cooley, R.L., and Barnhart, J.T., 1965, *Homotrema rubrum* (Lamark), A sediment transport indicator: *Journal of Sedimentary Petrology*, v. 35, no. 1, p. 265-272.

- Margolis, S.V., and Kennett, J.P., 1971, Antarctic glaciation during the Tertiary recorded in Sub-Antarctic deep-sea cores: *Science*, v. 170, p. 1085-1087.
- Marshall, P.R., 1976, Some relationships between living and total foraminiferal faunas on Pedro Bank, Jamaica: *Maritime Sediments*. Special Publication no. 1, Part A, p. 61-70.
- Matley, C.A., 1924a, Reconnaissance Geological Survey of Cayman Islands, B.W.I.: *The Pan-American Geologist*, v. XLII, p. 313-315.
- Matley, C.A., 1924b, Report of a reconnaissance geological survey of the Cayman Islands: Supplement to the *Jamaica Gazette*, 13 June, v. 47, p. 69-73.
- Matley, C.A., 1925, A Reconnaissance Geological Survey of the Cayman Islands, *British West Indies-Abstract 24: British Association for the Advancement of Science*, p. 392-393.
- Matley, C.A., 1926, The geology of the Cayman Islands (British West Indies) and their relation to the Bartlett Trough: *Quarterly Journal of the Geological Society of London*, v. 82, p. 352-387.
- McKenzie, J.A., Weissert, H., Poore, R.Z., Wright, R.C., Percival, S.F., Oberhänsli, H., and Casey, M., 1984, Paleooceanographic implications of stable-isotope data from Upper Miocene- Lower Pliocene Sediments from the southeast Atlantic (Deep Sea Drilling Project Site 519), *in* Hsü, K.J., LaBrecque, J.Z., *et al.*, eds., *Initial Reports of the Deep Sea Drilling Project: Washington (U.S. Government Printing Office)*, v. 73, p. 717-724.
- Mercer, J.H., and Sutter, J.F., 1982, Late Miocene-earliest Pliocene Glaciation in Southern Argentina: Implications for Global Ice-Sheet History: *Palaeogeography, Palaeoclimatology, Palaeoecology*, v. 38, p. 182-206.
- Minnery, G.A., 1990, Crustose Coralline Algae from the Flower Garden banks, Northwestern Gulf of Mexico: Controls on distribution and growth morphology: *Journal of Sedimentary Petrology*, v.60, no. 6, p.992-1007.
- Montpetit, J.C., 1998, *Sedimentology, Depositional Architecture, and Diagenesis of the Cayman Formation at Tarpon Springs Estates, Grand Cayman, British West Indies* [unpublished M.Sc. thesis]: University of Alberta.
- Perfit, M.R., and Heezen. B.C., 1978, The geology and evolution of the Cayman Trench: *Geol. Soc. Amer. Bull.*, v. 89, p. 1155-1174.
- Pickard, J., Adamson, D.A., Harwood, D.M., Miller, G.H., Quilty, P.G., and Dell, R.K., 1988, Early Pliocene marine sediments, coastline, and climate of East Antarctica: *Geology*, v. 16, p. 158-161.

- Pigram, C.J., Davies, P.J., Feary, D.A., and Symonds, P.A., 1992, Absolute magnitude of the second-order middle to late Miocene sea level fall, Marion Platform, northeast Australia: *Geology*, v. 20, p. 858-862.
- Pleydell, S.M., 1987, Aspects of diagenesis and ichnology in the Oligocene-Miocene Bluff Formation of Grand Cayman Island, British West Indies [unpublished M. Sc. thesis]: University of Alberta.
- Pleydell, S.M., and Jones, B., 1988, Boring of various faunal elements in the Oligocene-Miocene Bluff Formation of Grand Cayman, British West Indies: *Journal of Paleontology*, v. 62, p. 348-367.
- Pleydell, S.M., Jones, B., Longstaffe, F.J., and Baadsgaard, H., 1990, Dolomitization of the Oligocene-Miocene Bluff Formation on Grand Cayman, British West Indies: *Canadian Journal of Earth Sciences*, v. 27, p. 1098-1110.
- Reid, R.P. and MacIntyre, I.G., 1988, Foraminiferal-algal nodules from the Eastern Caribbean: Growth history and implications on the value of nodules as paleoenvironmental indicators: *Palaios*, v. 3, p. 424-435.
- Rosencrantz, E., Ross, M.I., and Sclater, J.G., 1988, Age and spreading history of the Cayman Trough as determined from depth: *Journal of Geophysical Research*, v. 93, p. 2141-2157.
- Scoffin, T.P., 1987, *An Introduction to Carbonate Sediments and Rocks*: Chapman and Hall, 274p.
- Shackleton, N.J., and Cita, M.B., 1976, Oxygen and Carbon isotope stratigraphy of benthic foraminifers at site 397: Detailed history of climatic change during the late Neogene. *in* von Rad, U., Ryan, W.B.F., *et al.*, eds., *Initial Reports of the Deep Sea Drilling Project*: Washington (U.S. Government Printing Office), v. 47, p. 433-445.
- Shackleton, N.J., and Opdyke, N.D., 1977, Oxygen isotope and palaeomagnetic evidence for early Northern Hemisphere glaciation: *Nature*, v. 270, p. 216-219.
- Shah, R., 1996, *Restoring our past, Key to Cayman*: Cayman Free Press, p. 110-113.
- Shourie, A., 1993, *Depositional Architecture of the Late Pleistocene Ironshore Formation, Grand Cayman, British West Indies* [unpublished M.Sc. thesis]: University of Alberta.
- Spencer, T., 1985, Marine erosion rates and coastal morphology of reef limestones on Grand Cayman Island, West Indies: *Coral Reefs*, v. 4, p. 59-70.

- Stroeven, A.P., Burckle, L.H., Kleman, J., and Prentice, M.L., 1998, Atmospheric Transport of Diatoms in the Antarctic Sirius Group: Pliocene Deep Freeze, *GSA Today*: v. 8, no. 4, p. 1-5.
- Tucker, M.E., and Wright, V.P., 1990, *Carbonate Sedimentology*: Blackwell Scientific Publications, Boston, p. 482.
- Vail, P.R., Mitchum, R.M., and Thompson, S., 1977, *Seismic Stratigraphy – Applications to Hydrocarbon Exploration*, American Association of Petroleum Geologists Memoir 26, p. 99-116.
- Vézina, J.L., 1997, *Stratigraphy and Sedimentology of the Pleistocene Ironshore Formation at Rogers Wreck Point, Grand Cayman: a 400 ka Record of Sea-Level Highstands* [unpublished M.Sc. thesis]: University of Alberta.
- Vézina, J., Jones, B., Ford, D., 1999, Sea-level highstands over the last 500'000 years; Evidence from the Ironshore Formation on Grand Cayman, British West Indies: *Journal of Sedimentary Research*, v.69, no. 2, p. 317-327.
- Wardlaw, B.R., and Quinn, T.M., 1991, The Record of Pliocene Sea-Level Change at Enewetak Atoll: *Quaternary Science Reviews*, v. 10, p. 247-258.
- Webb, P.N., and Harwood, D.M., 1991, Late Cenozoic Glacial History of the Ross Embayment, Antarctica: *Quaternary Science Reviews*, v. 10, p. 215-223.
- Wells, J.W., 1967, Corals as Bathometers: *Marine Geology*, v. 5, p. 349-365.
- Wignall, B.W., 1995, *Sedimentology and Diagenesis of the Cayman (Miocene) and Pedro Castle (Pliocene) Formations at Safe Haven, Grand Cayman, British West Indies* [unpublished M.Sc. thesis]: University of Alberta.
- Williams, N., 1970, *A History of the Cayman Islands: George Town, Grand Cayman, Cayman Islands Government*, 94p.
- Wineberg, J.L., 1994, Evolutionary patterns and biogeography of the Scleractinian coral *Madracis* in tropical America: Abstracts with programs – Geological Society of America, v. 26, no. 7, p. 122.
- Woodroffe, C.D., Stoddart, D.R., Harmon, R.S., and Spencer, T., 1983, Coastal morphology and Late Quaternary history, Cayman Islands, West Indies: *Quaternary Research*, v. 19, p. 64-84.

APPENDIX

CORE LOGS

Helen Harquail's Swamp #1 (HHS#1)
17Q, MM 471340, 2133780

Date logged: August 13, 1997

Logged by: Astrid Arts

Remarks: Spudded 14/06/93, Abandoned 16/06/93, KB: 2'0", TD: 98'4"

Location: End of southeastern most canal road, accessed through North Sound Estates.

Reason for termination: sand in the hole. Poor prospects for deepening.





LEGEND

- | | | | |
|--|--|---|---|
|  DOLOSTONE |  Ironshore Formation |  Cayman Formation |  Cavity |
|--|--|---|---|

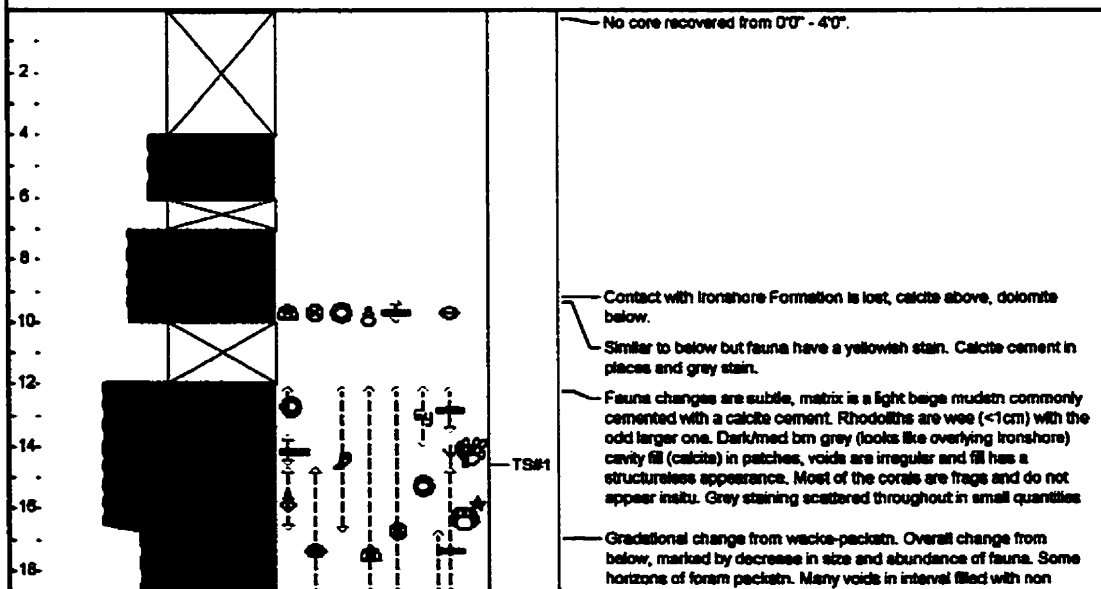
LITHOLOGIC ACCESSORIES

- | | |
|--|--|
|  Grey Staining |  Flowstone |
|--|--|

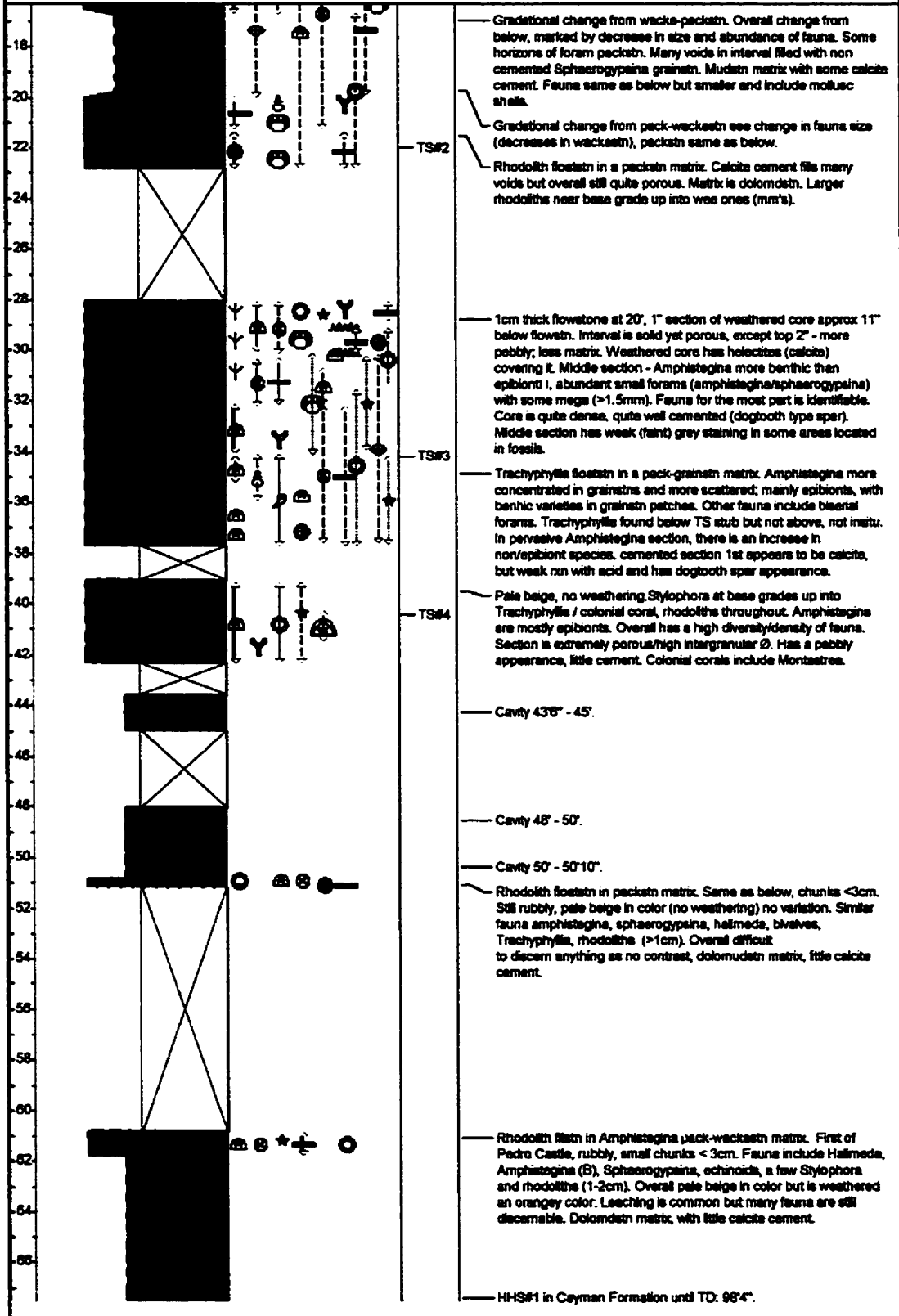
FOSSILS

- | | | |
|---|--|--|
|  - Sphaerogyparia |  - Rhodolith |  - Amphistegina |
|  - Trachyphylla |  - Echinoid Fragments |  - Stick Homotrema |
|  - Mollusca (undifferentiated) |  - Gastropods |  - Stylophora coral |
|  - Porites coral |  - Halimeda |  - Encrusting homotrema |
|  - Free Living Red Algae |  - Colonial coral | |

FEET	TEXTURE	ACCESSORIES	FOSSILS	SAMPLES	REMARKS
	framestn boundstn ballstn rudstn floatstn grainstn peckstn wackstn mudstn				



Helen Harquail's Swamp #1 (HHS#1)
17Q, MM 471340, 2133780



Lower Valley Reservoir #1 (LVR#1)
17Q, MM 469760, 2131560

Date logged: August 13, 1997

Logged by: Astrid Arts

Remarks: Spudded 17/06/93, Abandoned 18/06/93, KB: 8'0", TD 68'6".

Location: Lower Valley Reservoir, north side on grass strip besides chlorinating shed. Reason for termination: poor recoveries, sand in the hole. Prospects for deeping are poor, used by Water Authority for testing.

LEGEND

 DOLOSTONE

LITHOLOGIC ACCESSORIES

Gy - Grey Staining

Terra - Terra Rossa

FOSSILS


 - Sphaerogypsina

 - Rhodolith

 - Amphistegina

 - Trachyphyllia

 - Stick Homotrema

 - Molluscs (undifferentiated)

 - Styophora coral

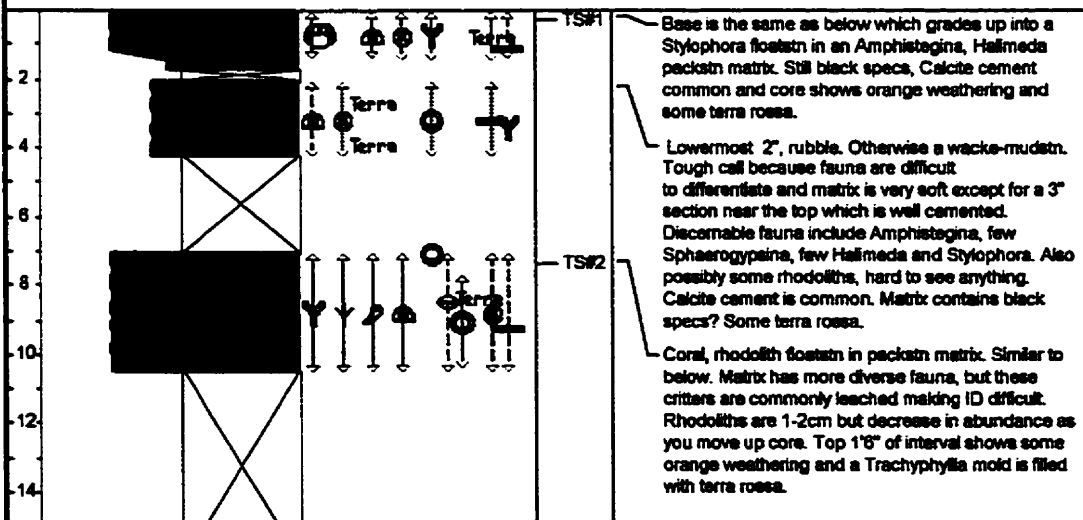
 - Porites coral

 - Halimeda

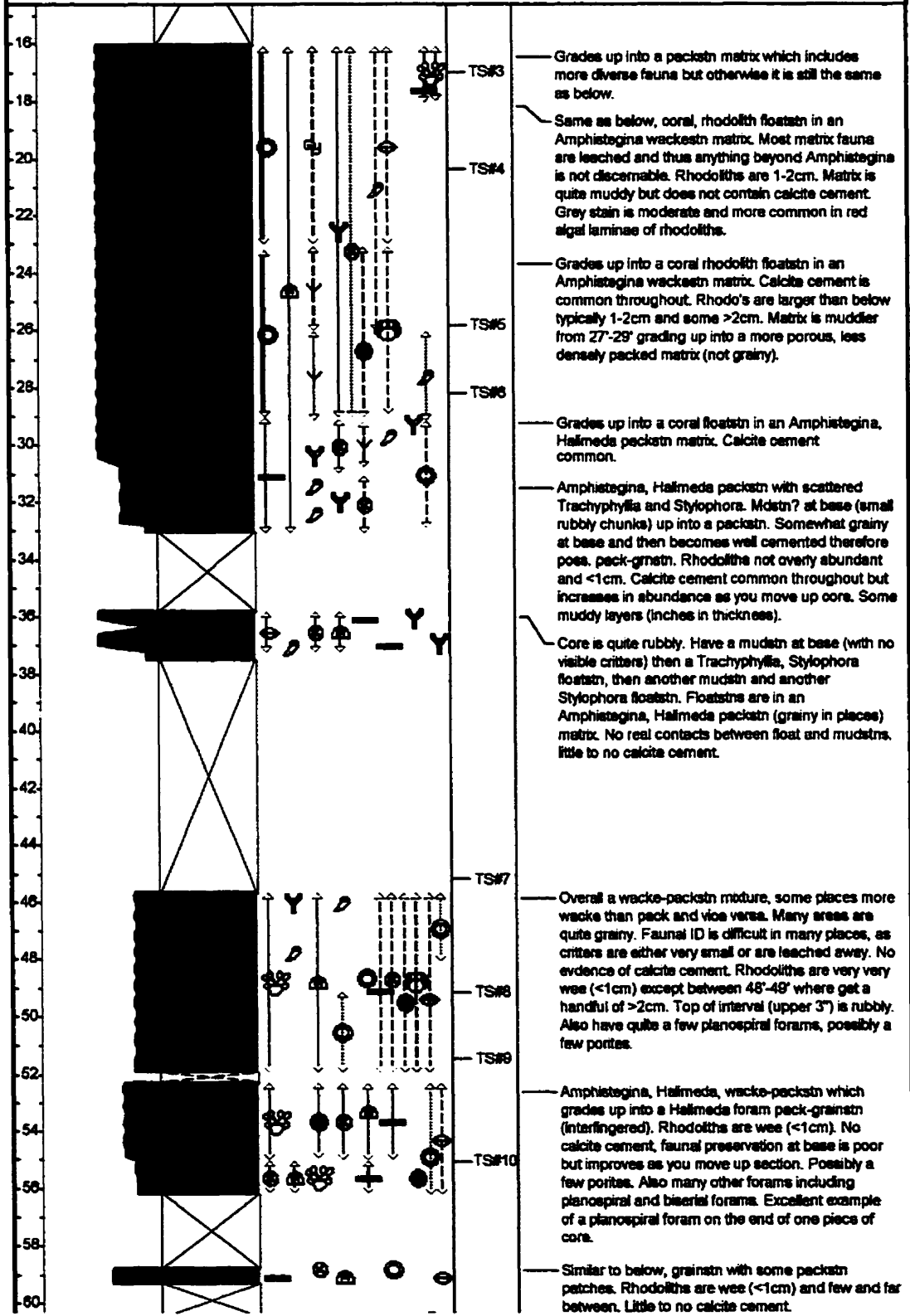
 - Encrusting homotrema

 - Free Living Red Algae

FEET	TEXTURE	ACCESSORIES	FOSSILS	SAMPLES	REMARKS
	framestn boundstn befllestn ruckstn floestn grainstn peckstn wackstn mudstn				



Lower Valley Reservoir #1 (LVR#1)
 17Q, NM 489760, 2131560



Grades up into a packstn matrix which includes more diverse fauna but otherwise it is still the same as below.

Same as below, coral, rhodolith floatstn in an Amphistegina wackestn matrix. Most matrix fauna are leached and thus anything beyond Amphistegina is not discernable. Rhodoliths are 1-2cm. Matrix is quite muddy but does not contain calcite cement. Grey stain is moderate and more common in red algal laminae of rhodoliths.

Grades up into a coral rhodolith floatstn in an Amphistegina wackestn matrix. Calcite cement is common throughout. Rhodo's are larger than below typically 1-2cm and some >2cm. Matrix is muddier from 27'-29' grading up into a more porous, less densely packed matrix (not grainy).

Grades up into a coral floatstn in an Amphistegina, Halimeda packstn matrix. Calcite cement common.

Amphistegina, Halimeda packstn with scattered Trachyphyllia and Stylophora. Mdstn? at base (small rubby chunks) up into a packstn. Somewhat grainy at base and then becomes well cemented therefore poss. pack-grainst. Rhodoliths not overly abundant and <1cm. Calcite cement common throughout but increases in abundance as you move up core. Some muddy layers (inches in thickness).

Core is quite rubby. Have a mudstn at base (with no visible criters) then a Trachyphyllia, Stylophora floatstn, then another mudstn and another Stylophora floatstn. Floatstns are in an Amphistegina, Halimeda packstn (grainy in places) matrix. No real contacts between float and mudstns. little to no calcite cement.

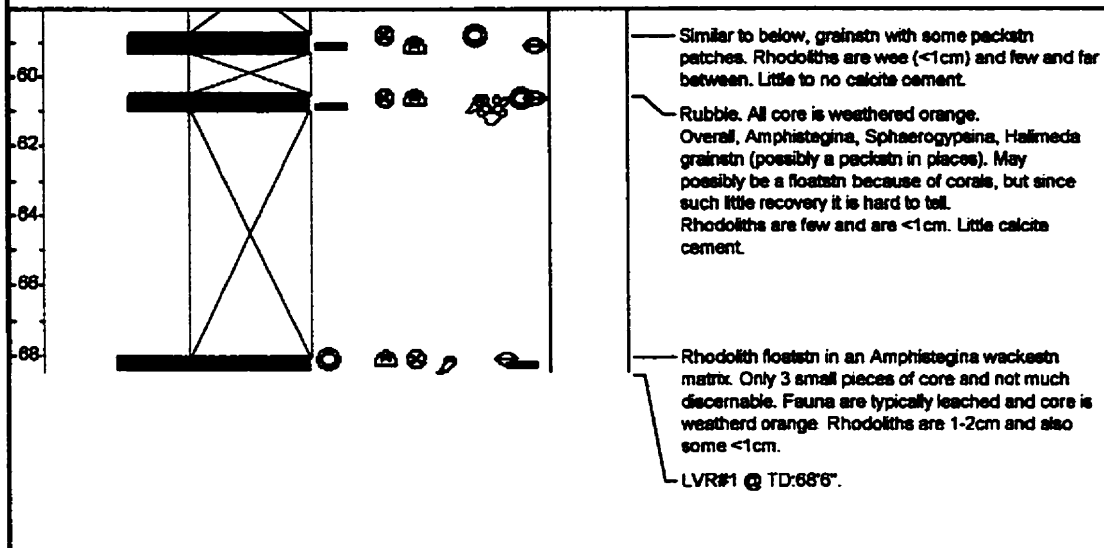
Overall a wacke-packstn mdture, some places more wacke than pack and vice versa. Many areas are quite grainy. Faunal ID is difficult in many places, as criters are either very small or are leached away. No evidence of calcite cement. Rhodoliths are very very wee (<1cm) except between 48'-49' where get a handful of >2cm. Top of interval (upper 3") is rubby. Also have quite a few planospiral forams, possibly a few porites.

Amphistegina, Halimeda, wacke-packstn which grades up into a Halimeda foram pack-grainstn (interfingred). Rhodoliths are wee (<1cm). No calcite cement, faunal preservation at base is poor but improves as you move up section. Possibly a few porites. Also many other forams including planospiral and biserial forams. Excellent example of a planospiral foram on the end of one piece of core.

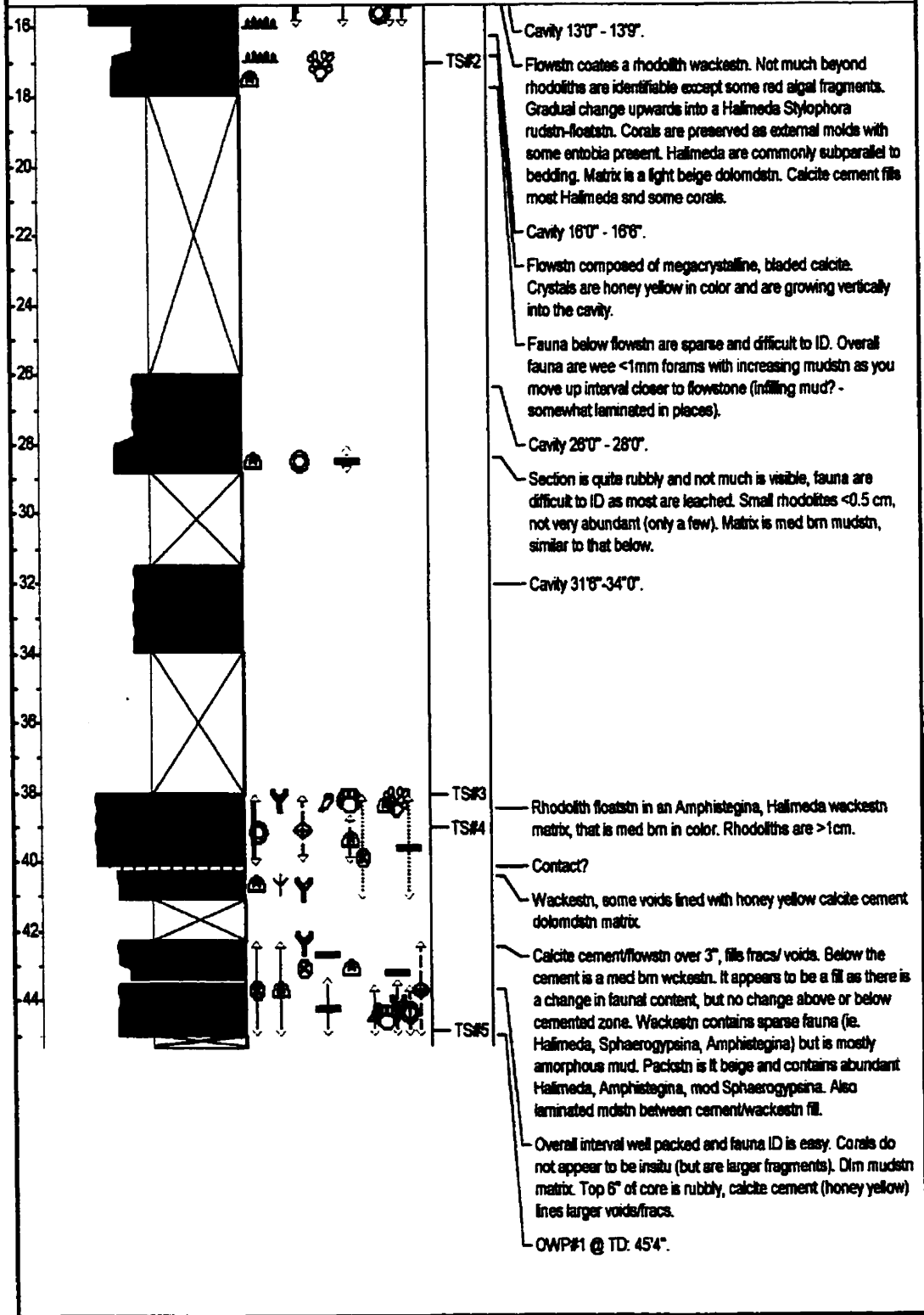
Similar to below, grainstn with some packstn patches. Rhodoliths are wee (<1cm) and few and far between. Little to no calcite cement.

Lower Valley Reservoir #1 (LVR#1)

17Q, MM 469760, 2131560



Otto Watler's Pasture #1 (OWP#1)
 17Q, NM 470540, 2132750



Otto Watler's Pasture #1A (OWP#1A)
17Q, MM 470540, 2132750

Date logged: August 13, 1997

Logged by: Astrid Arts

Remarks: Spudded 09/06/93, Abandoned 11/06/93, KB: 2'0", TD: 111'6". Location: Otto Watler's pasture, 4' WNW of OWP#1. Reason for termination: jamming, low recoveries. Prospects for deepening - possible, Water Authority using for testing.

LEGEND

 DOLOSTONE	 Ironshore Formation	 Cayman Formation	 Cavity
---	---	--	--

CONTACTS

 Sharp

LITHOLOGIC ACCESSORIES

 Grey Staining

 Flowstone

 Terra - Terra Rossa

FOSSILS

 Sphaerogypsina

 Rhodolith

 Amphistegina

 Trachyphylla

 Stick Homotrema

 Molluscs (undifferentiated)

 Gastropods

 Stylophora coral

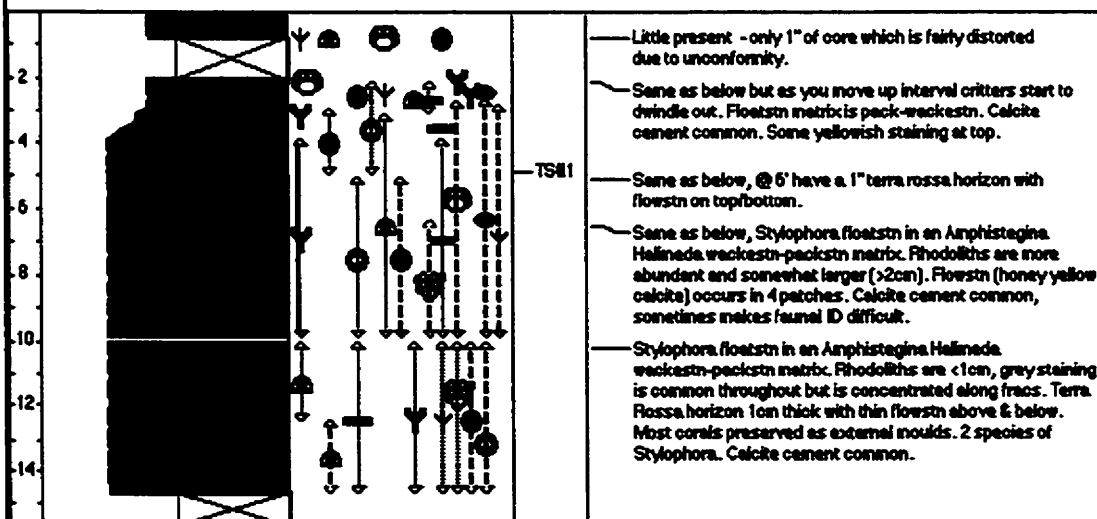
 Porites coral

 Halimeda

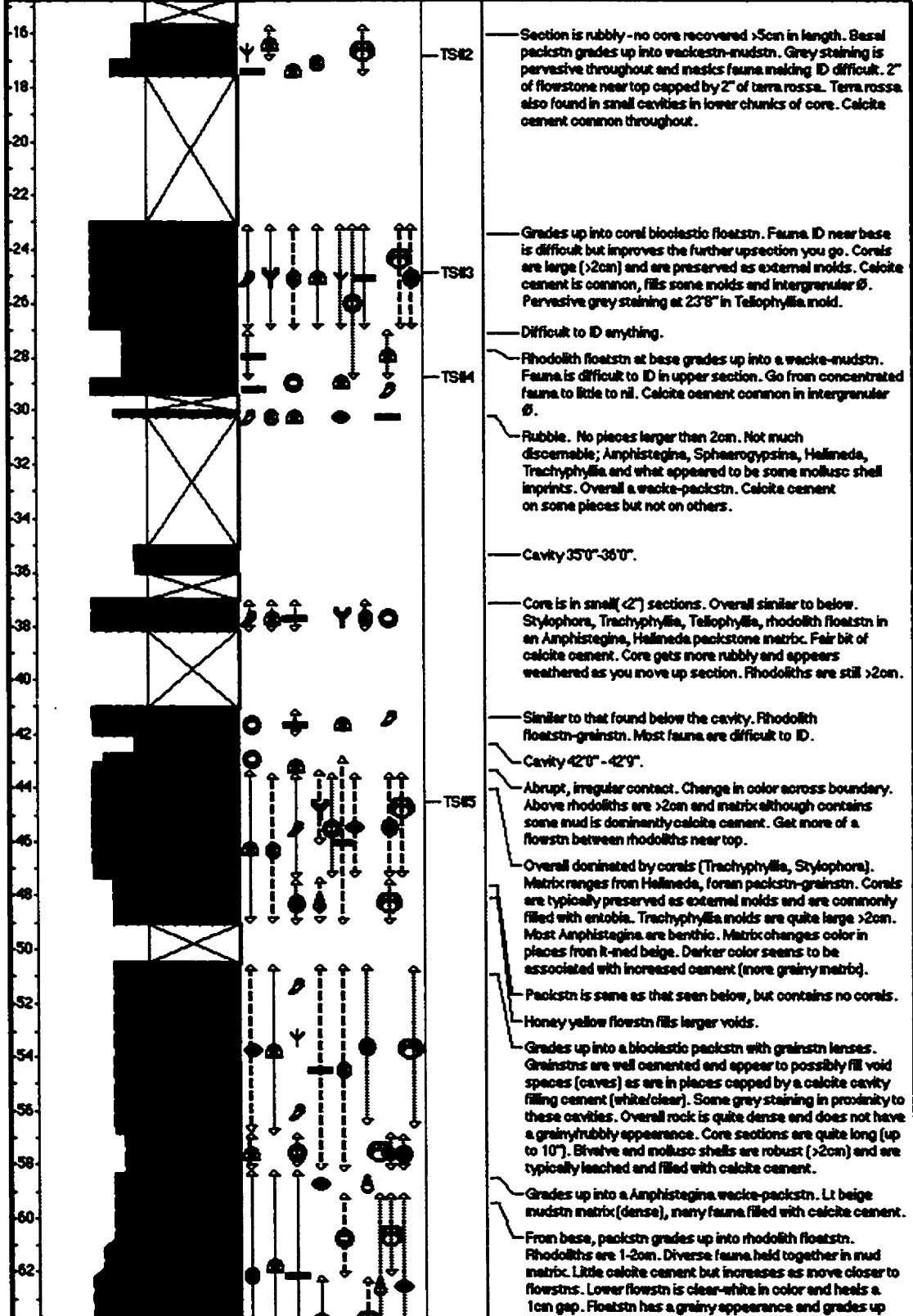
 Encrusting homotrema

 Free Living Red Algae

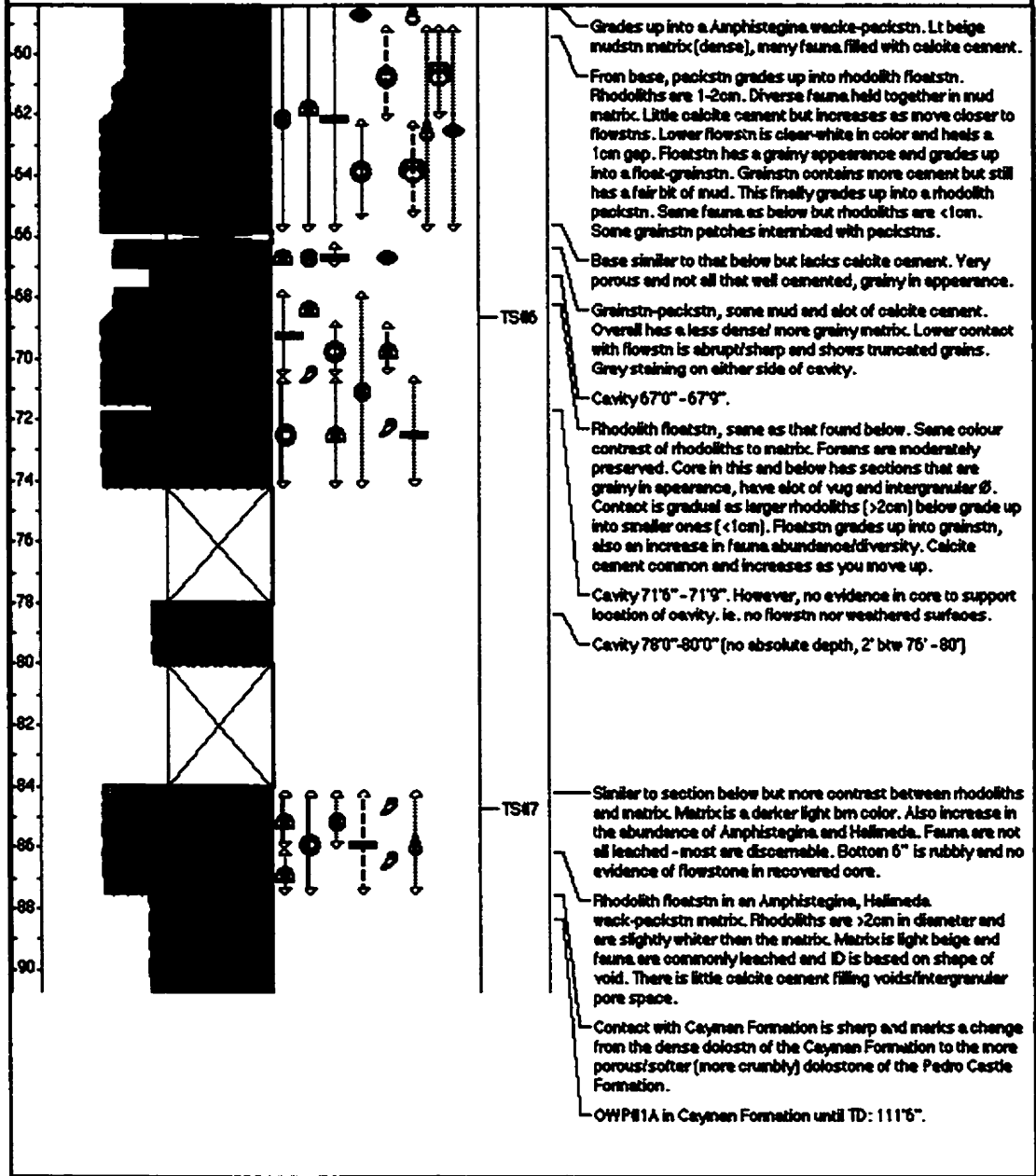
FEET	TEXTURE	ACCESSORIES	FOSSILS	SAMPLES	REMARKS
	<ul style="list-style-type: none"> — f. aneastn — boundstn — buffleestn — rudstn — floatstn — granstn — packstn — wackestn — mudstn 				



Otto Watler's Pasture #1A (OWP#1A)
 17Q, MM 470540, 2132750



Otto Watler's Pasture #1A (OWP#1A)
 17Q, MM 470540, 2132750



Otto Watler's Pasture #2 (OWP#2)
17Q, MM 469760, 2131560

Date logged: August 13, 1997

Logged by: Astrid Arts

Remarks: Spudded 11/06/93, Abandoned 14/06/93, KB: 2'6", TD: 94'8".

Location: Otto Watler's pasture, east side of track just before second gate.

Reason for termination: sand in the hole. Prospects for deepening are poor.

LEGEND

DOLOSTONE
 Ironshore Formation
 Cavity












CONTACTS

----- Uncertain

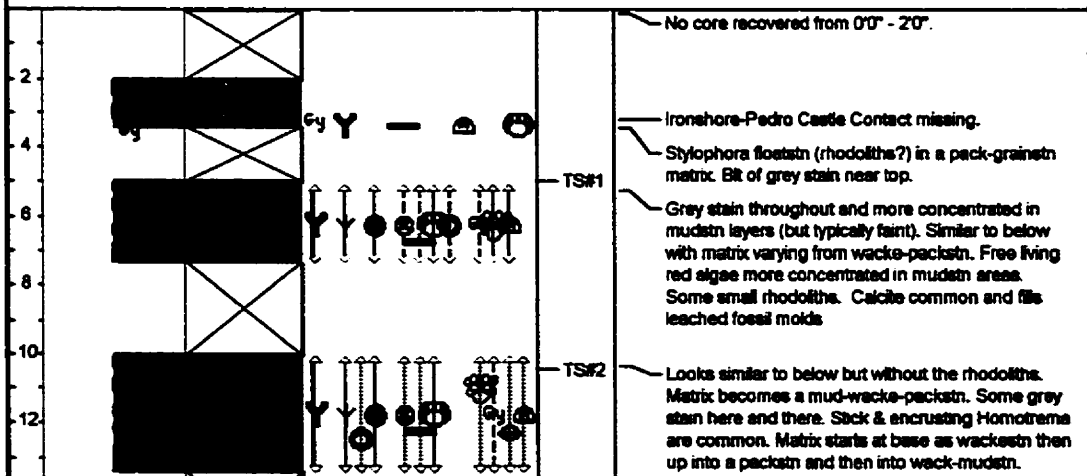
LITHOLOGIC ACCESSORIES

Gy - Grey Staining

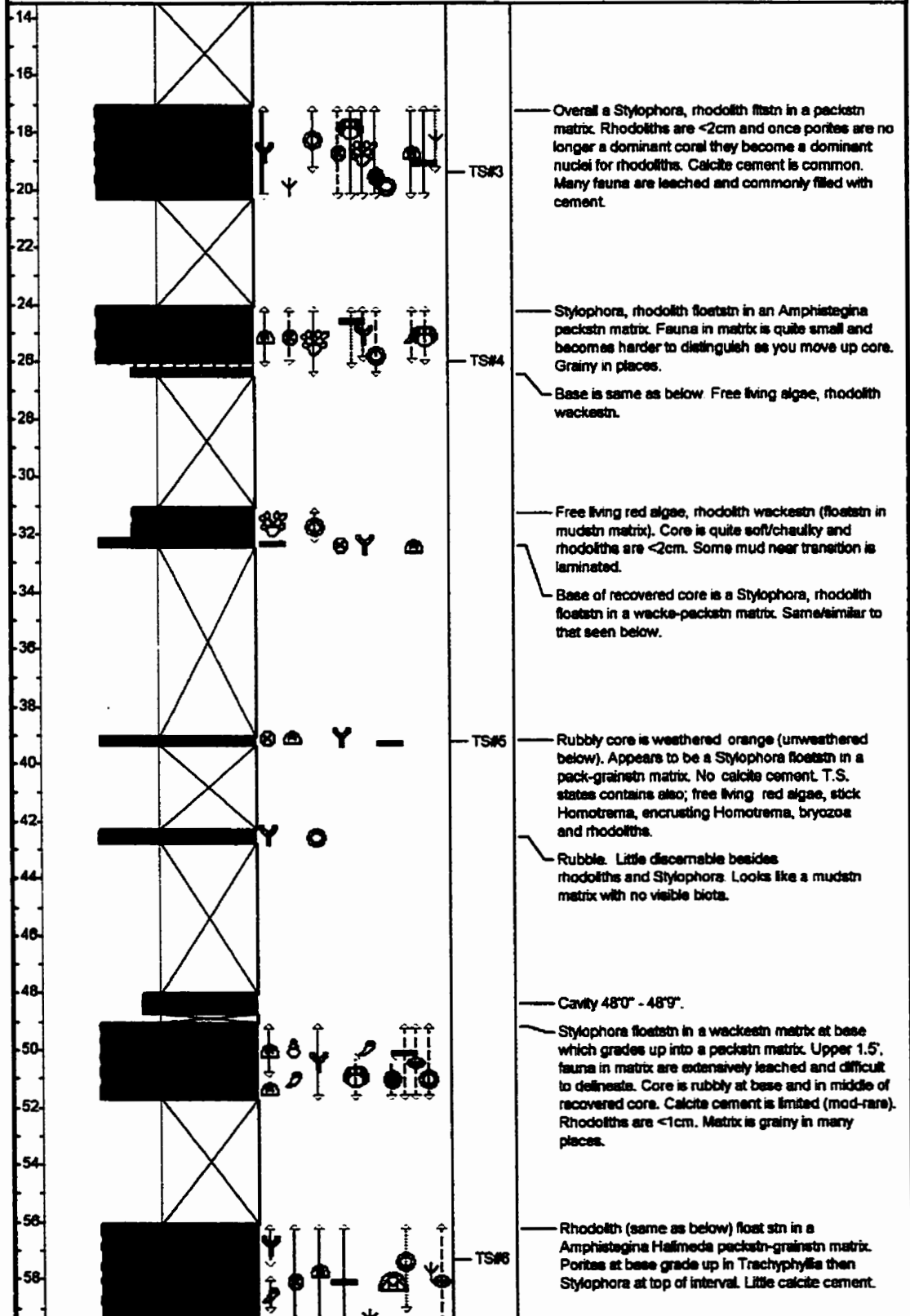
FOSSILS

 - Spherogypsa	 - Rhodolith	 - Amphistegina
 - Trachyphylla	 - Stick Homotrema	 - Mollusca (undifferentiated)
 - Gastropods	 - Stylophora coral	 - Montasrea coral
 - Porites coral	 - Halimeda	 - Encrusting homotrema
 - Free Living Red Algae	 - Colonial coral	

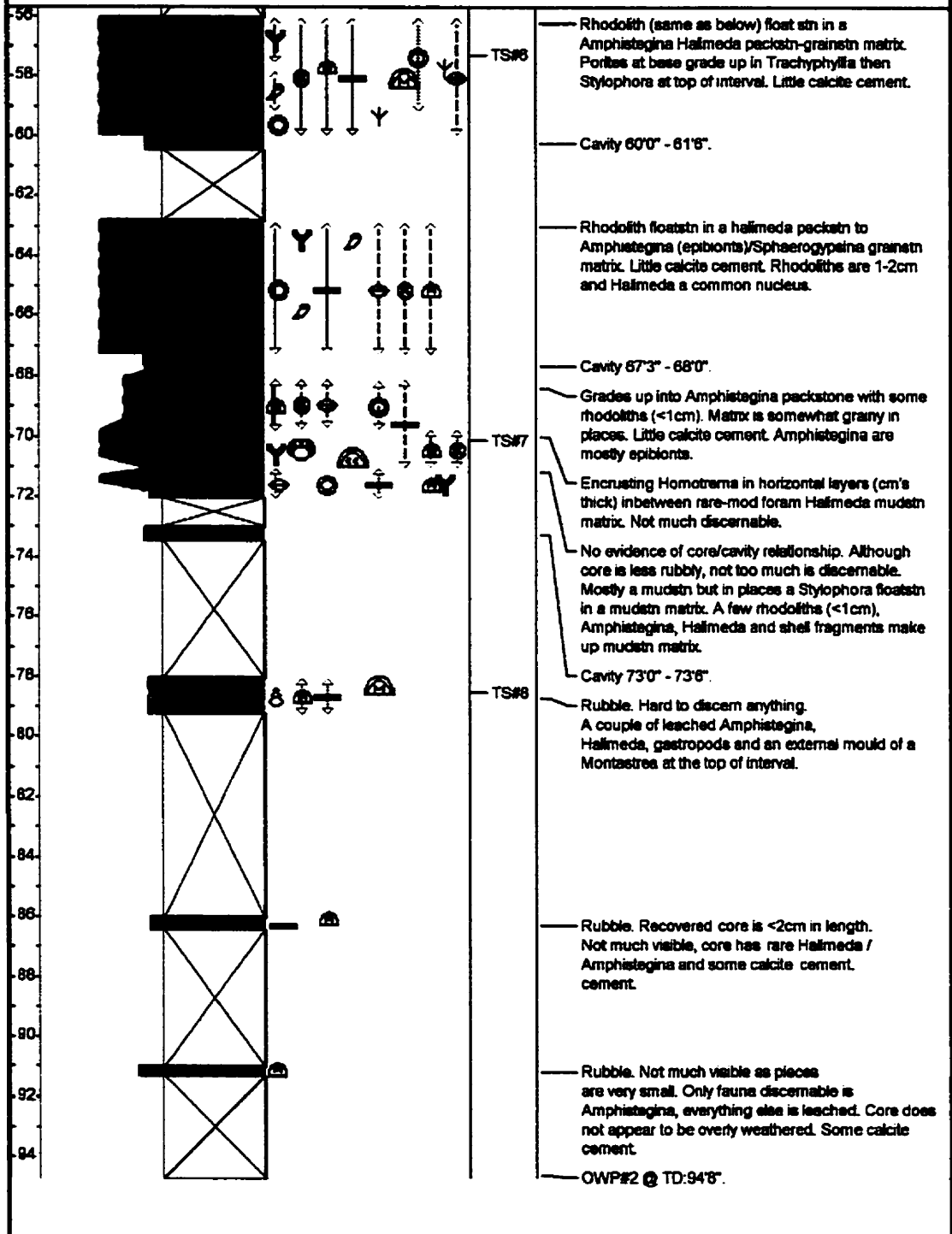
FEET	TEXTURE	ACCESSORIES	FOSSILS	SAMPLES	REMARKS
	framesn boundstn beflleatn rudstn floatstn grainstn packstn wackstn mudstn				



Otto Watler's Pasture #2 (OWP#2)
 17Q, MM 489760, 2131560



Otto Watler's Pasture #2 (OWP#2)
 17Q, MM 469760, 2131560



Otto Watler's Pasture #3 (OWP#3)
17Q, MN 470140, 2131530

Date logged:

Logged by: Astrid Arts

Remarks: Spudded 18/06/93, Abandoned 18/06/93, KB: 6'0", TD: 16'0".

Location: North edge of sinkhole just east of Lower Valley Reservoir.

Reason for termination: drilled as a test hole for Water Authority, had reached TD. Good prospects for deepening.











LEGEND

 DOLOSTONE

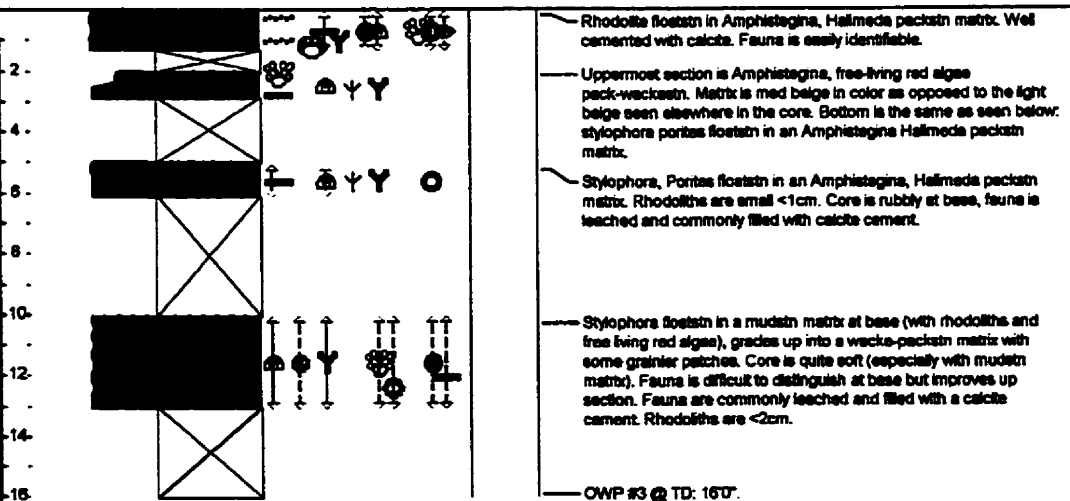
LITHOLOGIC ACCESSORIES

 grainy

FOSSILS

- | | | |
|---|---|--|
|  - Sphaerogypinae |  - Rhodolith |  - Amphistegina |
|  - Stick Homotrema |  - Molluscs (undifferentiated) |  - Stylophora coral |
|  - Porites coral |  - Halimeda |  - Encrusting homotrema |
|  - Free Living Red Algae | | |

FEET	TEXTURE	ACCESSORIES	FOSSILS	SAMPLES	REMARKS
	<ul style="list-style-type: none"> framestrn boundstrn bedstrn rudstrn floatstrn grainstrn peckstrn wackstrn mudstrn 				



Patrick Island Lagoon #2 (PIL#2)
17Q, MM 486080, 2133250

Date logged: August 12, 1997

Logged by: Astrid Arts

Remarks: Spudded 18/10/92, Abandoned 20/10/92, KB: 1'6", TD: 96'8".

Location: Patrick's Island Development, south shore of North Sound. Reason for termination: low recoveries. No prospects for deepening.

LEGEND

 DOLOSTONE  Cayman Formation

LITHOLOGIC ACCESSORIES

Gy - Grey Staining

FOSSILS


 - Sphaerogypaina

 - Rhodolith

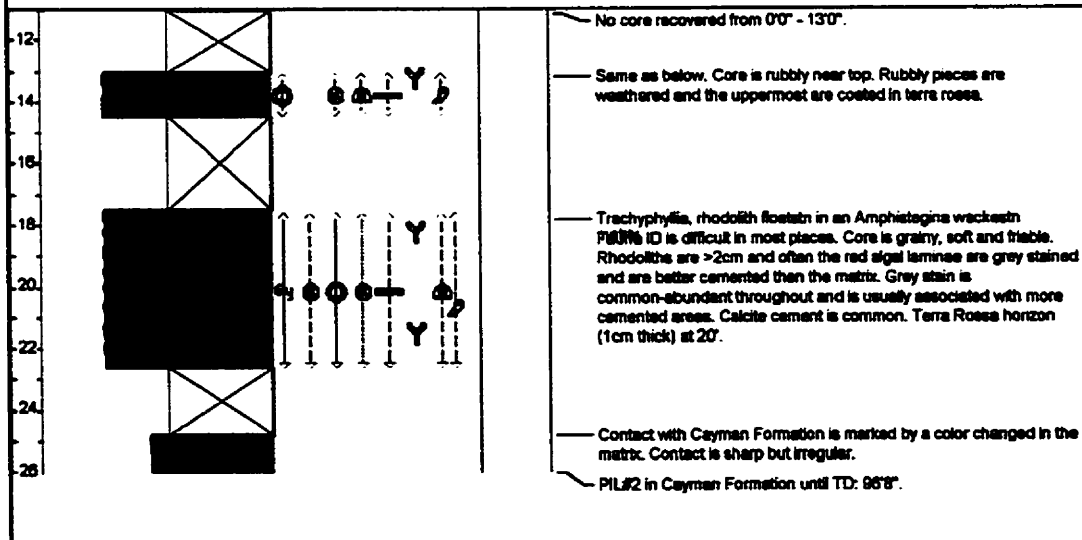
 - Amphistegina

 - Trachyphyllia

 - Stylophora coral

 - Helmedia

FEET	TEXTURE	ACCESSORIES	FOSSILS	SAMPLES	REMARKS
	framestr boundstr bedstr rudstr floestr grainstr packstr wackstr mudstr				



Sewage House and Treatment #1 (SHT#1)
17Q, MM 460750, 2135295

Date logged: August 12, 1997

Logged by: Astrid Arts

Remarks: Spudded 04/09/92, Abandoned 05/09/92, KB: 4'0", TD: 127'10".
 Location: Northwest corner of sewage lagoon compound at end of Seymour Rd. Reason for Termination: sand thicker'n 3yr old peanut butter and jamming frequently. No prospects for deepening.

LEGEND

DOLOSTONE
 Cayman Formation
 Cavity

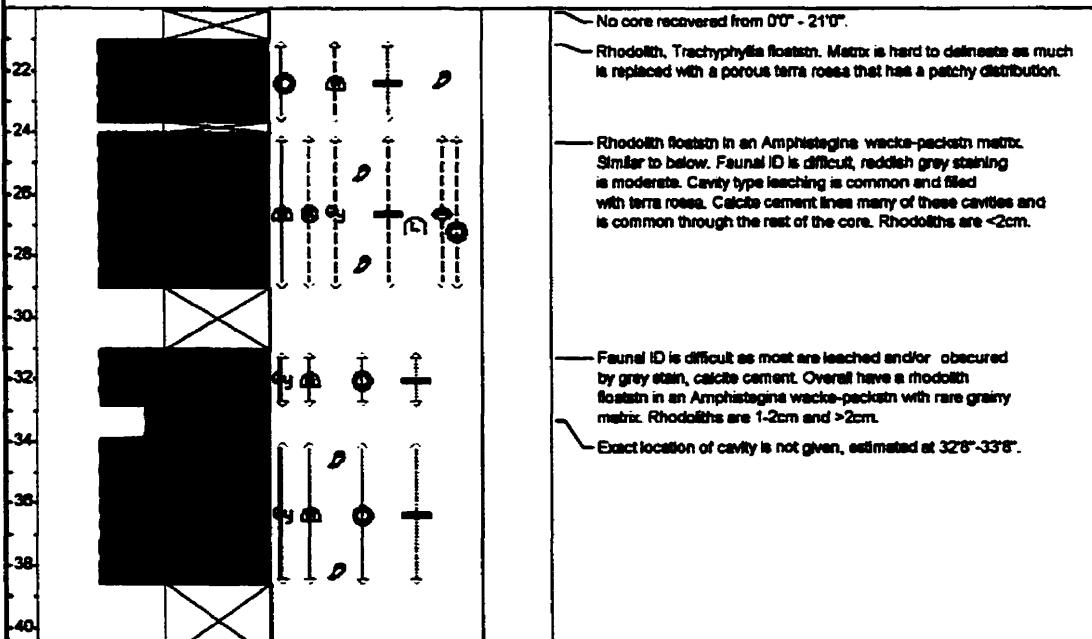
LITHOLOGIC ACCESSORIES

Gy - Grey Staining

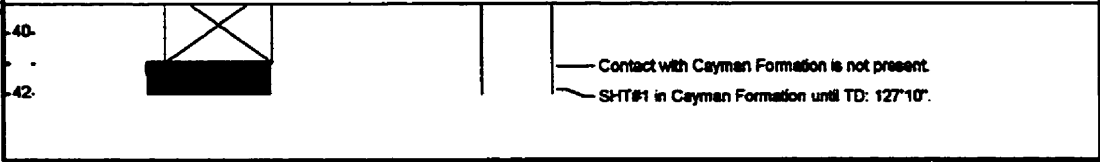
FOSSILS

- Sphaerogypaina
 - Rhodolith
 - Amphistegina
 - Trachyphyllia
 - Leptoseris
 - Mollusca (undifferentiated)
 - Halimeda

FEET	TEXTURE	ACCESSORIES	FOSSILS	SAMPLES	REMARKS
	framestn boundstn befllestn ruclestn foolestn grainstn packstn wackstn mudstn				



Sewage House and Treatment #1 (SHT#1)
17Q, MM 460750, 2135295



Sewage House and Treatment #2 (SHT#2)
17Q, MM 460925, 2135325

Date logged: August 12, 1997

Logged by: Astrid Arts

Remarks: Spudded 03/06/93, Abandoned 07/06/93, KB: 4'0", TD: 127'0". Location: Northeast corner of sewage lagoon compound at end of Seymour Rd. Reason for termination: poor recoveries. No prospect for deepening.

LEGEND

DOLOSTONE
 Cayman Formation
 Cavity

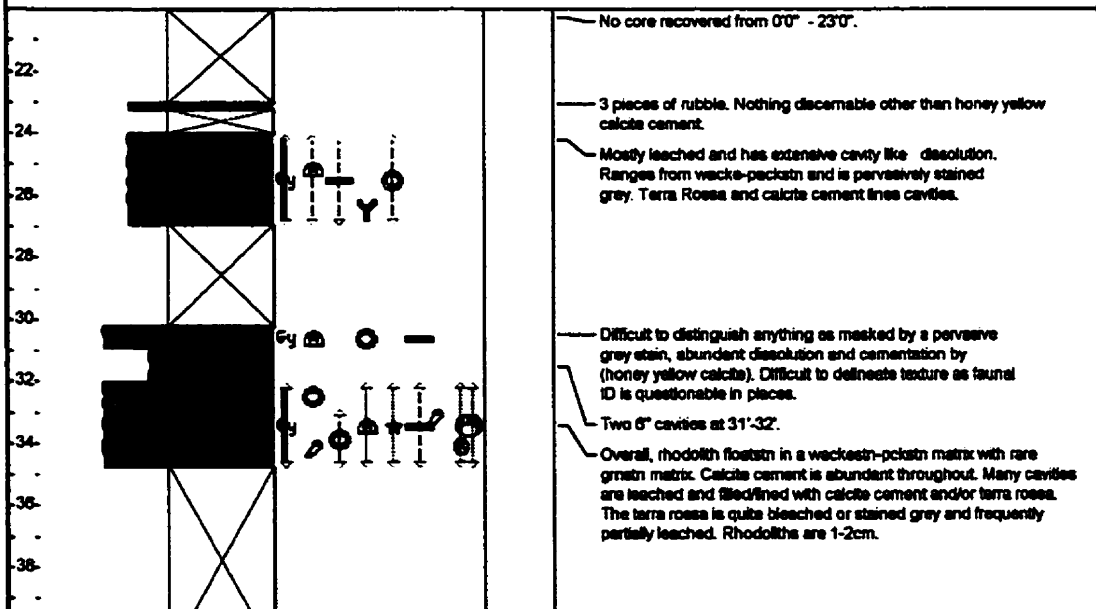
LITHOLOGIC ACCESSORIES

Gy - Grey Staining

FOSSILS

- Sphaerogypsina
 - Rhodolith
 - Amphistegina
 - Trachyphylla
 - Echinoid Fragments
 - Stylophora coral
 - Halimeda
 - Encrusting homotrema

	TEXTURE	ACCESSORIES	FOSSILS	SAMPLES	REMARKS
FEET	framestrn boundstrn buffstrn ruckstrn floatstrn grainstrn packstrn wackstrn mudstrn				



Sewage House and Treatment #2 (SHT#2)
17Q, MM 460925, 2135325

